ISSN 2537-6373 (Print)
ISSN 2537-6381 (Online)

The Moldovan Medical Journal

The Publication of the Scientific Medical Association of Moldova

Frequency – 4 per year
Category – B+

Vol. 65, No 2
December 2022

Welcome to the Moldovan Medical Journal!

The Moldovan Medical Journal is an international scientific double-blind peer reviewed periodical edition, 4 per year, of the Scientific Medical Association of the Republic of Moldova designed for specialists in the areas of medicine, dentistry, pharmacy, social medicine and public health. From its debut the journal has striven to support the interests of Moldovan medicine concerning the new concepts of its development.

The Editorial Board warmly welcomes both the readers of and the authors for the journal, all those who are enthusiastic in searching new and more effective ways of solving numerous medicine problems. We hope that those who want to make their contribution to the science of medicine will find our journal helpful and encouraging.

Editorial Board

Emeritus Members of the Editorial Board

INDEXING AND ABSTRACTING

1. DOAJ Aworded the Seal, Directory of Open Access Journals (www.doaj.org)
2. Google Scholar (https://scholar.google.com/citations?hl=en&user=weWUEMAAAAAJ)
3. VINITI, All-Russian Scientific and Technical Information Institute (www.viniti.ru)
4. Ulrichsweb Global Serials Directory (www.ulrichsweb.serialssolutions.com)
5. Directory of Open Access Scholarly Resources (https://portal.issn.org/resource/ISSN/2537-6381#)
6. CrossRef (https://search.crossref.org/?from_ui=&q=2537-6373) official Digital Object Identifier (DOI) Registration Agency of the International DOI Foundation
7. eLIBRARY.RU – Scientific Electronic Library (https://elibrary.ru/contents.asp?titleid=65889)
8. Sherpa Romeo, open access policies analyzer (https://v2.sherpa.ac.uk/id/publication/35606)
9. EuroPub, Directory of Academic and Scientific Journals (https://europub.co.uk/journals/19267)
10. Collective Catalogue of Moldovan University Libraries Consortium (www.primo.libuniv.md)
11. National Bibliometric Instrument (https://ibn.idsi.md/ro/vizualizare_revista/moldmedjournal)
12. Institutional Repository in Medical Sciences (http://library.usmf.md:8080/jspui/handle/123456789/5643)
13. WorldCat (https://www.worldcat.org/title/moldovan-medical-journal/oclc/1029854308&referer=brief_results)
14. NLM LocatorPlus (https://locatorplus.gov/cgi-bin/Pwebrecon.cgi)
15. BASE, Bielefeld Academic Search Engine (https://www.base-search.net/Search/Results?lookfor=moldovan+medical+journal&name=&oaboost=1&newsearch=1&refid=dcbasen)
16. Integrated Information System of Moldova's Libraries (SIBIMOL) (http://cc.sibimol.bnrm.md/opac/bibliographic_view/573823?pn=opac%2FSearch&q=moldovan+medical+journal#level=all&location=0&ob=asc&q=moldovan+medical+journal&sb=relevance&start=0&view=CONTENT)
17. CiteFactor Academic Scientific Journals (https://www.citefactor.org/journal/index/23553#.XAjn89szbIU)
18. Central and East European Index (https://www.ceendx.eu/?page_id=/93/moldovan-medical-journal/)
19. Electronic Journals Library University of Regensburg (http://rzblx1.uni-regensburg.de/detail.phtml?bibid=AAAAA&colors=7&lang=en&jour_id=431225)
20. Journal Factor (http://www.journalfactor.org/Journal.php?JOURNAL=JF3174&NAME=Moldovan_Medical_Journal)
21. CYBERLENINKA (https://cyberleninka.ru/journal/n/the-moldovan-medical-journal)
22. Index Copernicus International (https://journals.indexcopernicus.com/search/journal/issue?issueId=all&journalId=51450)
23. JIFACTOR, Global Society for Scientific Research (http://www.jifactor.org/journal_view.php?journal_id=4696)
24. Central Scientific Medical Library of Sechenov First Moscow State Medical University (www.scsml.rssi.ru)
25. East View Information Services (https://shop.eastview.com/results/item?SKU=5140480P)
26. Open Academic Journal Index (http://oaji.net/journal-detail.html?number=7489)
27. Cabell's International – Journal Quality Auditor, Scholarly Analytics (http://www.cabells.com)

9 772537 637004 >

Index for subscription – 32130

Editorial Staff

Anatol Calistru, MD, PhD, Head of the Editorial Office: +373 22 205 209
Ludmila Martinenko, English Corrector, telephone: +373 22 205 209
Irina Litvinova, Editorial Secretary, telephone: +373 32205877

Address of the Editorial Office
192, Stefan cel Mare Avenue, Chisinau, the Republic of Moldova
Phone: +373 22 205 209, Office: +373 79 429 274 mobile
www.moldmedjournal.md editor@moldmedjournal.md

Publisher

"Revista Curier Medical"
192, Stefan cel Mare Avenue
Chisinau, the Republic of Moldova

Printing House "Tipografia No1" SRL
46, 31 August 1989 str., Chisinau, MD-2001
the Republic of Moldova
www. tipografia.nr1@gmail.com

TABLE OF CONTENTS

ORIGINAL RESEARCHES

REVIEW ARTICLES

ANNIVERSARIES

ORIGINAL RESEARCHES

https://doi.org/10.52418/moldovan-med-j.65-2.22.01
UDC: 618.32+611.013

Evaluation of p57 expression in early disordered pregnancies with molar status vs non-molar ones

*[1,3]Valeriu David, [1,3]Vergil Petrovici, [1,2]Lilian Saptefrati, [1,2]Veaceslav Fulga, [1,2]Ecaterina Carpenco, [1]Elena Frant

[1]Laboratory of Morphology, [2]Department of Histology, Cytology and Embryology
Nicolae Testemitanu State University of Medicine and Pharmacy,
[3]Department of Pathomorphology, Institute of Mother and Child, Chisinau, the Republic of Moldova

Authors' ORCID iDs, academic degrees and contributions are available at the end of the article

*Corresponding author – Valeriu David, e-mail: valeriu.david@usmf.md
Manuscript received September 21, 2022; revised manuscript November 30, 2022; published online December 20, 2022

Abstract

Background: The molar and non-molar lesions are determined during histomorphological examination and treated as inconclusive. The establishing of a marker by immunohistochemical investigations could influence the accuracy of the morphopathological diagnosis. The aim is evaluation of p57 immunoexpression in the trophoblastic germ compartment in molar and non-molar pregnancies.
Material and methods: Abortion products from 15 patients with hydatidiform mole, 18 pregnancies solved on social indications and 16 short-term disordered pregnancies were evaluated depending on the immunoexpresion of p57.
Results: The hydatidiform mole was classified based on anti-p57 immunoexpression into: complete hydatidiform mole – 8 cases (negative immunoexpression or expression in <10% of villous cytotrophoblast) and partial hydatidiform mole – 7 cases (positive expression in >10% of the villous cytotrophoblast). Basal deciduous and extravillous cytotrophoblasts were positive in 100% of cases and served as internal control. Hepatocytes were used as negative control. In the control group, the positive immunoexpression was attested in >10% of cases in the villous trophoblast.
Conclusions: Differential immunoexpression of p57 protein in the germinal cytotrophoblast allows subclassification of molar pathology into complete and partial forms, while not allowing the differentiation between partial hydatidiform mole and non-molar lesions. Immunohistochemical evaluation of p57kip2 protein in molar and non-molar pathology is useful in differential diagnosis as a complementary method.
Key words: anti-p57, fetal concept, hydatidiform mole, trophoblastic disease.

Cite this article
David V, Petrovici V, Saptefrati L, Fulga V, Carpenco E, Frant E. Evaluation of p57 expression in early disordered pregnancies with molar status vs non-molar ones. *Mold Med J*. 2022;65(2):5-12. https://doi.org/10.52418/moldovan-med-j.65-2.22.01.

Introduction

The morphological profile that is evaluated in short-term dysregulated pregnancies includes a heterogeneous group of choriovillar abnormalities accompanied by polymorphic proliferative and hydropico-cystic lesions in the germinal compartment of the fetal conceptus. The complete, partial and non-molar molar lesions are established most often during the histomorphological examination in early-term deranged pregnancies in the germinal compartment, being often treated as inconclusive. This inconclusiveness of the histomorphopathological diagnosis is the result of the masking of the particularities attested at the level of the choriovillary stroma, in common with the degree of proliferation of the villous trophoblast in early terms of pregnancy [1, 2]. The histomorphological peculiarities are often not obvious and do not help in establishing of the differential diagnosis in molar pathology, particularly in the early period of evolution [3], including, in the association of morphological lesions with a hydropic or cystic character [4]. Gersell D. et al. (2011) indicate that the differential diagnosis becomes even more unpredictable in the case of the addition of hydropic degenerative changes in the chorionic villi (15%-40%), being more frequently attested in more advanced pregnancies [4]. The molar phenotypic profile of the fetal conceptus is usually diploid and has androgenic origin, with the establishment of the complete molar monospermatic or dyspermatic form, through the loss of maternal chromosomes before or after fertilization. In the case of the partial hydatidiform mole, it represents a fertilization of a normal egg by two spermatozoa or by a diploid spermatozoon in most cases [5-7]. Also, despite the fact that most molar pregnancies are diploid or triploid, they are quite frequently associated with molar pregnancies with numerical and structural

anomalies, or with a twin pregnancy, where the second fetus develops normally [8].

Thus, the establishment of a marker by immunohistochemical investigations could influence the accuracy of the morphopathological diagnosis in molar pregnancies. The protein p57kip2 (p57) is expressed in pregnancies with non-molar, pseudomolar choriovillary phenotype and is not expressed in complete molar pregnancies [9, 10]. A series of studies using p57 protein demonstrate its effectiveness in identifying the complete molar profile (by negative immunoexpression in the germinal compartment) vs partial hydatidiform mole, evaluated with positive p57 expression in most cases [11]. Therefore, the aim of the study was the differential evaluation of p57 immunoexpression in the trophoblastic germinal compartment in molar versus non-molar pregnancies.

Material and methods

The tissue samples were taken from the material obtained after medical abortion from 15 patients with short-term pregnancies (3-12 weeks) in the Mother and Child Institute, Perinatal Center of level III, during 2019-2021. All the samples were diagnosed as hydatidiform mole (group I). The age of the patients in this group varied between 17-47 years (28.4±9.36). All patients were previously examined by ultrasound and in 5 cases the molar ultrasound character was established.

The control group (group II) included the material taken from the germinal sac of pregnancies solved on social indications (SA) from 8 patients, aged between 22-40 years (30.5±5.6) and pregnancies solved on medical indications (MA) (16 patients) in the short term (with the diagnosis of spontaneous abortion or stagnant pregnancy, in the presence of hydropic and/or dysplastic morphopathological lesions), age between 23-41 years (31.3±6.7). Clinical data were obtained from each patient's medical records. The current research is part of a larger study of disordered early-term pregnancies.

Primary processing. The tissue material was collected fastly at the Obstetrics Department after the medical intervention, with rapid fixation in 10% formalin (pH 7.2-7.4) to reduce the risk of early lysis of tissue material and growth of bacterial flora. The time of fixation in formalin was no more than 24 hours. The paraffin embedding system was DP500/CIT2002 (Bio-Optica, Italy). Histochemical and histological processing of the samples was performed on the histoprocessor "TISSUE-TEK, VIP 6AI" (Sakura, Japan), sectioning on the microtome HM325 (Thermoscientific) (USA). Sections with a thickness of 5 μm were placed on positively charged slides (APTACA, Italy).

Histological method. Sections were stained by the classical conventional hematoxylin-eosin (H.E) method, using Mayer's hematoxylin (HEMM-36/21, BIOGNOST, Slovenia) and eosin Y 1% (EOY10-35/21, BIOGNOST, Slovenia). Sections for HE were automatically stained with autostainer AUS-240, (Bio-Optica, Italy) and automatically mounted (TISSUE-TEK, ClasTM, Sakura, Japan). Appropriate sections (sufficient tissue material) were selected for immunohistochemical staining.

Immunohistochemical method. Immunohistochemical assays were performed using the manual procedures adopted for the anti-p57 antibody (clone 25B2, Novocastra Liquid Mouse Monoclonal Antibody for human p57 protein (Product code: NCL-L-p57: Leica Biosystems Newcastle Ltd, Newcastle, UK) with the application of the Novolink™MaxPolimer detection system, Leica, (RE7280-K) [12]. Details regarding the antibody can be found in Table 1. Deparaffinization was performed in two toluene baths (code UN1294, Sigma-Aldrich), 5 minutes each, followed by a mixed bath of toluene and alcohol 99.9% (code 06-10077F) for 5 minutes, then – 2 baths of absolute alcohol 99.9% with rehydration in distilled water. In order to unmask the epitopes, the sections were exposed to Na citrate solution, pH 6.0, in a water bath at 95°C-96°C, with a total pretreatment and posttreatment time of 60 minutes. Incubation of the sections with the primary antibody was followed by blocking of endogenous peroxidase by applying the Peroxidase-Blocking solution for 5 minutes, and DAB (3,3'-diaminobenzidine) was applied as a chromogenic substrate for 5 minutes. Nuclei were counterstained with Leica hematoxylin (RE7164). The final product of the reaction was colored brown with a nuclear pattern. Then, the panel of histological slides was subjected to the procedure of dehydration and clarification in absolute alcohol, one shot of mixed alcohol and toluene, and three shots of toluene, each exposure being 5 minutes. The final procedure was mounting the slides with BMC-100 solution. In the manual immunohistochemical staining procedure, the Sequenza™ Immunostaining Center was applied using the Thermo Shandon Coverplate.

Table 1. Antibody used: source, dilution, unmasking system, detection system, incubation time

Antibody / clone	Sourse / incubation time / dilution	Retrieval system / time	Detection / time
p57/25B2	Leica Biosystems Newcastle Ltd, Newcastle, UK / 30 min / 1:100	Na citrate solution, pH 6.0 / Water bath at a temperature of 95°C-96°C / 20 min	Novolink™-MaxPolimer, Leica / 20 min

Microscopic evaluation. The positive expression of p57 in the choriovillar and gestational deciduo-endometrial germinal compartment was determined based on nuclear staining in decidual cells and intermediate extravillous trophoblast (positive internal control). p57 immunopositivity was interpreted as satisfactory (negative) when choriovillary stroma and chorionic villus trophoblast cells were completely negative or showed nuclear immunoexpression in less than 10% of the cells, in the concomitant presence of the positive internal control. Chorionic villi and decidual plates from normal human placenta served as positive ex-

ternal control. The negative external control was represented by the liver (negative immunoreaction), being included in each research set. Cytoplasmic expression was considered non-specific. The quantification method was applied after Gupta et al. [13] and was performed with the Axio Imager A2 microscope (Carl Zeiss, Germany) equipped with an AXIOCam MRc5 recording camera.

Statistical analysis. The results of the study were stored in the Access 2007 database (Microsoft Office 2007). Statistical processing was performed using Winstat 2012.1 software (R. Titch Software, Bad Krozingen, Germany) The threshold value for statistically significant results was $p \leq 0.05$.

Results

The study was carried out on a batch of 15 cases of short-term disordered pregnancies with the morphopathological diagnosis of hydatidiform mole, the age of the patients varying between 17-47 years (28.4±9.3). Most of the patients were between 17 and 35 years old (11 cases/73.3%). In 3 cases/20% the age was greater than 35 years. The cases were classified based on the gestational period as follows: the group with the gestational period of 8 weeks (6/40.0% of cases), 9 weeks (4/26.7% of cases), 10 weeks (2/13.3% of cases), 7 and 12 weeks – 1 case each (6.66%). Data regarding age and gestational period were missing in 2 cases. During the primary investigation of the fetal conceptus from the group with disordered early-term pregnancies (basic group), it corresponded to type V fetal conceptus (molar-hidatiform fetal conceptus, MHFC) in 8 cases (53.3%) and was characterized by macroscopic multicystic lesions in the choriovilar germinal compartment, with variable sizes from 0.15 to 0.6 cm, with fluid-transparent content (fig. 1a). In the rest of the cases, the abortive product corresponded to the disorganized fetal concept of type VI (growth disorganized embryos, GDE), consisting of various categories of tissue plates (thickened and thinned), germinal sac (fragmented, mush-like) (fig. 1b). The volume of the abortive product was abundant in 100% of cases, with dimensions of 5.0x6.0x2.0cm, including the hemorrhagic component organized in blood clots. Embryo fragments were attested only in one case (6.66%).

In the control group, most patients were between 17 and 35 years (25 cases/80.6%) or older than 35 years (6/19.35%). The cases were classified based on the gestational period as follows: the group with a gestational period of 6-9 weeks –

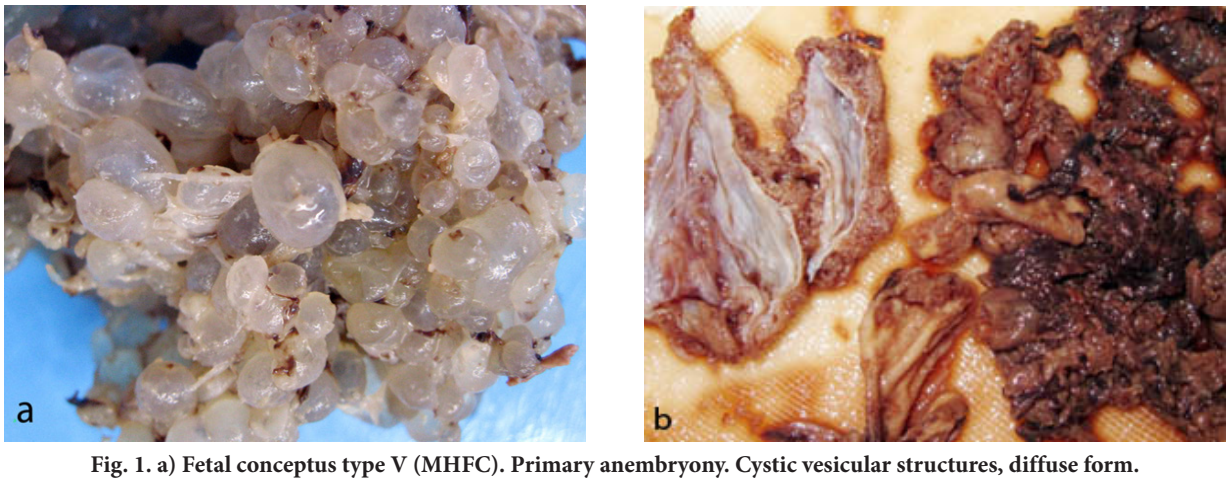

Fig. 1. a) Fetal conceptus type V (MHFC). Primary anembryony. Cystic vesicular structures, diffuse form. b) Fetal conceptus type VI (GDE). Secondary anembryony. Decidual and choriovillous tissue plates. Damaged germinal sac

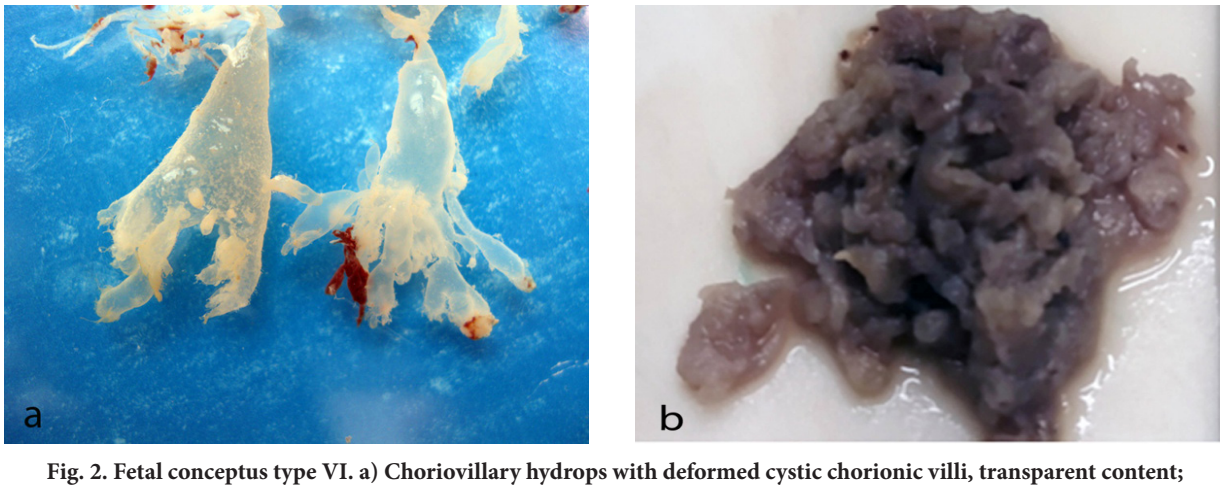

Fig. 2. Fetal conceptus type VI. a) Choriovillary hydrops with deformed cystic chorionic villi, transparent content; disordered dichotomous division; b) Mush-like appearance of the choriovillar product

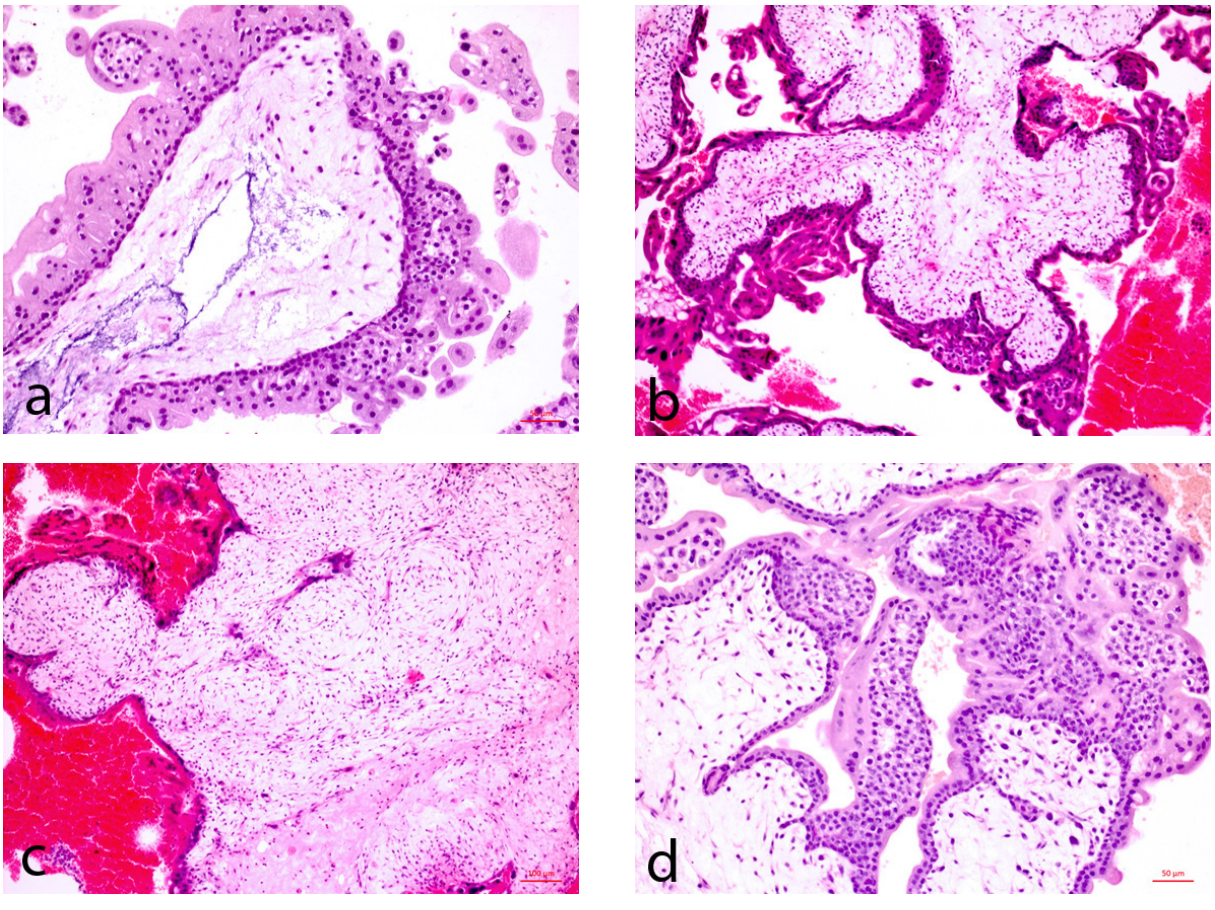

Fig. 3. Fetal conceptus type V (MHFC), complete type: a, d) Trophoblastic proliferation: mixed and cytotrophoblastic form; a, b) Stromal cystic structures with edema, hypo/hypercellularity; c) Stromal dysplasia with trophoblastic inclusions; a-d) Stromal anavascularization. HE, × 100, 400

22 cases (70.96%), and the group with a gestational period of 10-12 weeks – 9 cases (29.04%). During the primary investigation of the fetal conceptus obtained from 31 patients, in 21 cases (67.74%) the fetal conceptus was type VI (GDE), including embryo fragments in 5 cases (16.13%), and in 10 cases (32.25%) it had a mush-like appearance. The macroscopic peculiarities were mainly common, including a fragmented germinal sac, mush-like appearance, thinned and thickened tissue plates with various characters of expression, with or without embryo fragments. In some cases, lesions with a cystic appearance were associated, having variable sizes (from 0.4-1.9 cm) containing serous and transparent liquid (fig. 2). The volume of the abortive product was variable, predominantly abundant, including a hemorrhagic component in the form of blood clots or in a dispersed form with a mottled appearance.

When comparing the clinical diagnosis with the morphological one, in 33.3% of cases, the primary clinical diagnosis contained the notion of hydatidiform mole. In the rest of the cases, the clinical data were evaluated as endometrial gland hyperplasia or stagnant pregnancy.

By applying the complementary histological investigation by hematoxylin-eosin with the evaluation of histopathological lesions, the complete hydatidiform mole was observed in 8 cases (53.35%) out of 15 (fig. 3), and the partial one – in 7 cases (46.6%) (fig. 4).

In the group of early disturbed pregnancies (n=16), morphological lesions corresponding to the hydropic pattern at the level of the villous chorion were established in 10 cases (62.5%), and the dysplastic component – in 6 cases (37.5%) (fig. 5, 6).

Subsequently, all cases were subjected to immunostaining with anti-p57 (nuclear pattern), with the evaluation of two distinct compartments: germinal site (choriovilar) and gestational (deciduo-endometrial). In the molar group, the villous cytotrophoblastic site was positive in 7 cases (46.7%) and negative or <10% positive in 8 cases (53.3%) (fig. 7).

In the control group with pregnancies solved on social indications and or disordered at early term with hydropic and dysplastic stromal component, anti-p57 nuclear immunoexpression in the villous trophoblastic compartment was attested in 100% of cases (fig. 8).

In all cases, the internal positive control was attested in the region of the extravillous trophoblast, associated with the intense expression in the cells of the basal decidua (fig. 9 a, b). Hepatocytes served as external negative control (fig. 9 c).

Data analysis revealed statistically significant correlations of p57 expression in the following groups: CHM vs PHM ($p<0.003$), CHM and SA/MA ($p<0.001$). When analyzing the results of the given study, a series of correlations were found in relation to the age of the patient. This criterion correlated positively and statistically significantly with the term of gestation in the group of pregnancies with molar pathology: CHM ($rs=0.89$, $p<0.02$) and PHM

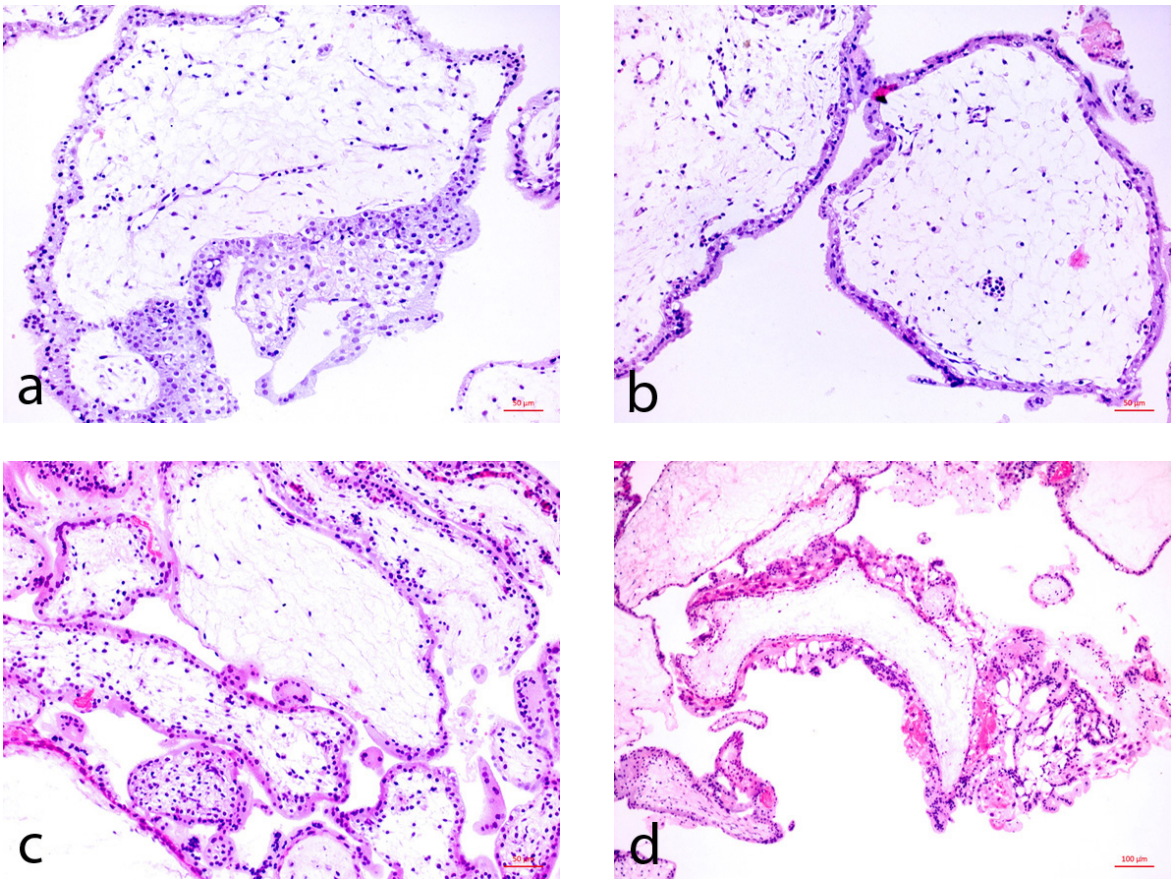

Fig. 4. Fetal conceptus type V (MHFC), partial type: a) Focal trophoblastic proliferation with anemic vascular component; b) Trophoblastic atrophy with absence of microvilli, vascular component with intravascular nucleated erythrocytes; c) Clusters of deformed villi with diverse stromal cellularity; d) chorionic villi with multifocal trophoblastic proliferation vs villi with acellular, hydropic stroma and trophoblastic atrophy. HE, × 100, 400

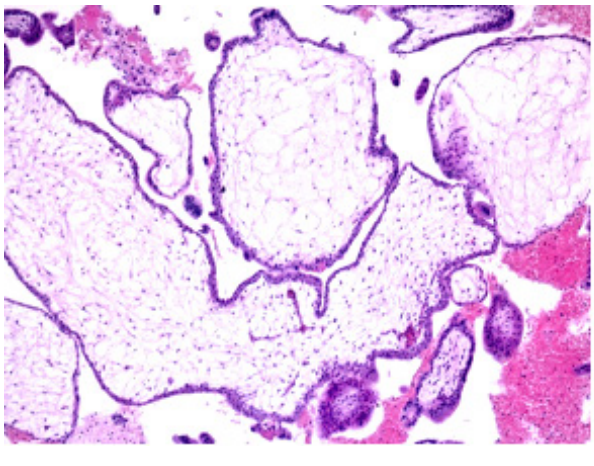

***Fig. 5.* Fetal conceptus type VI (GDE): Vilar hydrops. Hydropic/cystic choriovillar component. HE. × 100**

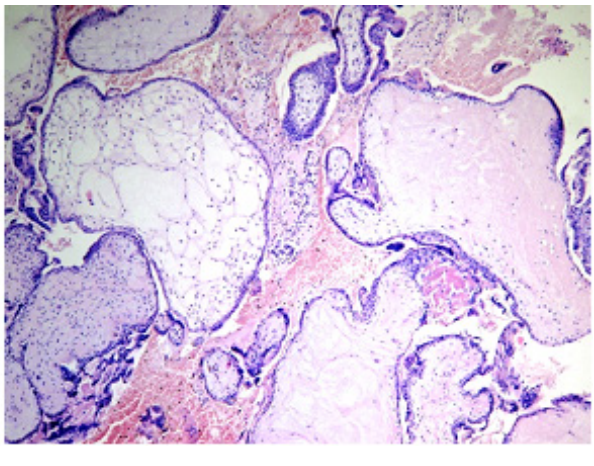

Fig. 6. Fetal conceptus type VI (GDE): Vascular stromal mesenchymal dysplasia. HE; × 100.

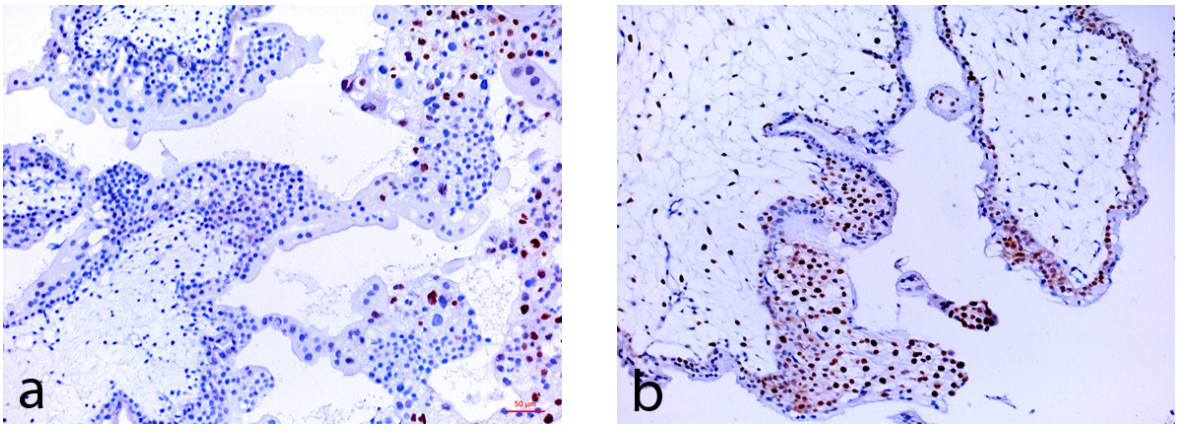

Fig. 7. Fetal conceptus type V (MHFC): a) CHM. Negative villous trophoblast immunoexpression. Intense nuclear immunoexpression in the extravillous trophoblast (internal control). Mixed cyto-syncytiotrophoblastic proliferation; b) PHM. Intense positive villous cytotrophoblast immunoexpression. Cytotrophoblastic proliferation. Immunoreaction for anti-p57, DAB

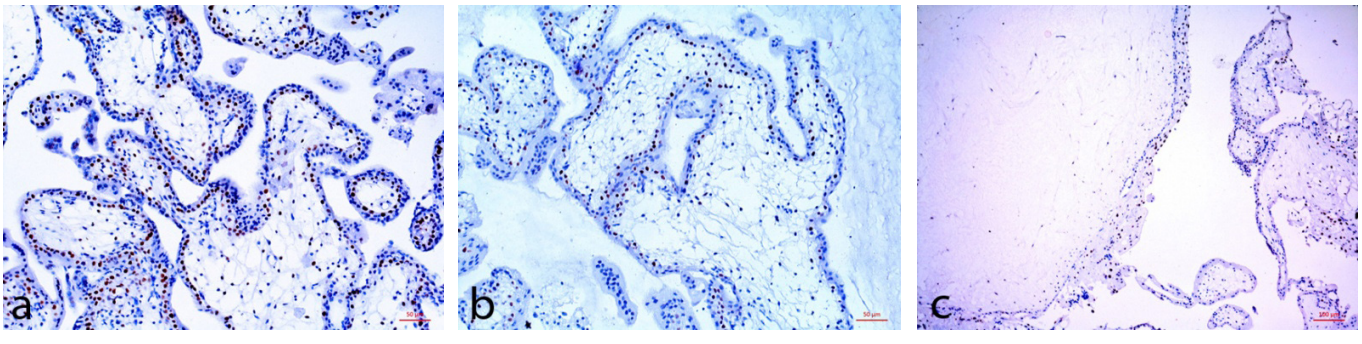

Fig. 8. Fetal conceptus type VI (GDE): a) Social abortion; b) Vilar hydrops; c) Mesenchymal dysplasia; Intense positive villous trophoblast immunoexpression. Immunoreaction for anti-p57, DAB

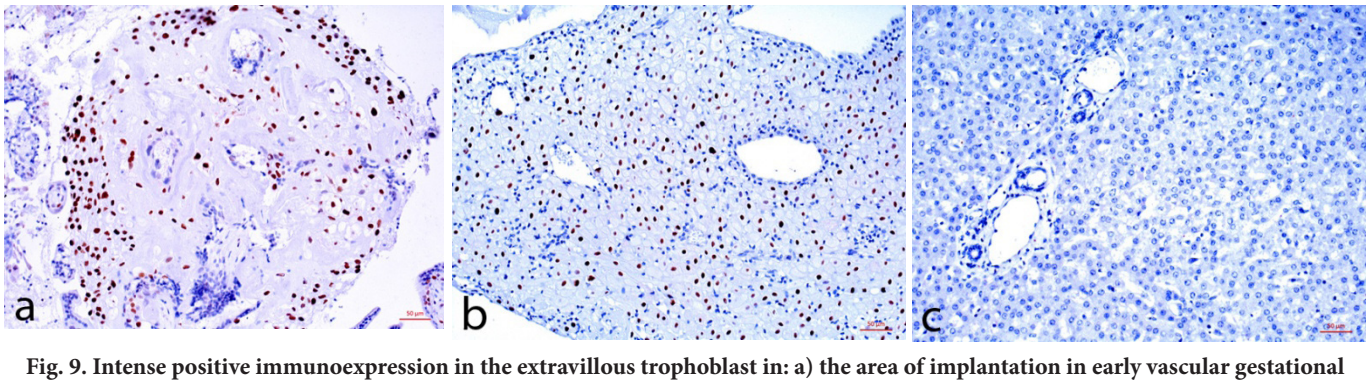

Fig. 9. Intense positive immunoexpression in the extravillous trophoblast in: a) the area of implantation in early vascular gestational conversion, b) the decidualocytes of a decidual plate (positive internal control); c) negative immunoexpression in hepatocytes (positive external control). Immunoreaction for anti-p57, DAB

(rs=0.75, p<0.04). The value of this marker, however, did not correlate statistically significantly in the group of control pregnancies and those that evolved with spontaneous abortion or stagnated in evolution (rs=0.17, p>0.28).

Discussion

Molar trophoblastic pathology represents a nosological entity describing an early placentation with choriovillary abnormalities of a proliferative and hydropic-cystic-malformative nature in the germinal compartment of the fetal conceptus in the case of abnormal fertilization. The histomorphological peculiarities are often confusing in establishing of the differential diagnosis of the molar pathology (CHM vs PHM) in the early period [3], because they also describe morphological lesions with a hydropic or cystic character [4].

Cytogenetic and ploidy analysis described the molar hydatidiform profile by several features. CHM is usually diploid and presents a 46XX karyotype and less often 46XY. Ocasionally, it can be tetraploid, including a small

percentage of cases with the biparental genome [7]. Androgenic origin is characterized by the lack of the maternal genome, as a result of the reduplication of a haploid paternal genome or being obtained by dispermatic fertilization. PHM presents as a triploid genome, in most cases with a 69XXX or 69XYY karyotype. The tetraploid genome includes a maternal and paternal haploid genome, paternal one being reduplicated as a result of dispermatic fertilization [6].

Thus, the evaluation of a marker through immunohistochemical investigations can influence the adjustment of the particularities of the morphopathological profile in molar pregnancies. In this context, the protein p57kip2 (p57) is the protein product of the paternally imprinted CDKN1C gene, the expression of which is associated with the presence of maternal DNA. It is present in pregnancies with a non-molar, pseudomolar choriovillous phenotype and absent in complete molar pregnancies [9, 10].

Kinara M. et al. (2005), Sasaki S. et al. (2015) highlight the impact of differential p57kip2 immunoreactivity in molar pathology of androgenic origin [14, 15].

In the present study it was possible to differentiate 2 forms of hydatidiform mole (CHM vs PHM) by evaluating the immunoexpression of p57 in the villous cytotrophoblast. It should be mentioned that p57 did not express at the site of the villous cytotrophoblast in all cases, which allowed to evaluate these pathological forms in the context of differential immunostaining. The results obtained in the given study are consistent with a series of studies according to which the complete hydatidiform mole does not contain a maternal genomic component, the application of the immunohistochemical reaction with p57 being important in the differential diagnosis of the molar pathology by indirectly identifying the presence of the maternal genome [16-18]. The authors mention that the application of the p57 protein demonstrates its effectiveness in identifying the complete molar profile by negative immunoexpression in the germinal compartment vis a vis the partial hydatidiform mole, which is p57 positive in most cases [11]. This divergent expression of p57 (positive or negative) in the germinal site of complete or partial hydatidiform mole denotes the loss or preservation of the maternal copy of the DNA [15]. In the systematic review and meta-analysis, Madi J. M. et al (2018) found a summary sensitivity of 0.984 (95% CI: 0.916-1.000) and a specificity of 0.625 (CI 95%: 0.503-0.736), with a curve diagnostic performance below 0.980 [19]. Ronnett B. M. (2018) indicates that the immunohistochemical evaluation of p57kip2 is practical and can be applied in histopathological practice as an adjunctive investigation in addition to the histomorphological one to help in the differential diagnosis of MHC [20].

When evaluating the statistical tests, significant differences were established in the groups between CHM vs PHM, CHM vs SA/MA, but not in PHM vs SA/MA, results that do not contradict with the literature data [21-25]. The given study highlighted that the majority of patients with the diagnosis of molar pathology were between 17 and 35 years old and the gestational period was within the limits of 6 to 9 weeks. Similar studies in the given field denote a minimal variability of the age interval [19].

In clinical practice, the differential evaluation of the hydatidiform molar profile is important. The most important reason for differentiating the subtypes of molar pathology in early terms is the possibility of the association of trophoblastic disease or choriocarcinoma [22]. Hydropic abortion is completely benign, while hydatidiform mole has a significant risk of transformation into persistent gestational trophoblastic disease, the incidence of which is higher in patients with complete hydatidiform mole (10-30%) vs patients presenting a partial molar form (0.5-5 %) [25].

Conclusions

Differential immunoexpression of p57 protein in the germinal cytotrophoblast allows subclassification of molar pathology into complete and partial form. It does not allow the differentiation between partial hydatidiform mole and non-molar lesions. Immunohistochemical evaluation of p57kip2 protein in molar and. non-molar pathology is useful in differential diagnosis as a complementary method.

References

1. Tse KY, Ngan HY. Gestational trophoblastic disease. Best Pract Res Clin Obstet Gynaecol. 2012;26(3):357-370. doi: 10.1016/j.bpobgyn.2011.11.009.
2. Golfier F, Clerc J, Hajri T. Contribution of referent pathologists to the quality of trophoblastic diseases diagnosis. Hum Reprod. 2011;26(10):2651-2658. doi: 10.1093/humrep/der265.
3. Fukunaja M, Katabuchi H, Nagasaka T, et al. Interobserver and intraobserver variability in the diagnosis of hydatiform mole. Am J Surg Pathol. 2005;29(7):942-947. doi: 10.1097/01.pas.0000157996.23059.c1.
4. Gersell D, Kraus F. Diseases of placenta. In: Kurman RJ, et al., editors. Blausteins pathology of the female genital tract. 6th ed. New York: Springer; 2011. p. 1000-1073.
5. Seckl MJ, Sebire NJ, Berkowitz RS. Gestational trophoblastic disease. Lancet. 2010;376:717-729. doi: 10.1016/S0140-6736(10)60280-2.
6. Slim R, Mehio A. The genetics of hydatiform moles: new lights on an ancient disease. Clin Genet. 2007;71(1):25-34. doi: 10.1111/j.1399-0004.2006.00697.x.
7. Van den Veyver IB, Al-Hussaini TK. Biparental hydatiform moles: a meternal effect mutation affecting imprinting in the offspring. Hum Reprod Update. 2006;12(3):233-242. doi: 10.1093/humupd/dmk005.
8. Sebire NJ, Foskett M, Paradinas FJ, et al. Outcome of twin pregnancies with complete hydatidiform mole and healthy co-twin. Lancet. 2002;359:2165-2166. doi: 10.1016/S0140-6736(02)09085-2.
9. Chilosi M, Piazzola E, Lestani M, et al. Differential expression of p57kip2 a maternally imprinted CDK inhibitor in normal human placenta and gestational trophoblastic disease. Lab Invest. 1998;78(3):269-276.
10. Ronnett BM, DeScipio C, Murphy KM. Hydatidiform moles: ancillary techniques to refine diagnosis. Int J Gynecol Pathol. 2011;30(2):101-116. doi: 10.1097/PGP.0b013e3181f4de77.
11. Banet N, DeScipio C, Murphy KM. Characteristics of hydatidiform moles: analysis of a prospective series with p57 immunohistochemistry and molecular genotyping. Mod Pathol. 2014;27(2):238-254. doi: 10.1038/modpathol.2013.143.

12. David V, Fulga V, Sinițîna L, Carpenco E, Cecoltan S, inventors. Protocolul tehnicii imunohistochimice manuale cu utilizarea anticorpului anti-p57, monoclonal antimouse, NCL-L-p57, clona 25B2, sistemul de detecție NovolinkTMMaxPolimer (RE7280-k) [Manual immunohistochemical technique protocol with the use of anti-p57 antibody, anti-mouse monoclonal, NCL-L-p57, clone 25B2, NovolinkTMMax-Polimer detection system (RE7280-k)]. Innovator certificate no. 5893.
13. Gupta M, Vang R, Yemelyanova A, et al. Diagnostic reproducibility of hydatidiform moles: ancillary techniques (p57 immunohistochemistry and molecular genotyping) improve morphologic diagnosis for both recently trained and experienced gynecologic pathologists. Am J Surg Pathol. 2012;36(12):1747-1760. doi: 10.1097/PAS.0b013e31825ea736.
14. Kihara M, Matsui H, Seki K, et al. Genetic origin and imprinting in hydatidiform moles. Comparison between DNA polymorphism analysis and immunoreactivity of p57kip2. J Reprod Med. 2005;50(5):307-312.
15. Sasaki S, Sasaki Y, Kunimura T, et al. Clinical usefulness of immunohistochemical staining of p57kip2. BioMed Res Int. 2015;2015:905648. http://dx.doi.org/10.1155/2015/905648.
16. Merchant SH, Amin MB, Viswanatha DS, et al. p57kip2 immunohistochemistry in early molar pregnancies: emphasis on its complementary role in the differential diagnosis of hidroic abortuses. Hum Pathol. 2005;36(2):180-186. doi: 10.1016/j.humpath.2004.12.007.
17. Fukunaga M. Immunohistochemical characterization of p57 (kip2) expression in early hydatiform moles. Hum Pathol. 2002;33(12):1188-1192. doi: 10.1053/hupa.2002.129421.
18. Castrillon DH, Sun D, Weremowicz S, et al. Discrimination of complete hydatiform mole from its mimics by immunohistochemistry of the paternally imprinted gene product p57kip2. Am J Surg Pathol. 2001;25(10):1225-30. doi: 10.1097/00000478-200110000-00001.
19. Madi JM, Braga A, Paganella MP, et al. Accuracy of p57kip2 compared with genotyping to diagnose complete hydatiform mole: a systematic review and meta-analysis. BJOG. 2018;125(10):1226-33. doi: 10.1111/1471-0528.15289.
20. Ronnett BM. Hydatiform moles: ancillary techniques to refine diagnosis. Arch Pathol Lab Med. 2018;142(12):1485-502. doi: 10.5858/arpa.2018-0226-RA.
21. Fisher RA, Lavery SA, Carby A, et al. What a difference an egg makes. Lancet. 2011;378(9807):1974. doi: 10.1016/S0140-6736(11)61751-0.
22. Berkowitz RS, Goldstein DP. Diagnosis and management of primary hydatidiform mole. Obstet Gynecol Clin North Am. 1988;15(3):491-503.
23. Soper JT. Gestational trophoblastic disease. Obstet Gynecol. 2006;108(1):176-87. doi: 10.1097/01.AOG.0000224697.31138.a1.
24. Banet N, DeScipio C, Murphy KM, et al. Characteristics of hydatiform moles: analysis of a prospective series with p57 immunohistochemistry and molecular genotyping. Mod Pathol. 2014;27(2):238-254. doi: 10.1038/modpathol.2013.143.
25. Madi JM, Braga AR, Paganella MP, et al. Accuracy of p57kip2 compared with genotyping for the diagnosis of complete hydatiform mole: protocol for a systematic review and meta-analysis. Syst Rev. 2016;5(1):169-175. doi: 10.1186/s13643-016-0349-7.

Authors' ORCID iDs and academic degrees
Valeriu David, MD, PhD, Associate Professor – https://orcid.org/0000-0001-9799-7369
Vergil Petrovici, MD, PhD, Associate Professor – https://orcid.org/0000-0001-8352-4202
Lilian Saptefrați, MD, PhD, Professor – https://orcid.org/0000-0003-2779-718X
Veaceslav Fulga, MD, PhD, Associate Professor – https://orcid.org/0000-0002-7589-7188
Ecaterina Carpenco, MD, PhD, Assistant Professor – https://orcid.org/0000-0003-1464-3149
Elena Frant, MD, PhD, Scientific Researcher – https://orcid.org/0000-0002-4223-3991

Authors' contributions
VD designed the study, conducted the laboratory work, interpreted the data, drafted the first manuscript; VP conducted the laboratory work, collected the material, interpreted the data; LS reviewed the manuscript; EC performed the laboratory work, interpreted the data; EF performed the laboratory work. All the authors reviewed and approved the final version of the manuscript.

Funding
This work was carried out as a part of the state project "Morphological approach by conventional, histo- and immunohistochemical methods of the peculiarities of the pathological profile of early placentogenesis in short-term disordered pregnancies". Project code 20.80009.8007.17.

Ethical approval and consent to participate
No approval was required for this study.

Conflict of interests
There are no conflicts of interest.

https://doi.org/10.52418/moldovan-med-j.65-2.22.02
UDC: 618.36-006.325+618.32+611.013

The expression of Ki-67 marker in the hydatidiform mole

[1,2]Ecaterina Carpenco, [1,3]Vergil Petrovici, [1,3]Lilia Sinitina, [1,2]Veaceslav Fulga, *[1,3]Valeriu David

[1]Laboratory of Morphology, [2]Department of Histology, Cytology and Embryology
Nicolae Testemitanu State University of Medicine and Pharmacy
[3]Department of Pathomorphology, Institute of Mother and Child, Chisinau, the Republic of Moldova

Authors' ORCID IDs, academic degrees and contributions are available at the end of the article

*Corresponding author – Valeriu David, email: valeriu.david@usmf.md
Manuscript received October 07, 2022; revised manuscript November 21, 2022; published online December 20, 2022

Abstract

Background: The hydatiform mole is charcaterized by a pathological proliferation of the trophoblast. Its evaluation could predict the progression to gestational trophoblastic neoplasia. The aim of the study was the analysis of the proliferative activity of the villous trophoblast in the molar vs non-molar lesions.
Material and methods: p-57 and Ki-67 were evaluated by immunohistochemistry in 15 cases of hydatidiform mole and 18 cases of abortions.
Results: The hydatidiform mole was divided based on the immunoexpression of anti-p57 into: complete (8 cases) and partial type (7 cases). The distribution score of Ki67 immunoreactivity in the villous cytotrophoblast was: complete mole: +3 – 8 cases; partial mole: +1 – 1 case, +2 – 3 cases, +3 – 3 cases; abortions on social indications: +1 – 6 cases, +2 – 9 cases; +3 – 2 cases. The mean and standard deviations were: 2.88±0.354; 2.29±0.756 and 1.82±0.728, respectively. The following statistical correlations were determined: complete vs partial mole ($p=0.014$), complete mole vs abortion ($p<0.01$) and overall cases of mole vs abortion ($p=0.000034$).
Conclusions: Villous cytotrophoblast proliferative activity is high in the complete hydatidiform mole, and the immunoreactivity distribution index is highly positive and statistically true in the molar versus non-molar group. Immunohistochemical evaluation of Ki-67 in molar pathology is useful in differential diagnosis as a complementary method.
Key words: hydatidiform mole, Ki-67, trophoblastic proliferation.

Cite this article
Carpenco E, Petrovici V, Sinitina L, Fulga V, David V. The expression of Ki-67 marker in the hydatidiform mole. *Mold Med J*. 2022;65(2):13-19. https://doi.org/10.52418/moldovan-med-j.65-2.22.02

Introduction

The hydatidiform mole, as a component of gestational trophoblastic disease, is categorized into two subtypes: complete hydatidiform mole (CHM) and partial hydatidiform mole (PHM). The maternal genetic component is present in the case of the partial form and absent in the case of the complete form [1]. CHM is a non-invasive placental disease characterized by hydropic, cystic deformations of the chorionic villi accompanied by pronounced trophoblastic proliferation. PHM comprises mainly two populations of chorionic villi: corresponding to the gestational age and villi with hydropic changes in the presence of expressed focal proliferative character [2, 3].

Complete molar, partial molar, as well as non-molar lesions in the germinal compartment are established during histomorphological examination and are frequently treated as inconclusive due to interobserver and intraobserver diagnostic variability. This lack of clarity in the diagnosis of early-term disturbed pregnancies with molar and non-molar profile is the result of the masking of morphological peculiarities in the choriovillary compartment [4, 5]. The histomorphological lesions are quite non-specific and do not facilitate the differential diagnosis in molar pathology, especially in the early period of evolution [6], considering also the association of hydropic and/or cystic stromal lesions [7].

The assessment of the risk of the development of persistent gestational trophoblastic disease and its subsequent management are affected by the variability of the diagnosis of histopathological lesions in early-term disturbed pregnancies, including molar pathology. Therefore the assessment of the trophoblastic epithelial proliferative profile has a priority importance in the diagnostic management. Thus, the elucidation of a marker for the differential diagnosis, together with the evaluation of the proliferative pattern, remains a subject for studies. A number of studies have shown the impact of paternally imprinted p57 gene expression in the differential diagnosis of molar vs non-molar pathology with incomplete differentiation [8, 9].

Ki-67 is a non-histone nuclear protein present in all active phases of the cell cycle, being virtually absent in quiescent G_0 cells. Ki-67 protein expression is strictly associated with cell proliferation, therefore it can be applied as a marker for dividing cells [10]. Therefore, the aim of the

study was to evaluate the proliferative activity of the villous trophoblast in the hydatidiform mole.

Material and methods

General characteristic. The study material was represented by the tissue samples obtained after medical abortion from 15 patients with short-term pregnancies (3-12 weeks) from the level III Perinatal Center, Mother and Child Institute, during 2019–2021, with the morphopathological diagnosis of hydatidiform mole. They were included in the L_I study group. The age of the patients was between 17-47 years with an average of 28.4±9.36 years. All the patients were examined by USG, in 5 cases morphological ultrasound aspects characteristic of molar hydatidiform structures were established.

The control material included tissue samples of the fetal conceptus taken after abortion on social indications/desire from 18 patients who constituted the control group (L_{II}). The age of the patients in this group was between 22-40 years with an average of 30.5±5.6 years. Clinical data were obtained from each patient's medical records. Specimens of liver were used for external negative control. The current research is the part of a larger study of disrupted early-term pregnancies.

The histological examination included the histoprocessing of tissue samples, the application of the usual histological method (hematoxylin-eosin) and the immunohistochemical method (anti-Ki67 and anti-p57) with the evaluation of microscopic features, as well as statistical processing.

Primary processing. The tissue material of the product of conception was collected at short term in obstetrics department with rapid fixation in 10% formalin solution, pH 7.2-7.4 to reduce the risk of early lysis of tissue material and superimposition of bacterial flora. The period of fixation in formalin solution was not more than 24 hours. The paraffin embedding system was DP500/CIT2002 (Bio-Optica, Italy). Histochemical and histological processing of the samples was performed on the histoprocessor „TISSUE-TEK, VIP 6AI" (Sakura, Japan), sectioning on the microtome HM325 (Thermoscientific) (USA). Sections with a thickness of 5 μm were spread on positively charged slides (APTACA, Italy).

Histological method. Sections were stained by the classical conventional hematoxylin-eosin (HE) method, using Mayer's hematoxylin (HEMM-36/21, BIOGNOST, Slovenia) and eosin Y 1% (EOY10-35/21, BIOGNOST, Slovenia). Sections for H&E were automatically stained with autostainer AUS-240, (Bio-Optica, Italy) and automatically mounted (TISSUE-TEK, ClasTM, Sakura, Japan). Appropriate sections (sufficient tissue material) were selected for immunohistochemical staining.

Immunohistochemical method. The immunohistochemical assays were performed by manually adapted operational procedures for two antibodies: anti-Ki67 (clone MIB-1, ready-to-use, FLEX, monoclonal mouse anti-human, Dako, IS626) and anti-p57 (clone 25B2, Novocastra Liquid Mouse Monoclonal Antibody for human p57 protein (Product code: NCL-L-p57: Leica Biosystems Newcastle Ltd, Newcastle, UK) with the application of 2 detection systems: EnVision™FLEX, high pH (K8000) [11] and Novolink™MaxPolimer, Leica (RE7280-K) [12]. The conventional immunohistochemical method was applied (Table 1). Deparaffinization was performed in two toluene baths (code UN1294, Sigma-Aldrich) of 5 minutes each, a mixed toluene and 99.9% alcohol bath (code 06-10077F) for 5 minutes, followed by 2 baths in 99.9% alcohol with rehydration in distilled water in 2 intakes of 10 minutes each.

Application of primary antibodies was preceded by exposure of tissue sections to Target Retrieval Solution, Flex, high pH (50x) (code DM828, Dako) for anti-Ki67 antibody and Na citrate solution, pH 6.0 for anti-p57. The exposure took place in a water bath at a temperature of 95°C-96°C of the unmasking solution, for 20 minutes, with a total pretreatment and posttreatment time of 60 minutes. Sections were incubated with primary antibodies for 30 minutes at room temperature. Endogenous peroxidase blocking was performed by applying Peroxidase-Blocking Solution for 5 minutes, and DAB (3,3'-diaminobenzidine) was applied as a chromogenic substrate for 5 minutes. Nuclei were counterstained with Mayer's hematoxylin (HEMM-36/21, BIOGNOST, Slovenia) when using the EnVision™FLEX detection system, high pH. In the case of the Novolink™MaxPolimer system, Leica hematoxylin (RE7164) was applied. The final product of the reaction was expressed by staining the nuclei in brown. Then, the panel of histological slides was subjected to the procedure of dehydration and clarification in 2 batches of absolute alcohol, one batch of mixed alcohol and toluene, and three batches of toluene, each exposure being 5 minutes. The final procedure consisted of mounting the slides with BMC-100 solution. In the manual immunohistochemical staining procedure, the Sequenza™ Immunostaining Center was applied using the Thermo Shandon Coverplate.

Microscopic evaluation. Ki67 (nuclear proliferation receptor) protein expression was analyzed in the chorionic villus compartment (trophoblastic epithelial component). The regions with the highest cell density and nuclear expression (hot-spots) were identified at x100 magnification.

Table 1. Antibodies used: source, dilution, unmasking system, detection system, incubation time

Antibody/ clone	Sourse/ incubation time/ dilution	Retrieval system/ time	Detection/ time
p57/ 25B2	Leica Biosystems Newcastle Ltd, Newcastle, UK/ 30 min/ 1:100	Na citrate solution, pH 6.0/ Water bath at a temperature of 95°C-96°C/ 20 min	Novolink™Max Polimer, Leica/ 20 min
Ki67/ MIB-1	Dako/ 30 min/ ready to use	Dako Target Retrieval Solution, high pH/ Water bath at a temperature of 95°C-96°C/ 20 min	EnVision™-FLEX, High pH/ 20 min

Subsequently, was counted the number of immunopositive cells per 100 cells from 3 fields of view at x400 magnification. Then was determined the value of the Ki-67 proliferation index (PI/ %), that represented the percentage of immunopositive cells vs the total number of cells. The following score was assigned: 0 – absent, weakly positive (+1 in <10% of cells), moderately positive (+2 in 10-50% of cells) and strongly positive (+3 in >50% of cells).

Positive expression of p57 in the choriovillary and gestational deciduo-endometrial germinal compartment was determined based on nuclear positivity in decidual cells, villous trophoblast and intermediate extravillous trophoblast (positive internal control). p57 immunopositivity was interpreted as satisfactory (negative) when choriovillary stroma and chorionic villus trophoblast cells were completely negative or showed nuclear immunoexpression in less than 10% of cells, in the concomitant presence of the positive internal control. Chorionic villi and decidual plaques from normal human placenta served as positive external controls. The negative external control was represented by the hepatocytes (negative immunoreaction), being included in each research group. In all research sites cytoplasmic expression was considered nonspecific. The quantification method was applied according to Gupta M. et al. [13]. Quantification of positive cells was performed with an Axio Imager A2 microscope (Carl Zeiss, Germany) equipped with an AXIOCam MRc5 recording camera.

Statistical methods. The study results were stored and grouped in the MS Excel 2010 database. Data analysis was performed using the SPSS program (SPSS Statistics 23.0; IBM, Chicago, IL, USA). Descriptive statistics were applied with the determination of the arithmetic mean (M) of the Ki67 values and the standard deviation (SD). Were also compared the values of Ki-67 PI in the L_I vs L_{II}, as well as inside the L_I (complete vs partial hydatiform mole) by applying the t test. The results were considered statistically significant at a $p<0.05$.

Results

The evaluation of the cases included in the L_I study group showed that the definite diagnosis of hydatidiform mole was established in 33.3% of cases. In 66.7% of cases, due to the predominance of hemorrhagic syndrome, the clinical diagnosis was of endometrial glandular hyperplasia, ongoing pregnancy with spontaneous abortion or stagnant pregnancy.

Morphological examinations by usual methods of the abortive product in the early period in both groups determined 2 morphological types of fetal conceptus: type V – molar hydatidiform fetal conceptus (HMFC) and type VI – disorganized fetal conceptus (DFC) in various macroscopic variations of the material. In the material classified as type VI fetal concept, in 5 cases the predominantly mushy character was macroscopically attested (figure 1a-b).

Following the application of the anti-p57 antibody, according to the particularities of the immunomorphological profile attested at the site of the villous trophoblast (negative or positive immunoreaction from the villous cytotrophoblast), two subtypes of hydatidiform mole were deciphered: complete hydatidiform mole – 7 cases (46.7%) and partial hydatidiform mole – 8 cases (53.3%) (fig. 2). In all cases studied, the extravillous trophoblast was analyzed for the internal positive control, together with the intense expression in the decidual cells (fig. 3a). The hepatocytes that did not present a positive immunoreaction served as an external negative control (fig. 3b).

Later, the cases were analyzed in terms of the proliferative character of the villous trophoblastic epithelium, expressed by the Ki67 proliferation index (PI). The numerical values and their distribution in relation to the hydatidiform mole subtypes and the control group are elucidated in table 1.

According to the results, the maximum immunoexpression of the anti-Ki67 reaction at the level of the villous cytotrophoblast was attested in the group with molar pathology, the values of the complete molar subtype being

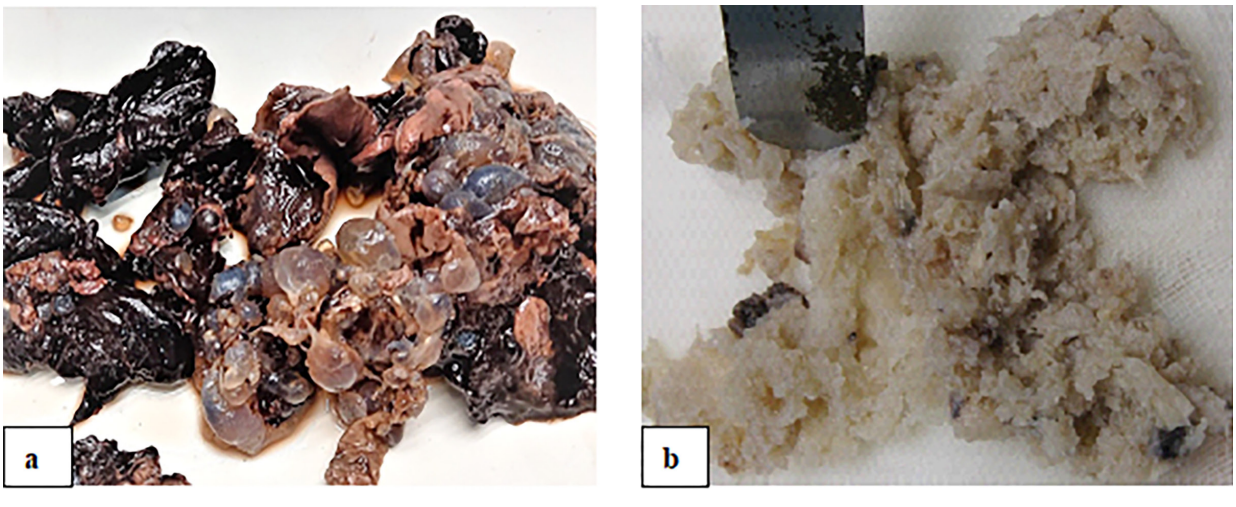

Fig. 1. Macroscopic features of the fetal concept: a) Molar aspect of the germinal sac in abortion with brown and hemorrhagic changes of the decidual plaques (HMFC); b) The mushy aspect of the disintegrated conceptus in medical abortion (DFC)

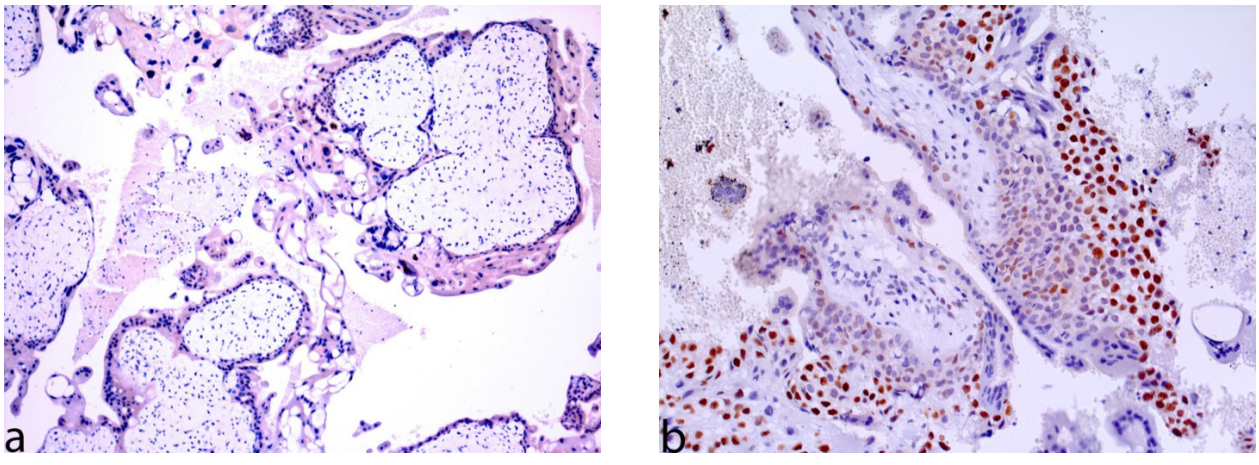

Fig. 2. Hydatidiform mole. a) CHM: Negative immunoexpression of villous trophoblast; b) PHM: Positive immunoexpression of villous trophoblast. Immunoreaction for anti-p57, DAB, × 100, 200

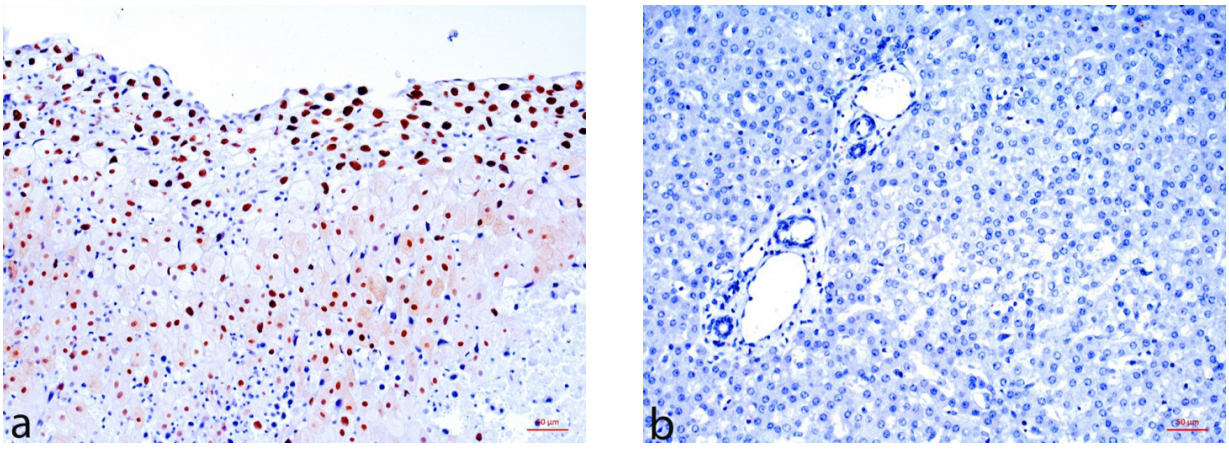

Fig. 3. a) Intense positive immunoexpression of p57 in decidual cells and extravillous trophoblast (positive internal control); b) negative imunoexpression in hepatocytes (positive external control). Immunoreaction for anti-p57, DAB, × 200

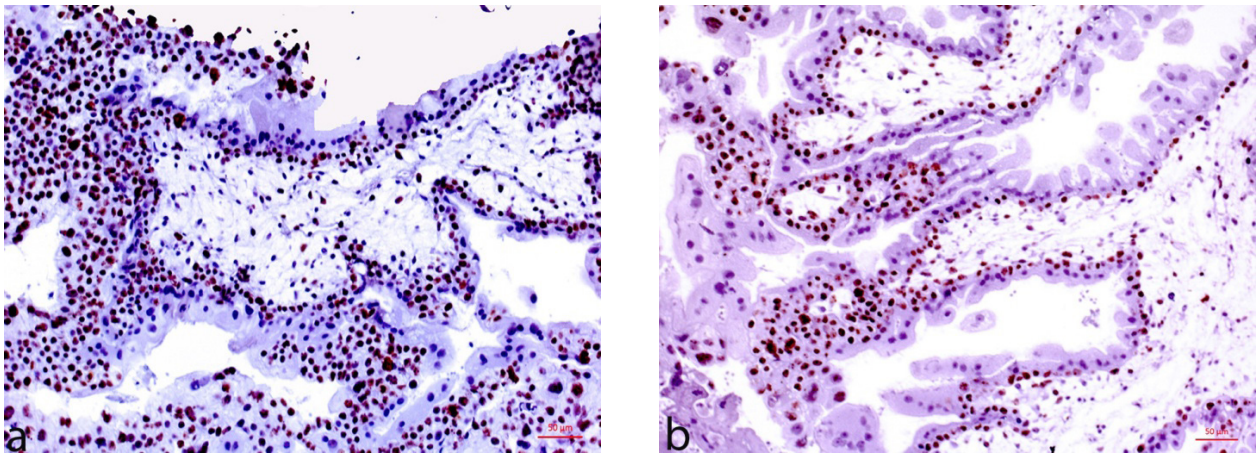

Fig. 4. CHM (a, b). Positive immunoexpression in the villous trophoblast. Mitotic activity with pronounced cytotrophoblastic proliferation. Distribution score +3. Immunoreaction for anti-Ki67, DAB, × 200

clearly superior both inside the group and also in relation to the abortion group. Immunoreactivity in the syncytiotrophoblast was not attested. The distribution of Ki67 immunoreactivity in the studied groups is reflected in table 2.

In the CHM group, the score was a maximum of +3 in 100% of cases (fig. 4). In PHM, equal values of +3 and +2 scores were attested (42.9% each) and only one case (14.2%) of a weak positive (+) immunoexpression (fig. 5). In the overall molar pathologies, the maximum score of +3

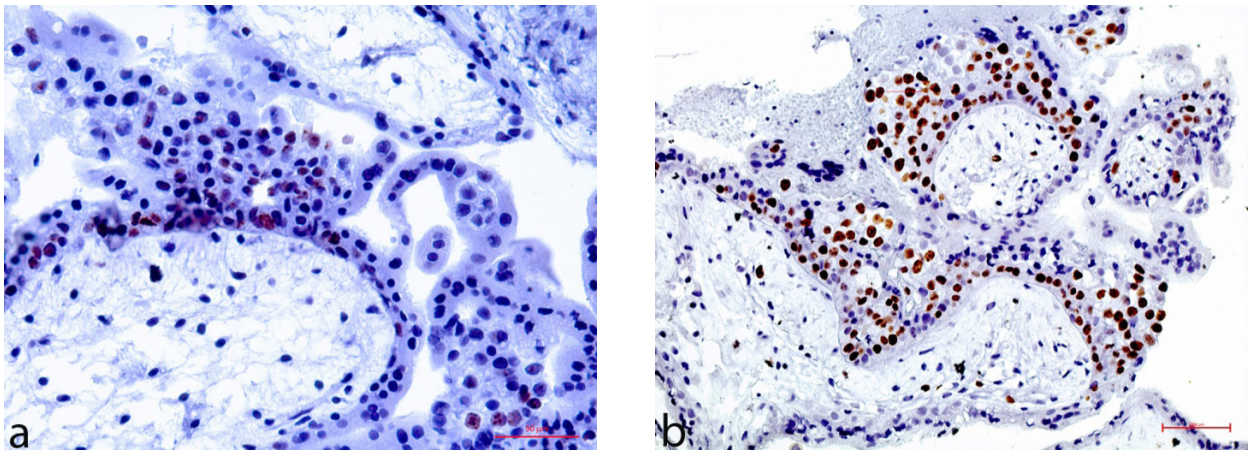

Fig. 5. PHM (a, b). Positive immunoexpression in the villous trophoblast. Distribution score: a) +2; b) +3. Focal proliferation. Immunoreaction for anti-Ki67, DAB, × 400, 200

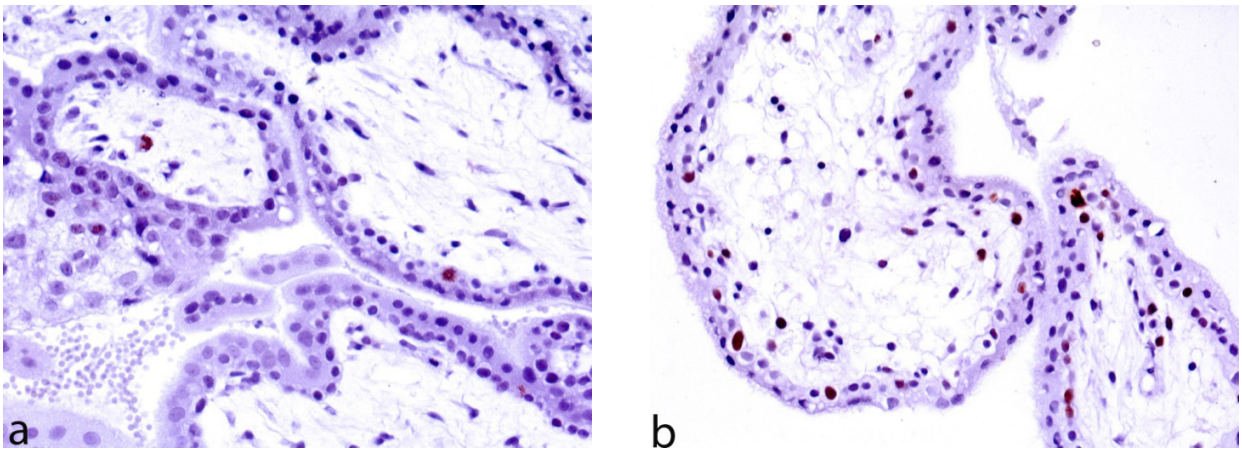

Fig. 6. Abortion on social indications/ desire (a, b). Positive immunoexpression in the villous trophoblast. Distribution score: a) +1; b) +2. Focal proliferation. Immunoreaction for anti-Ki67, DAB, × 400

Table 1. Mean value and standard deviation (M±SD) of the Ki67 marker in relation to the study group

Study group	Ki67 (PI)	
	Villous cyto-trophoblast	Villous syncytio-trophoblast
	M±SD	M±SD
CHM	87.25±4.59	0±00
PHM	48.71±29.66	0±00
HM (total)	69.26±27.99	0±00
AS/D	25.05±20.84	0±00

Table 2. Distribution of Ki67 immunoreactivity (%)

Study group	Cytotrophoblast/ score				Syncytiotrophoblast / score			
	0	+	++	+++	0	+	++	+++
CHM	-	-	-	8	-	-	-	-
PHM	-	1	3	3	-	-	-	-
HM (total)	-	1	3	11	-	-	-	-
AS/D	-	6	9	2	-	-	-	-

Note: „0" – absent immunoexpression; „+" weakly positive (<10%), „++" moderately positive (10-50%), „+++" strongly positive (>50%)

was attested in 11 cases, +2 in 3 cases and +1 in one case. When evaluating the distribution of immunoreactivity in the control group, the +2 score (9 cases/52.9%) was dominant, followed by the +1 score (6 cases/35.3%) and the +3 score (2 cases/11.7%) (fig. 6). The mean and standard deviations were: 2.88±0.354; 2.29±0.756 and 1.82±0.728, respectively

At the same time, when analyzing the obtained results, a coincidence of Ki67 immunoreactivity was observed in the following groups: CHM/ PHM/ AS/D in case of +3 score, PHM/ AS/D in case of +2 score and PHM/ AS/D in case of +1 score.

The mean values of Ki67 PI in each study group can be found in the table 3.

To test the hypophysis that each morphological entity was associated with statistically significant different mean values of Ki67 PI, a t-test was performed. The following statistical correlations were found: MHC vs MHP ($t_{15,71}$=3,402, p=0,014), MHC vs AS/D ($t_{13,16}$=11,71, p<0,01) and mole vs AS/D ($t_{1,64}$=5,105, p=0,000034).

Table 3. The mean values of Ki67 PI

	MD	N	Mean	Std. Deviation
Ki67citovPI	CHM	8	87.2500	4.59036
	PHM	7	48.7143	29.66319
Ki67citovPI	CHM	8	87.2500	4.59036
	AS/D	17	25.0588	20.84907
Ki67citovPI	PHM	7	48.7143	29.66319
	AS/D	17	25.0588	20.84907
Ki67citovPI	mole	15	69.2667	27.99354
	AS/D	17	25.0588	20.84907

Note: citov – cytovillous, PI – proliferative index, MD – morphological diagnosis, N – number of cases, CHM – complete hydatiform mole, PHM – partial hydatiform mole, mole – overall cases of hydatiform mole (CHM+PHM), AS/D – abortion on social indications/desire.

Discussion

Hydatidiform mole (HM) represents a heterogeneous group of lesions characterized by trophoblastic proliferative and hydropic-cystic choriovillary abnormalities in the germinal compartment, caused by abnormal fertilization. The differentiation of the two forms (subtypes) of HM is possible by cytogenetic analysis and based on ploidy. The 46XX karyotype, less often 46XY and very rarely the tetraploid for CHM were appreciated. In the case of PHM, a triploid genome (69XXX or 69XYY karyotype) or tetraploid consisting of a maternal and paternal haploid genome were determined, the latter reduplicated as a result of bisperm fertilization [14, 15]. This differentiation is of major importance in clinical management, a fact determined by the increased risk of persistence of trophoblastic disease or evolution into choriocarcinoma [16], patients presenting CHM being more frequently affected [17].

For the purpose of distinguishing the molar profile, the literature mentions the application of differential immunoreactivity of p57kip2 [18, 19], which is the product of the paternally imprinted CDKN1C gene, the expression of which is associated with the presence of maternal DNA [9]. According to data from the literature, as well as received results, by immunohistochemical investigation of the product of conception taken in early terms of short-term dysregulated pregnancies, by evaluating the immunoexpression of p57 in the villous cytotrophoblast, it was possible to distinguish two evolutionary subtypes of HM: complete and partial. At the same time, when evaluating the statistical tests, significant differences were established in the CHM vs PHM, CHM vs AS/AM groups, but not in the PHM vs AS/AM groups, results that do not contradict the literature data [20, 21].

Complete, partial, and non-molar molar lesions in the germinal compartment are established during histomorphological examination and frequently treated as inconclusive due to interobserver and intraobserver variability. This inconclusiveness in the differential diagnosis of the molar and non-molar profile is the result of the lack of certain morphological peculiarities in the choriovilar compartment [4, 5] and frequently presents diagnostic difficulties in the early period of pregnancy [6]. The evaluation of the trophoblastic epithelial proliferative profile has a priority importance in the diagnostic management, thanks to the variable deciphering of the histopathological lesions in early-term pregnancies, and thanks to the impact on the clinical management. Thus, the elucidation of an applicative marker for differential diagnosis, together with the evaluation of the proliferative pattern, remains a subject for studies.

Ki67 is a non-histone nuclear protein present in all active phases of the cell cycle, being virtually absent in quiescent (G_0) cells. Ki-67 protein expression is strictly associated with cell proliferation, therefore it can be used to determine dividing cells [10]. According to the bibliographic data, being a marker of proliferative activity, the expression of the Ki67 oncogene can also be applied in trophoblastic disease, including HM subtypes, with predictive value for the progression to a gestational trophoblastic neoplasia [22].

In the presented study, Ki67 immunoexpression was limited to villous cytotrophoblast, syncytium being negative. Ki67 expression in stromal cells was in most cases limited to a score of +1 in the group of abortions on social indications/ desire and a moderate score of +2 for molar pathology. The given results are in accordance with a series of studies, which denote the accentuated and differentiated immunoexpression in the villous cytotrophoblastic compartment [24]. The obtained data do not contradict the literature data. They denote the presence of different expression of Ki67 in molar and non-molar pathology, as well as in the CHM and PHM subtypes [23-25].

The histopathological features described in the literature as morphological criteria for differentiating molar and non-molar pathology remain uncertain due to interobserver and intraobserver variability. This discrepancy may also be determined by various technical factors, protocols and examination techniques, polymorphic tissue material. Overall, the immunohistochemical investigation by applying the anti-Ki67 antibody comes in handy as a complementary method in the differential diagnosis of molar pathology in early-term pregnancies.

Conclusions

Villous cytotrophoblast proliferative activity is high in the complete hydatidiform mole, and the immunoreactivity distribution index is highly positive and statistically true in the molar versus non-molar group. Immunohistochemical evaluation of Ki-67 protein in molar pathology is useful in differential diagnosis as a complementary method.

References

1. Lai CY, Chan KY, Khoo HY, et al. Analysis of gestional trophoblastic disease by genotyping and chromosome in situ hybridization. Mod Pathol. 2004;17(1):40-8. doi: 10.1038/modpathol.3800010.
2. Tham BWL, Everard JE, Tidy JA, et al. Gestational trophoblastic disease in the Asian population of Northern England and North Wales. BJOG. 2003;110(6):555-9.
3. Smith HO, Kohorn E., Cole LA. Choriocarcinoma and gestational trophoblastic disease. Obstet Gynecol Clin North Am. 2005; 32(4):661-84. doi: 10.1016/j.ogc.2005.08.001.
4. Tse KY, Ngan HY. Gestational trophoblastic disease. Best Pract Res Clin Obstet Gynaecol. 2012;26(3):357-370. doi: 10.1016/j.bpobgyn.2011.11.009.
5. Golfier F, Clerc J, Hajri T. Contribution of referent pathologists to the quality of trophoblastic diseases diagnosis. Hum Reprod. 2011;26(10):2651-2658. doi: 10.1093/humrep/der265.
6. Fukunaja M, Katabuchi H, Nagasaka T, et al. Interobserver and intraobserver variability in the diagnosis of hydatiform mole. Am J Surg Pathol. 2005;29(7):942-947. doi: 10.1097/01.pas.0000157996.23059.c1.
7. Gersell D, Kraus F. Diseases of placenta. In: Kurman RJ, et al., editors. Blausteins pathology of the female genital tract. 6th ed. New York: Springer; 2011. p. 1000-1073.
8. Chilosi M, Piazzola E, Lestani M, et al. Differential expression of p57kip2 a maternally imprinted CDK inhibitor in normal human placenta and gestational trophoblastic disease. Lab Invest. 1998;78(3):269-276.
9. Ronnett BM, DeScipio C, Murphy KM. Hydatidiform moles: ancillary techniques to refine diagnosis. Int J Gynecol Pathol. 2011;30(2):101-116. doi: 10.1097/PGP.0b013e3181f4de77.
10. Scholzen T, Gerdes J. The Ki-67 protein: from the known and the unknown. J Cell Physiol. 182;(3):311-322. doi: 10.1002/(SICI)1097-4652(200003)182:3<311::AID-JCP1>3.0.CO;2-9.
11. David V, Petrovici V, Siniţîna L, Şaptefraţi L, Marin N, inventors. Protocolul tehnicii IHC manuale cu utilizarea anticorpului Ki-67, clona MIB-1, sistemul de vizualizare EnVision™FLEX [Manual IHC technique protocol using Ki-67 antibody, MIB-1 clone, EnVisionTM-FLEX visualization system]. Innovator certificate No 5866. Romanian.
12. David V, Fulga V, Siniţîna L, Carpenco E, Cecoltan S, inventors. Protocolul tehnicii imunohistochimice manuale cu utilizarea anticorpului anti-p57, monoclonal antimouse, NCL-L-p57, clona 25B2, sistemul de detecţie Novolink™MaxPolimer (RE7280-k) [Manual immunohistochemical technique protocol with the use of anti-p57 antibody, anti-mouse monoclonal, NCL-L-p57, clone 25B2, Novolink-TMMaxPolimer detection system (RE7280-k)]. Innovator certificate No 5893. Romanian.
13. Gupta M, Vang R, Yemelyanova A, et al. Diagnostic reproducibility of hydatiform moles: ancillary techniques (p57 immunohistochemistry and molecular genotyping) improve morphologic diagnosis for both recently trained and experienced gynecologic pathologists. Am J Surg Pathol. 2012;36(12):1747-1760. doi: 10.1097/PAS.0b013e31825ea736.
14. Van den Veyver IB, Al-Hussaini TK. Biparental hydatiform moles: a maternal effect mutation affecting imprinting in the offspring. Hum Reprod Update. 2006;12(3):233-242. doi: 10.1093/humupd/dmk005.
15. Slim R, Mehio A. The genetics of hydatiform moles: new lights on an ancient disease. Clin Genet. 2007;71(1):25-34. doi: 10.1111/j.1399-0004.2006.00697.x.
16. Berkowitz RS, Goldstein DP. Diagnosis and management of primary hydatidiform mole. Obstet Gynecol Clin North Am. 1988;15(3):491-503.
17. Soper JT. Gestational trophoblastic disease. Obstet Gynecol. 2006;108(1):176-87. doi: 10.1097/01.AOG.0000224697.31138.a1.
18. Kihara M, Matsui H, Seki K, et al. Genetic origin and imprinting in hydatidiform moles. Comparison between DNA polymorphism analysis and immunoreactivity of p57kip2. J Reprod Med. 2005;50(5):307-312.
19. Sasaki S, Sasaki Y, Kunimura T, et al. Clinical usefulness of immunohistochemical staining of p57kip2. BioMed Res Int. 2015;2015:905648. http://dx.doi.org/10.1155/2015/905648.
20. Banet N, DeScipio C, Murphy KM. Characteristics of hydatidiform moles: analysis of a prospective series with p57 immunohistochemistry and molecular genotyping. Mod Pathol. 2014;27(2):238-254. doi: 10.1038/modpathol.2013.143.
21. Madi JM, Braga AR, Paganella MP, et al. Accuracy of p57kip2 compared with genotyping for the diagnosis of complete hydatiform mole: protocol for a systematic review and meta-analysis. Syst Rev. 2016;5(1):169-175. doi: 10.1186/s13643-016-0349-7.
22. Hasanzadehy M, Sharifi N, Esmaieli H, Daloe MS, Tabari A. Immunohistochemical expression of the proliferative marker Ki67 in hydatidiform moles and its diagnostic value in the progession trophoblastic neoplasia. J Obstet Gynecol Res. 2013;39(2):572-7. doi: 10.1111/j.1447-0756.2012.01981.x.
23. Khooei A, Atabaki P, Fazel A, et al. Ki-67 expression in hydatiform moles and hydropic abortions. Iran Red Crescent Med J. 2013;15(7):590-594. doi: 10.5812/ircmj.5348.
24. Schammel DP, Bocklage T. p53 PCNA and Ki-67 in hydropic molar and non-molar placentas: imuunohistochemical study. Int J Ginecol Pathol. 1996;15(2):158-66. doi: 10.1097/00004347-199604000-00011.
25. Cheville JC, Robinson R, Benda JA. Evaluation of Ki-67 (MIB-1) in placentas with hidropic change and partial and complete hydatidiform mole. Pediatr Pathol Lab Med. 1996;16(1):41-50.

Authors' ORCID IDs and academic degrees
Ecaterina Carpenco, MD, PhD applicant, Assistant Professor – https://orcid.org/0000-0003-1464-3149
Vergil Petrovici, MD, PhD, Associate Professor – https://orcid.org/0000-0001-8352-4202
Lilia Sinitina, MD, PhD, Associate Research – https://orcid.org/0000-0001-9646-8860
Veaceslav Fulga, MD, PhD, Associate Professor – https://orcid.org/0000-0002-7589-7188
Valeriu David, MD, PhD, Associate Professor – https://orcid.org/0000-0001-9799-7369

Authors' contributions
EC designed the study, performed the laboratory work, interpreted the data; VP conducted the laboratory work, collected the material, interpreted the data; LS collected the material, interpreted the data; VF revised the manuscript; VD designed the study, conducted the laboratory work, interpreted the data, drafted the first version of the manuscript. All the authors reviewed and approved the final version of the manuscript.

Funding
This work was carried out within the framework of the state project "Morphological approach by conventional, histo- and immunohistochemical methods of the peculiarities of the pathological profile of early placentogenesis in short-term dysregulated pregnancies". Project number 20.80009.8007.17.

Ethical approval and consent to participate. No approval was required for this study.
Conflict of interests. Nothing to declare.

DOI: https://doi.org/10.52418/moldovan-med-j.65-2.22.03
UDC: 616.72-018.3-089.844-092.9

Joint cartilage experimental defect regeneration by hierarchic biphasic combined grafts

***Vitalie Cobzac, Mariana Jian, Tatiana Globa, Viorel Nacu**

Laboratory of Tissue Engineering and Cellular Culture
Nicolae Testemitanu State University of Medicine and Pharmacy, Chisinau, the Republic of Moldova

Author's ORCID iD, academic degrees and contribution are available at the end of the article

*Corresponding author – Vitalie Cobzac, e-mail: vitalie.cobzac@usmf.md
Manuscript received October 03, 2022; revised manuscript December 02, 2022; published online December 20, 2022

Abstract

Background: The existing surgical techniques used to regenerate articular cartilage fail. Utilisation of hierarchical, biphasic structures obtained from osteochondral tissue, through demineralisation, decellularization, longitudinal perforation and combination with chondroprogenitor cells, presents a high potential in cartilage defects regeneration.
Material and methods: The research was performed on 36 rabbits, separated equally in two experimental and one control group. In the experimental groups, the experimental osteochondral defects of 4-4.5 mm in depth, were performed with a 3.7 drill bit at the level of weight bearing surface of the medial femoral condyle. In the 1st group the defects were treated with grafts combined with autologous chondrocytes, and in the 2nd group with grafts combined with autologous mesenchymal stem cells. In the control group, cartilaginous defects were treated by transferring the osteochondral plugs taken from the trochlear groove. The rabbits were removed from the experiment at 6 and 12 weeks. The results were evaluated by Unified Histological Score of Regenerated Cartilage (UHSRC).
Results: At 6 weeks, according to UHSRC, the 1st group had 28.33±1.53 points, the 2nd group –27.67±2.08 points and the control group –26.33±1.53 points ($p>0.1$; $p>0.2$). At 12 weeks the 1st group had 18.68±5 points, the 2nd group –14.89±3.76 points and the control group –17.22 ±4.84 points ($p>0.5$; $p>0.2$).
Conclusions: According to UHSRC, the experimental groups don't show a significant difference compared to the control group at 6 and 12 weeks, also the quality of regenerated cartilage is poor.
Key words: cartilage, regeneration, biphasic hierarchic graft, chondroprogenitor cells, unified histological score.

Cite this article
Cobzac V, Jian M, Globa T, Nacu V. Joint cartilage experimental defect regeneration by hierarchic biphasic combined grafts. *Mold Med J.* 2022;66(2):20-29. https://doi.org/10.52418/moldovan-med-j.65-2.22.03.

Introduction

Articular cartilage is a tissue with a very poor regenerative capacity, and in the case of large defects this is impossible [1-4]. The surgical treatment techniques used today mostly lead to the formation of fibrous or fibrocartilaginous tissue within the defect, with very low mechanical properties [2, 3, 5-7]. Combining of grafts obtained from synthetic or biological structures with various types of cells, seems to be an effective way to regenerate organs and tissues. There are several ways described in the literature to regenerate tissues and organs by combining three-dimensional matrices with various cells. Human amniotic membrane combined with bone marrow mesenchymal stem cells is used in the treatment of rabbit skin defects [8], combining of synthetic trachea obtained from polycaprolactone by 3D printing with bone marrow mesenchymal stem cells (BM-MSC), chondrocytes induced from pluripotent stem cells and human bronchial epithelial cells, to obtain a functional organ [9]. It is also known that biphasic blood vessels can be synthesized from polycaprolactone and type I collagen combined with smooth muscle cells and endothelial cells [10]. The combination of different three-dimensional monophasic structures obtained from collagen type I, I/III or atelocollagen type I with cells was also used to restore articular cartilage [7, 11].

As a result, the treatment methods with high perspective for articular cartilage regeneration, seem to be those that use multiphasic grafts combined with cells that have chondroprogenitor potential [3, 5, 12-15]. Utilization of hybrid structures, bi- or triphasic, obtained by mixing collagen with chitosan [5], with hyaluronic acid with or without chondroitin sulfate [12, 13, 16], with silk threads [17], and other non collagenic structures agarose [18], sodium alginate, gelatin [19], polycaprolactone [20] and others, are widely used in obtaining grafts that can be combined with mesenchymal stem cells (MSC) or chondrocytes with the aim of regenerating articular cartilage. The most of those three-dimensional matrices used in combination with chondroprogenitor cells are of synthetic origin, which tend to correspond to the specific properties of cartilage in order to be used in combination with MSC or chondrocytes [21, 22]. Elaboration of the graft that was used in the ex-

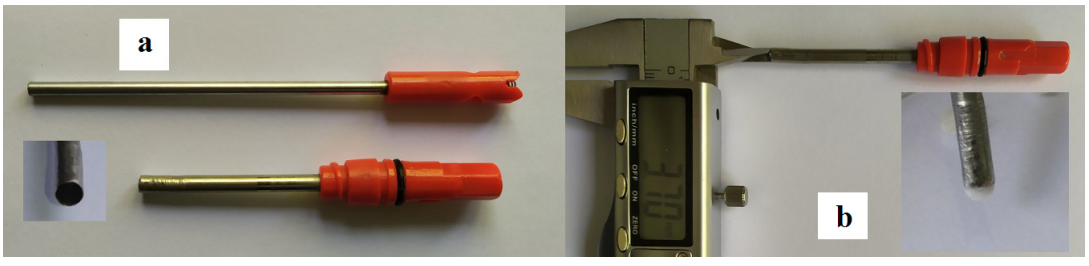

Fig. 1. The selfmade circular knife which was used to make circular sections of the grafts: (a) the device consists of circular knife and the trocar to push out the graft, (b) presentation of knife internal diameter and the device with a sectioned graft

periment from osteochondral tissue through demineralization, decellularization and longitudinal perforation [4], shows a high potential for utilization in combination with MSCs or chondrocytes for articular cartilage regeneration at the level of weight-bearing regions of the femoral condyle by creating favorable conditions that will protect the graft from deterioration after transplantation [6]. Since the graft is obtained of tissue with a biphasic, hierarchical structure [23], and the ability of cellular penetration and proliferation through it is ensured by its high degree of perforation, the use of such a graft seems to be reasonable. Also, the lack of immune response to decellularized bone and cartilage reduces the possibility of a graft rejection reaction, and its combination with autologous cells such as chondrocytes and bone marrow MSC could ensure the tissue remodeling process [24].

Material and methods

The *in vivo* experimental researches were carried out on 36 domestic rabbits with an average age of 4.5 ±0.5 months. The animals were divided into three groups, by 12 rabbits per group as follows:

- Group I – rabbits treated with osteochondral demineralised decellularized (OCDD) grafts combined with chondrocytes, consists of 4 males and 8 females, average weighing 3.52 ±0.42 kg;
- Group II – rabbits treated with OCDD grafts combined with MSC, consists of 7 males and 5 females, average weight 3.37 ±0.57 kg;
- Control group – rabbits treated with autologous osteochondral grafts, consists of 7 males and 5 females, average weight 3.52 ±0.62 kg.

There was no significant difference between the age, body mass and gender of the rabbits in the created experimental groups ($p > 0.2$).

Preparation of the hierarchic biphasic grafts

During the experiment 6 additional rabbits were sacrificed, from which were collected the distal femurs needed for grafts preparation. The collected distal femurs were stored in ultra-freezer (ULUF 450-2M, Arctiko) at -84°C until use. After removing the soft tissues from the distal femurs, they were demineralized in 0.6 M HCl [3, 4]. Then with a self-made circular knife (fig. 1) from the weight-bearing surface of each condyle, pieces of osteochondral tissues were sectioned with the diameter of 3.61 ±0.1mm and the height of 4.33 ±0.11mm, with the average volume of 44.05 ±1.15mm^3. The grafts were longitudinally perforated with a 23G syringe needle more than 120 times, degreased with 3% H_2O_2 (Eurofarmaco, the Republic of Moldova) for 24 hours and and with 70% alcohol (Eladum Pharma, the Republic of Moldova) for 6 hours by shaking at 200 rpm in a shaker-incubator (ES-20, Biosan).

The grafts were washed with distilled water by shaking 3 hours, the water was changed every hour, and decellularized in 1% sodium dodecyl sulphate (SDS) during 24 hours also by shaking at room temperature. After decellularization the grafts were washed with distilled water during 3 days, changing the water 2-3 times a day. In the laminar flow hood (LN 090, Nuve) the grafts were washed with 70% alcohol (Eladum Pharma, the Republic of Moldova) a few minutes. The graft sterilization was performed also with 70% alcohol in a laminar flow hood during 2 hours. Then, the sterilized grafts were washed with HBSS (Lonza, Belgium) for 24 h, changing the solution 3 times. The next day by 2-3 small strips of sterile gauze were inserted into the sterile 15 ml tubes, and the grafts by one were placed on the sterile gauze from the tubes. In order to dry the grafts, the test tubes were centrifuged at 4000 rpm for 20 minutes (Universal 32R, Hettich Zentrifugen), and then stored at -84°C (ULUF 450-2M, Arctiko) until use (fig. 2).

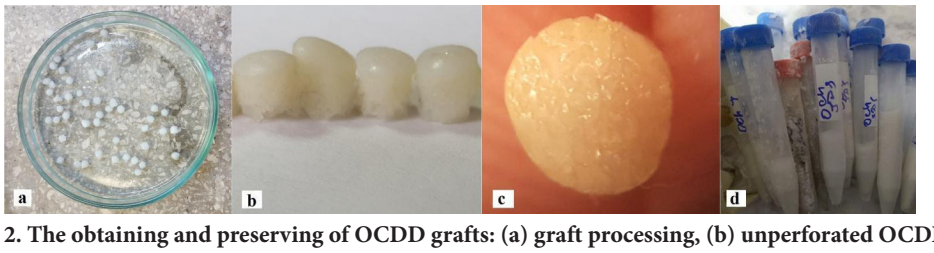

Fig. 2. The obtaining and preserving of OCDD grafts: (a) graft processing, (b) unperforated OCDD grafts, (c) longitudinally perforated OCDD graft, (d) OCDD grafts preserved at –84°C

The isolation of cells with chondroprogenitor potential

The necessary cells with chondroprogenitor potential to obtain the combined grafts were isolated according to the methods presented in previous publications carried out in the laboratory. MSCs were isolated by culture from rabbit bone marrow, which was collected into a heparinized syringe by aspiration under general anesthesia from the iliac bone [1, 25]. There were aspirated 4 ±1.2 ml of bone marrow. After centrifugation with concentration gradient HiSep 1077 (HiMedia, India), the mononuclear cell layer was extracted and washed in other 15 ml tube with HBSS (HiMedia, India) and cell culture media composed of DMEM/F-12 Ham (Sigma, UK) and FBS (Lonza, Belgium) and 1% antibiotic antimycotic solution (HiMedia, India). Then the cells were transferred to a 25 cm^2 cell culture flask (Nunc, Denmark) with 5 ml of cell culture media and incubated at 37°C, 5% CO_2, changing the media every 2-3 days until a 80-90% confluence.

Chondrocytes were isolated by enzymatic digestion of articular cartilage taken from one of knes under general anesthesia. The harvested cartilage pieces were digested with 0.6% collagenase using the continuous monitoring method [2], the process being stopped when the chondrocytes from the digested cartilage occupied the entire field of view. After washing, the chondrocytes were counted and seeded in 25cm^2 cell culture flasks (Nunc, Denmark) at a density of 7100 ±2100 cells/cm^2, in 5 ml of cell culture medium composed of DMEM (Sigma, UK) with SFB (Lonza, Belgium) and 1% antibiotic antimycotic solution (HiMedia, India). The cell culture media was changed every 2-3 days until a 80-90% confluence.

The combined grafts obtaining

OCDD grafts were combined with rabbits autologous cells and transplanted on the day when MSCs and chondrocytes reached 80-90% confluence. Initially, OCDD grafts were thawed and heated to 37°C in a thermostat, followed by cells detachment from the cell culture surface of the flask by trypsinization [3]. After trypsin inactivation with cell culture medium specific for each type of cells, the contents of the flasks were placed in 15 ml tubes and centrifuged at 1000 rpm for 10 minutes at room temperature (Universal 32R, Hettich Zentrifugen).

After centrifugation, the cell culture media with inactivated trypsin was removed, and by 1 ml of fresh cell culture media specific to the cells type was poured into the tubes. After pipetting, the cellular suspension was transferred to 1.5 ml Eppendorf tubes, which were centrifuged at 3500 rpm for 3 minutes (Combi-Spin FVL-2400N, Boeco) (fig. 3). After centrifugation from the Eppendorf tubes, the medium was extracted, except for 50-60 µl. Meanwhile the 15 ml tubes with the OCDD grafts and the sterile devices for fixation and cellularization of small sized grafts (DFCSSG) [3, 6] were placed in the hood (LN 090, Nuve). The used device was necessary for cellularization of grafts by the gravitational method, and its utilisation has been described in previous work [6]. The device was placed into

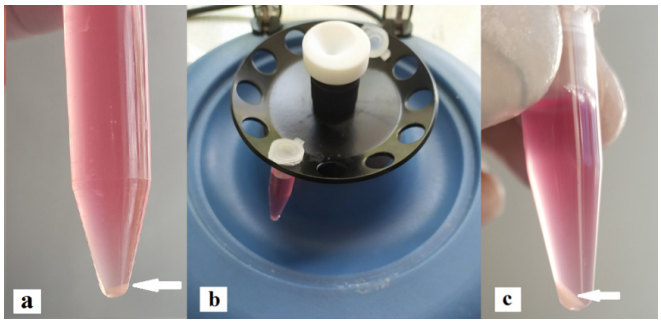

Fig. 3. Cells preparation to be combined with OCDD grafts: (a) cellular pellet in 15 ml tube after first centrifugation, (b) centrifugation of Eppendorf tube with cellular suspension in microcentrifuge, and (c) cells pellet at the bottom of Eppendorf tube, the pellet is indicated with white arrow

a stand, the cap from the tube with the graft was removed and with a tweezer the graft was extracted from the tube and inserted into the container of the fixation device. With a micropipette (LightDrop 10-100 µl, Thermo Fisher) the cellular pellets from the Eppendorf tubes were pipetted into the remaining 50-60 µl, and the cellular suspensions were poured onto the OCDD grafts which were fixed in the container of DFCSSG. Then, the lid was applied on the device and it was placed in a 15 ml tube [6], with the slightly opened cap and the divice was placed in incubator (SmartCell, Heal Force) at 37°C, 5% CO_2 humid environment.

Transplantation of combined grafts

After introduction of the combined grafts in the incubator, the rabbits were weighed and anesthetized. After preparing the operating field at the level of the unoperated knee joints, through a medial parapatellar approach of approximately 4-5 cm the knee joints were opened. After hemostasis, the patella was laterally dislocated and the knee flexed. Then, on the weight-bearing articular surface of the medial femoral condyle, with drill-bits of 1.5, 2, 3, 3.5 and 3.7 mm diameter, consecutively, with caution, at low speed and without opening the medullary canal, the defects of 3.7 mm in diameter and 4-4.5 mm in depth were created. Then the combined grafts were taken to the operating room. The containers with the combined grafts were placed on the operating table respecting all sterility principles. Intraoperatively, the base of the support with one of the combined grafts was sectioned with scissors and the graft was slowly pushed out into the defect with a K-wire, without damaging it or squeezing out the cells from the graft. All grafts were transplanted with its cartilaginous part facing up (fig. 4). After graft implantation, the dislocated patella was reduced and with the knee in extension, the wound was closed and aseptic dressing was applied. Maintaining the knees in extension, at the lateral side of the operated lower limbs thin planks were applied, wider than the limb and with the length corresponding to the distance from the hip to the ankle, which were fixed to the operated limbs with a cast from the pelvis to the ankle, holding a window at the level of the postoperative wound for dressings (fig. 6).

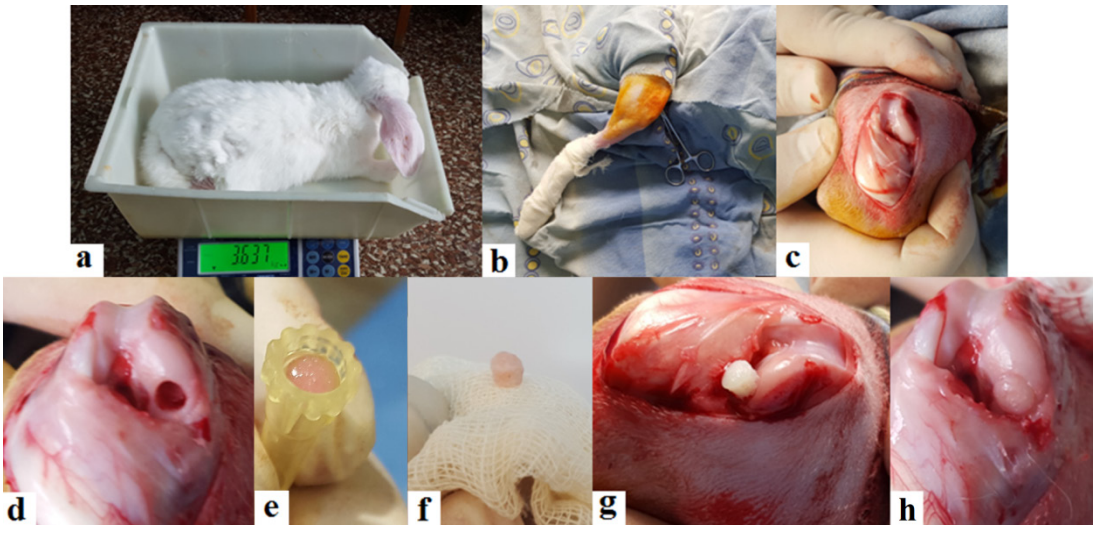

Fig. 4. Transplantation of the OCDD grafts combined with MSCs autologous chondrocytes, (a) animal weighing and general anesthesia performing, (b) operating field preparation, (c) medial parapatellar arthrotomy with lateral dislocation of patella, (d) creatig of the experimental defect, (e, f) aspect of the graft populated with autologous cells and (g, h) graft implantation into the experimental defect

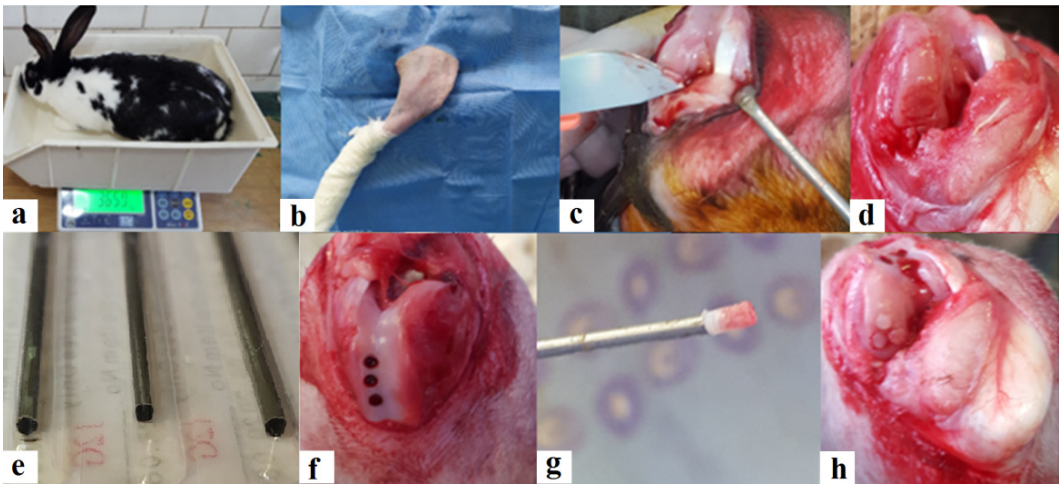

Fig. 5. Transplantation of autologous osteochondral tissue: (a, b) general anesthesia of the animal and preparation of the operating field, (c, d) creating the experimental cartilage defect, (e, f, g) harvesting of the autologous osteochondral tissue grafts from the non weight-bearing surface of the femoral trochlear groove with 12G needle and (h) their transplantation.

Transplantation of autologous osteochondral tissue

To the rabbits from the control group was performed transplantation of autologous osteochondral tissue (AOCT). The rabbits were prepared for surgery in the same way as the rabbits from the experimental groups. Through the same approach, after arthrotomy, lateral dislocation of the patella and knee flexion, with a scalpel, a cartilaginous defect was made on the articular weight-bearing surface of the medial femoral condyle of 3.7 mm in diameter, at the same level where were transplanted the combined grafts. In the created cartilage defect with a small diameter drill-bit, 3 holes of approximately 1.7 mm in diameter were made, in the form of a triangle, with a depth of 4-4.5 mm. With a 12 G piercing needle, that has internal diameter of 1.7 mm, at low speed, to avoid overheating the osteochondral tissue, from the trochlear groove were taken pieces of autologous osteochondral tissue and implanted in the drilled holes at the same height or with almost 1 mm higher than the adjacent normal car-

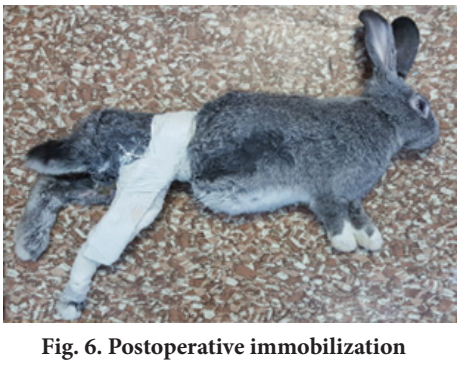

Fig. 6. Postoperative immobilization of the operated knees in rabbits

tilage (fig. 5). After reducing the dislocation of the patella and keeping the knee in extension, the wound was sutured and aseptic dressing was applied, followed by knee immobilization as described above (fig. 6).

Postoperative care

The cast immobilization of the operated knees was removed after 10 days. Postoperatively the rabbits received antibiotics for another 2-3 days depending on the case. Dressings were performed every 1-2 days, with monitoring of the general condition of the animals. All animals were kept in clean conditions, fed and watered daily.

The operated rabbits were removed from the experiment after 6 weeks – by 3 rabbits from each group, and after 12 weeks the rest, and the operated distal femurs were sampled. After removing of all soft tissues, the distal femurs were placed in 10% buffered formaldehyde, pH=7.4. For the microscopic examination slides of 5 µm were sectioned with microtome and fixed on the coverslip. Histochemical staining was performed with Hematoxylin-Eosin (H-E), Safranin O and Toluidine Blue with Fast Green. The evaluation of the results was performed according to the Unified Histological Score of Regenerated Cartilage (UHSRC) [3], which was composed by combining 3 scores widely used in the evaluation of regenerated articular cartilage in animals, whose authors are Sellers R. (1997), Wakitani S. (1994) and O'Driscoll S. (1986) [3, 26]. Each of the scores proposed by the authors contain many similar evaluation criteria, which evaluate the general morphology of the regenerated tissue and make difference between hyaline cartilage, fibrocartilage and fibrous tissue. Those scores also evaluate the degree of defect filling, thickness of the regenerated cartilage and the presence of lesions in it, the metachromasia of the regenerated tissue and the degree of integration of the regenerated tissue with the healthy one. Each score also contains specific individual criteria, such as the cellularity level of the regenerated cartilage in the O'Driscoll score, or the cellular pattern in the regenerated tissue present in the Wakitani score, and formation of chondrocytes clusters in the Sellers and O'Driscoll scores. At the same time, the Sellers score includes such criteria like evaluation of the subchondral bone condition and formation of the demarcation line between the normal and the calcified cartilage in the repaired osteochondral unit, which is very important, because the subchondral bone was also involved in the process of *in vivo* testing of combined biphasic hierarchical grafts [23] for articular cartilage regeneration. The UHSRC is presented in Table 1, and consists of evaluation of 13 criteria, the values assigned to each criteria on the scale are in descending order, in other words, the higher is the quality of the regenerated tissue, the lower will be the evaluation score, and vice versa, the higher is the evaluation score, the lower is the quality of the regenerated tissue, the value of the lowest quality being 43 points.

Table 1. Unified histological score of regenerated cartilage (Sellers, Wakitani and O'Driscoll)

	Criteria			Scale
1	Cellular pattern in regenerated cartilage	Hyaline cartilage		0
		Predominantly hyaline cartilage		1
		Predominantly fibrocartilage		2
		Only non-cartilaginous structure		3
2	Cellular morphology (category – a, b, c, d)	(a)	**Normal**	0
		(b)	**Mostly round cells with chondrocytic morphology**	
			> 75% of tissue with columns in the radial zone	0
			25-75% of tissue with columns in the radial zone	1
			<25% of tissue with columns in the radial zone (disorganized structure)	2
		(c)	**About 50% round cells with chondrocytic morphology**	
			> 75% from tissue with columns in the radial zone	2
			25-75% from tissue with columns in the radial zone	3
			<25% of tissue with columns in the radial zone (disorganized structure)	4
		(d)	**Mostly spindle-shaped cells (fibroblast-like)**	5
3	Chondrocytes clusters formation	Absent		0
		<25% of cells		1
		25-100% of cells		2
4	The cellularization level	Normal cellularity		0
		Mild hypocellularity		1
		Moderate hypocellularity		2
		Severe hypocellularity		3
5	Matrix metachromasia	Normal		0
		Slightly reduced		1
		Moderately reduced		2
		Severely reduced		3
		Staining is absent		4
6	The articular surface aspect	Smooth and intact		0
		Superficial horizontal lamination		1
		Cracks from 25% to 100% of the thickness		2
		Severe disorders, ruptures, including fibrillation		3
7	Integration of the graft with the surrounding articular cartilage	Normal continuity and integration at the border		0
		Reduced cellularity at the border		1
		Gap or lack of continuity on one side		2
		Gap or lack of continuity on both sides		3
8	The architecture of entire defect without including edges	Normal		0
		1-3 small defects		1
		1-3 large defects		2
		severe destruction		3
9	The thickness of the newly formed cartilage	100% of the neighboring normal cartilage		0
		50-100% of the neighboring normal cartilage		1
		0-50% of the neighboring normal cartilage		2

10	The presence of degenerative changes in the adjacent cartilage	Normal cellularity, no clusters, normal staining	0
		Normal cellularity, few clusters, moderate staining	1
		Moderate cellularity, moderate number of clusters, moderate staining	2
		Severe hypocellularity, without staining	3
11	Filling of the defect in relation to the adjacent normal cartilage surface	111-125 %	1
		91-110 %	0
		76-90 %	1
		51-75 %	2
		26-50 %	3
		<25 %	4
12	Formation of the demarcation line	Complete	0
		75-99 %	1
		50-74 %	2
		25-49 %	3
		<25 %	4
13	The percentage of newly restored subchondral bone	90-100 %	0
		75-89 %	1
		50-74 %	2
		25-49 %	3
		<25 %	4

Results

In order to combine OCDD grafts with cells that have chondroprogenitor potential, $1.64x10^5 \pm 7x10^4$ chondrocytes were isolated from hyaline articular cartilage with a viability of 96.79%, from which in the first passage during 10±3 days of culture were obtained $2.94x10^6 \pm 3.77x10^5$ chondrocytes with a viability of 99.89%. Also, from 4 ±1.2 ml of bone marrow collected from the rabbits, during 11±3 days were obtained $1.55x10^6 \pm 3.76x10^5$ MSC with a viability of 98%.

As a result of the implementation of the UHSRC, the animals removed from the experiment at 6 weeks in all cases had an almost similar histological score. The group of rabbits whose experimental defects were treated with OCDD grafts combined with chondrocytes had a score of 28.33±1.53 points, the group treated with grafts combined with MSC obtained a score of 27.67±2.08 points and the control group had a score of 26.33±1.53 points. As a result, there is no significant difference between the control group and the experimental groups in which tissue defects were treated with OCDD grafts combined with chondrocytes ($p > 0.1$) and in that treated with grafts combined with MSC ($p > 0.2$) (fig. 7).

At the animals removed from the experiment at 12 weeks after surgery, according to the UHSRC were determined the following results: the experimental group in which the experimental defects were treated with OCDD grafts combined with chondrocytes had a score of 18.68 ±5 points, the experimental group treated with OCDD grafts combined with MSC had a score of 14.89 ±3.76 points and the control group had a score of 17.22 ±4.84 points. According to obtained results, it was determined that there was no significant difference between the control group

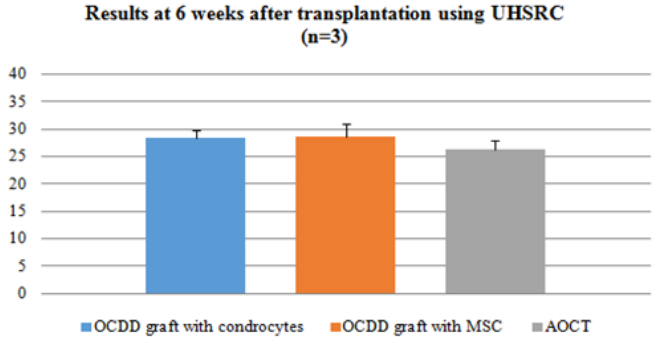

Fig. 7. Comparative results of experimentally created defects and treated with hierarchical biphasic grafts combined with chondrocytes and BM-MSC at 6 weeks after transplantation

and the group in which the cartilaginous defects were treated with OCDD grafts combined with chondrocytes ($p > 0.5$) and the group in which the defects were treated with OCDD grafts combined with MSC ($p > 0.2$) (fig. 8).

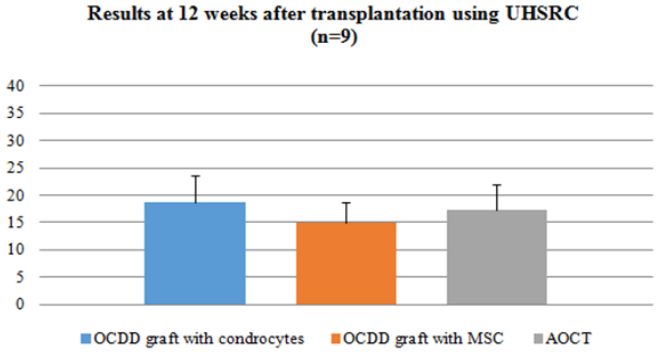

Fig. 8. Comparative results of regenerated defects at 12 weeks after surgery

At comparison of the results obtained within the same group of animals that were removed from the experiment at 6 and 12 weeks after surgery, a significant difference is determined between the obtained results, which are much better in the case of animals that were removed from the experiment later, the data are shown in table 2.

Table 2. The comparison of UHSRC obtained by groups depending on the evaluation term of the regenerated defects

	UHSRC at 6 weeks (n=3)	UHSRC at 12 weeks (n=9)	t-test
OCDD grafts combined with chondrocytes	28.33±1.53	18.68±5	p=0.009
OCDD grafts combined with BM-MSC	27.67±2.08	14.89±3.76	p<0.001
Transplantation of AOCT	26.33±1.53	17.22±4.84	p=0.004

During the histological examination of the regenerated articular cartilage after transplantation of grafts that

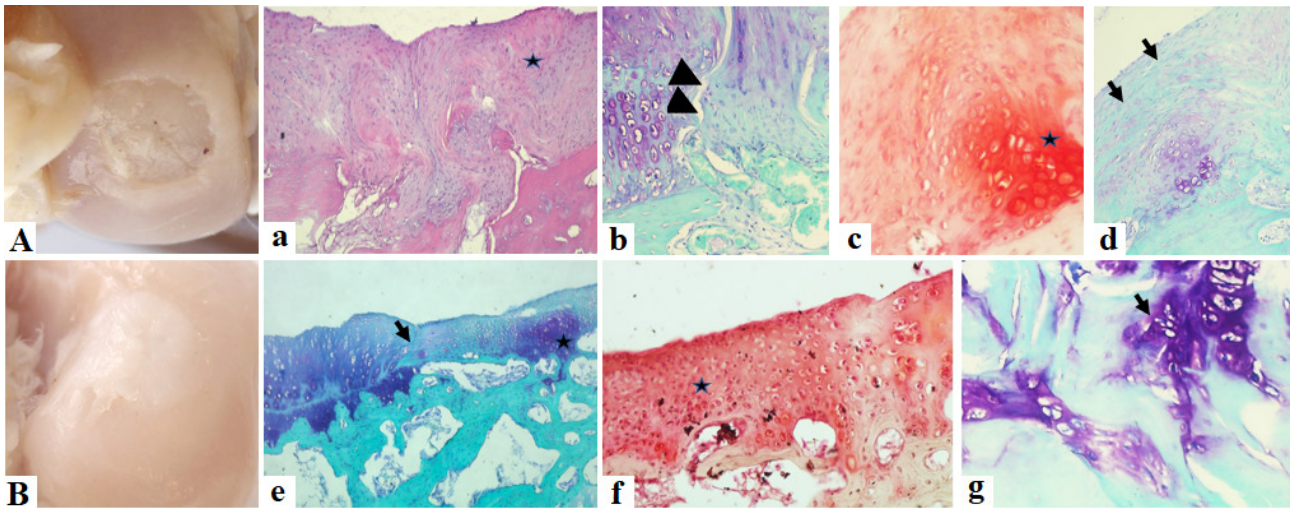

Fig. 9. Regeneration of articular cartilage using grafts combined with chondrocytes at 6 (A) and 12 weeks (B) after transplantation: (a, d) moderate cellularised fibrocartilage (× 40), H-E and Toluidine Blue with Fast Green; (b) regenerated cartilage cracks (× 100); (c) uneven GAGs distribution (x100), Safranin O; (e, g) chondrocytic clusters delimited by fibrous tissue (× 40, × 100), Toluidine Blue with Fast Green and H-E; (f) GAGs homogeneous content (× 40), Safranin O

were combined with chondrocytes (fig. 9), at 6 weeks after transplantation was determined that the defects were filled with fibrocartilage with moderate cellularity unevenly distributed. It was also determined that the deep areas of the neo-cartilage were populated by chondrocytes, arranged in isogenous groups, with signs of cellular hypertrophy and preservation of their integrity, and the superficial part of the regenerated cartilage was represented by fibroblast-like cells surrounded by a predominantly fibrous matrix. The collagen fibers were determined as being thinned and fragmented, and the concentration of glycosaminoglycans (GAG) was gradually reduced from the deep areas to the periphery. In the place of contact with the native cartilage, long and deep cracks were observed. At 12 weeks after transplantation, the quality of regenerated articular cartilage was significantly better, it was smoother, and its thickness was thinner compared to the native cartilage. In the deep and middle areas newly formed hyaline cartilage was identified, and fibrous cartilage was frequently detected in the superficial areas. The cells in the regenerated cartilage were unevenly distributed, being predominantly of the chondrocytic type, organized in isogenic groups. At the border with the native cartilage chondrocytic clusters were identified, which were delimited by masses of fibrous tissue. The collagen fibers were highly disorganized, and the content of GAGs was more homogeneous, being identified in all areas of the newly formed cartilage.

In the case of experimental defects regenerated by using grafts combined with MSC, no big difference was observed compared to grafts combined with chondrocytes from the

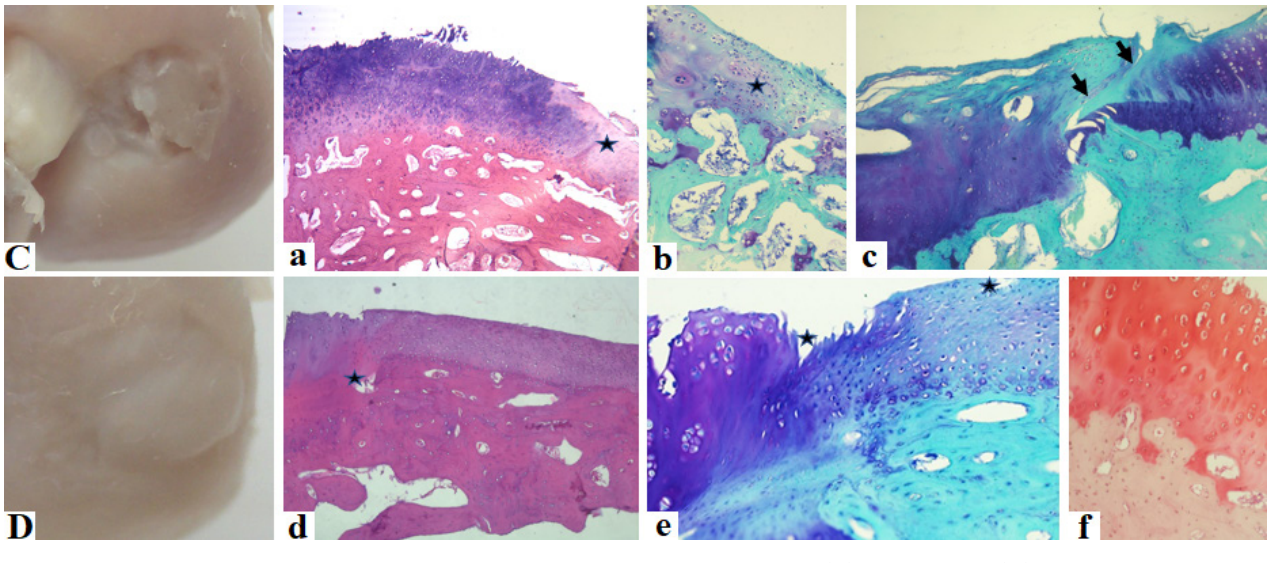

Fig. 10. Regeneration of articular cartilage using grafts combined with MSC at 6 (C) and 12 weeks (D) after transplantation: (a) moderate cellularised fibrocartilage (× 40), H-E; (b, f) GAGs homogeneous content with cells in upper part of the cartilage (× 40, × 100), Toluidine Blue with Fast Green and Safranin O; (c, e) regenerated cartilage cracks and fibrillation (× 40); (d) chondrocytic clusters delimited by fibrous tissue (× 40), H-E

same periods. At 6 weeks was determined that the presence of chondrocytes and chondroblasts was predominantly in the superficial and middle areas of the regenerated cartilage. While at 12 weeks was determined that the thickness of the regenerated cartilage is similar to that of the native one, the concentration of GAGs being slightly lower, and the demarcation line was better visualized (fig. 10).

In the case of cartilage defects regeneration by autologous osteochondral tissue transfer, at 6 weeks, in all cases, were identified areas where the defects were not completely filled with regeneration tissue, but also the areas with the lack of adherence to native articular cartilage. There are cases when the autologous transplant was located in the same plane as the surface of native articular cartilage, or even slightly protruding into the joint cavity. The cartilage within the autologous grafts underwent partial or in some cases total lytic changes, with partially or totally destroyed chondrocytes. In the contact areas of the native cartilage with the transplanted tissue, were observed structural changes like hypercellularity with uneven cellular distribution and their tendency to form large clusters of chondrocytes and extracellular matrix with intense metachromasia. At 12 weeks, the defects areas were incompletely filled, the recovery of the defect was achieved only at the level of bone tissue, with its non-homogeneous filling. Also, at the periphery of the transplanted tissue, immature cartilaginous tissue was observed, on some places with signs of maturity, and in the center of the transplant area a fibrillar matrix with fibroblast-like cells was present, with the content of GAGs being inhomogeneous (fig. 11).

Discussion

The process of obtaining cells for articular cartilage regeneration with combined grafts is an essential one. It is necessary to mention that there is an obvious difference between the number of MSC and chondrocytes transplanted within the experiment ($p<0.001$). This significant difference between the groups is due to the fact that MSC are larger than chondrocytes, for this reason, the amount of transplanted MSCs is almost twice lower comparing to chondrocytes. However, in each transplantation, one cell culture flask with 80-90% cells confluence was used. As a result, if the amount of transplanted cells during the experiment is reported to have a defect of 1 cm^3, then it turns out that for the treatment of a defect of 1 cm^3 will be necessary to transplant approximately $6.67x10^7 \pm 8.55x10^6$ chondrocytes or $3.51x10^7 \pm 8.53x10^6$ MSC.

During the performed research, the experimental defects should have been only of articular cartilage, without involving the subchondral bone, according to the main objective of the research, which is the regeneration of the articular cartilage, but not of the subchondral bone. This was not done because it was practically impossible to prepare and fix a decellularized cartilaginos graft combined with cells, which after transplantation would be constantly subjected to mechanical stress forces, because the articular cartilage has a very weak regeneration potential, even being combined with cells that have chondroprogenitor potential, it has poor possibility to adhere at the adjacent bone and cartilage. At the same time, the subchondral bone in the region with degenerated cartilage is important for the nutrition of the deep layers of the cartilage and the transfer of mechanical stimuli from the cartilage to the rest of the bone [27], as a result, the bone within the biphasic graft being demineralized ensures a rapid regeneration of the subchondral bone due to its osteoinductive and osteoconductive properties [15, 23], but also a more stable fixation of the graft. Because the demineralized, decellularized and longitudinally perforated grafts have much lower mechanical strength than normal osteochondral tissue [4],

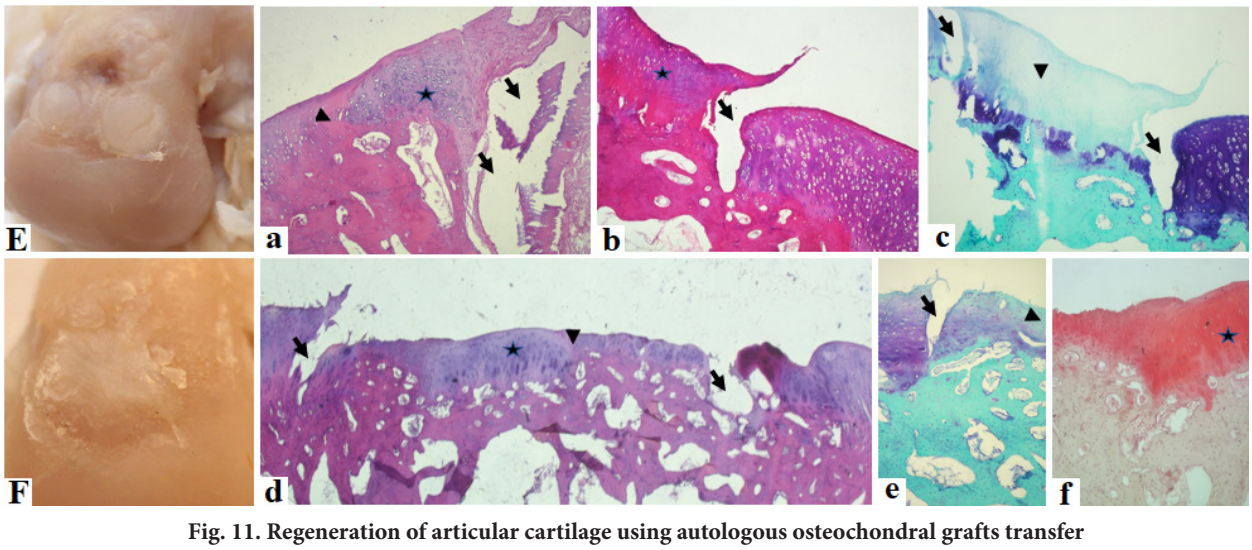

Fig. 11. Regeneration of articular cartilage using autologous osteochondral grafts transfer at 6 (C) and 12 weeks (D) after implantation: (a, b, c, d, e) lack of regeneration between the transferred tissue and the native cartilage with signs of partial or total osteo- and chondrolysis (× 40), H-E and Toluidine Blue with Fast Green; (a, d) hypercellularity at the level of transferred tissue and lack of cells at the border between graft and native cartilage; (e, f) inhomogeneous GAGs content (× 40), Toluidine Blue with Fast Green and Safranin O

in order to ensure joint rest for the process of osteogenesis and chondrogenesis, plaster immobilization was applied for a period of 10 days.

Transplantation of biphasic osteochondral, allogeneic, demineralized, decellularized, longitudinally perforated grafts and combined with autologous cells with chondroprogenitor potential to regenerate the articular cartilage, can be qualified as articular cartilage regeneration through tissue engineering techniques. The tissue engineering technique that uses three-dimensional matrices combined with autologous chondrocytes is called Matrix-assisted Autologous Chondrocyte Implantation (MACI) [2, 3], and the technique that uses three-dimensional matrices populated with MSC is called Matrix Autologous Stem-cells Implantation (MASI) [14]. Thus, in the performed research, were compared two tissue engineering techniques of articular cartilage regeneration with the autologous osteochondral tissue transfer through the mosaicplasty technique [28]. Given that the UHSRC at 12 weeks in the groups that used grafts combined with chondrocytes and grafts combined with MSC are different (fig. 8), the best score being in the case of grafts combined with MSC – 14.89±3.76 points, comparatively to those combined with chondrocytes with a score of 18.68 ±5 points, from a statistical point of view, there is no significant difference between these 2 groups ($p = 0.08$). The research that compares the MACI and MASI techniques, using chondrocytes isolated from the articular cartilage and MSC isolated from the articular synovium, shows slightly better results when MASI technique was performed [14].

Considering that the UHSRC obtained in the experimental groups do not show a significant difference compared to the control group at 6 and 12 weeks, and the histological picture is far from ideal, the obtained cartilage results are far from good.

Conclusions

There was no big difference at 6 and 12 weeks between results of the grafts combined with chondrocytes and those combined with MSC, even though the number of transplanted chondrocytes was almost twice bigger ($p > 0.8$; $p = 0.08$), and the control group did not show better results.

Utilisation of UHSRC allowed a thorough evaluation of the obtained results. Thus, a weak regeneration degree of the experimental cartilage defects was achieved in both cases: using grafts combined with chondrocytes and MSC, and the control group.

References

1. Cobzac V, Mostovei A, Jian M, Nacu V. An efficient procedure of isolation, cultivation and identification of bone marrow mesenchymal stem cells. Mold Med J. 2019;62(1):35-40. doi: 10.5281/zenodo.2590011.
2. Cobzac V, Verestiuc L, Jian M, Nacu V. Chondrocytes isolation from hyaline cartilage by continuous monitoring method. Mold Med J. 2021;64(6):13-19. https://doi.org/10.52418/moldovan-med-j.64-6.21.03.
3. Cobzac V, Jian M, Globa T, Nacu V. The cartilaginous tissue regeneration on weight bearing and non-weight bearing surfaces of the knee. In: Tiginianu I, Sontea V, Railean S, editors. 5th International Conference on Nanotechnologies and Biomedical Engineering, ICNBME 2021. IFMBE Proceedings. 2021;87:334-341. https://doi.org/10.1007/978-3-030-92328-0_44.
4. Cobzac V, Verestiuc L, Jian M, Nacu V. Assesment of ionic and anionic surfactants effect on demineralized osteochondral tissue. IOP Conference Series: Materials Science and Engineering. 2019;572:012084. doi: 10.1088/1757-899X/572/1/012084.
5. Chicatun F, Pedraza CE, Muja N, Ghezzi CE, McKee MD, Nazhat SN. Effect of chitosan incorporation and scaffold geometry on chondrocyte function in dense collagen type I hydrogels. Tissue Eng Part A. 2013;19(23-24):2553-64. doi: 10.1089/ten.TEA.2013.0114.
6. Cobzac V, Jian M, Nacu V. Cellularization of small-sized grafts from biological material using the gravitational modality principle. J Phys Conf Ser. 2021;1960:012004. doi:10.1088/1742-6596/1960/1/012004.
7. Irawan V, Sung TC, Higuchi A, Ikoma T. Collagen scaffolds in cartilage tissue engineering and relevant approaches for future development. Tissue Eng Regen Med. 2018;15(6):673-697. doi: 10.1007/s13770-018-0135-9.
8. Kim SS, Song CK, Shon SK, Lee KY, Kim CH, Lee MJ, Wang L. Effects of human amniotic membrane grafts combined with marrow mesenchymal stem cells on healing of full-thickness skin defects in rabbits. Cell Tissue Res. 2009;336(1):59-66. doi: 10.1007/s00441-009-0766-1.
9. Kim IG, Park SA, Lee SH, Choi JS, Cho H, Lee SJ, Kwon YW, Kwon SK. Transplantation of a 3D-printed tracheal graft combined with iPS cell-derived MSCs and chondrocytes. Sci Rep. 2020;10(1):4326. https://doi.org/10.1038/s41598-020-61405-4.
10. Ju YM, Ahn H, Arenas-Herrera J, Kim C, Abolbashari M, Atala A, Yoo LL, Lee SJ. Electrospun vascular scaffold for cellularized small diameter blood vessels: a preclinical large animal study. Acta Biomater. 2017;59:58-67. doi: 10.1016/j.actbio.2017.06.027.
11. Zak L, Albrecht C, Wondrasch B, Widhalm H, Vekszler G, Trattnig S, Marlovits S, Aldrian S. Results 2 years after matrix-associated autologous chondrocyte transplantation using the novocart 3d scaffold: an analysis of clinical and radiological data. Am J Sports Med. 2014;42(7):1618-27. doi: 10.1177/0363546514532337.
12. Chen S, Zhang Q, Kawazoeb N, Chen G. Effect of high molecular weight hyaluronic acid on chondrocytes cultured in collagen/hyaluronic acid porous scaffolds. RSC Adv. 2015;5:94405-94410. https://doi.org/10.1039/C5RA18755A.
13. Vázquez-Portalatı NN, Kilmer CE, Panitch A, Liu JC. Characterization of collagen type I and II blended hydrogels for articular cartilage tissue engineering. Biomacromolecules. 2016;17(10):3145-3152. doi: 10.1021/acs.biomac.6b00684.
14. Akgun I, Unlu MC, Erdal OA, Ogut T, Erturk M, Ovali E, Kantarci F, Caliskan G, Akgun Y. Matrix-induced autologous mesenchymal stem cell implantation versus matrix-induced autologous chondrocyte implantation in the treatment of chondral defects of the knee: a 2-year randomized study. Arch Orthop Trauma Surg. 2015;135(2):251-263. doi: 10.1007/s00402-014-2136-z.
15. Zhang H, Yang L, Yang XG, Wang F, Feng JT, Hua KC, Li Q, Hu YC. Demineralized bone matrix carriers and their clinical applications: an overview. Orthop Surg. 2019;11(5):725-737. doi: 10.1111/os.12509.
16. Schuette HB, Kraeutler MJ, McCarty EC. Matrix-assisted autologous chondrocyte transplantation in the knee: a systematic review of mid- to long-term clinical outcomes. Orthop J Sports Med. 2017;5(6):2325967117709250. doi: 10.1177/2325967117709250.
17. Chomchalao P, Pongcharoen S, Sutheerawattananonda M, Tiyaboonchai W. Fibroin and fibroin blended three-dimensional scaffolds for rat chondrocyte culture. Biomed Eng Online. 2013;12:28. doi: 10.1186/1475-925X-12-28.
18. Enders JT, Otto TJ, Peters HC, Wu J, Hardouin S, Moed BR, Zhang Z. A model for studying human articular cartilage integration *in vitro*. J Biomed Mater Res A. 2010;94(2):509-14. doi: 10.1002/jbm.a.32719.
19. Li L, Yu F, Zheng L, Wang R, Yan W, Wang Z, Xu J, Wu J, Shi D, Zhu L, Wang X, Jiang Q. Natural hydrogels for cartilage regeneration: Modifi-

cation, preparation and application. J Orthop Translat. 2018;17:26-41. doi: 10.1016/j.jot.2018.09.003.
20. Malinauskas M, Jankauskaite L, Aukstikalne L, Dabasinskaite L, Rimkunas A, Mickevicius T, Pockevicius A, Krugly E, Martuzevicius D, Ciuzas D, Baniukaitiene O, Usas A. Cartilage regeneration using improved surface electrospun bilayer polycaprolactone scaffolds loaded with transforming growth factor-beta 3 and rabbit muscle-derived stem cells. Front Bioeng Biotechnol. 2022;10:971294. doi: 10.3389/fbioe.2022.971294.
21. Irawan V, Sung TC, Higuchi A, Ikoma T. Collagen scaffolds in cartilage tissue engineering and relevant approaches for future development. Tissue Eng Regen Med. 2018;15(6):673-697. doi: 10.1007/s13770-018-0135-9.
22. Lin S, Lee WYW, Feng Q, Xu L, Wang B, Man GCW, Chen Y, Jiang X, Bian L, Cui L, Wei B, Li G. Synergistic effects on mesenchymal stem cell-based cartilage regeneration by chondrogenic preconditioning and mechanical stimulation. Stem Cell Res Ther. 2017;8(1):221. doi: 10.1186/s13287-017-0672-5.
23. Lin X, Chen J, Qiu P, Zhang Q, Wang S, Su M, Chen Y, Jin K, Qin A, Fan S, Chen P, Zhao X. Biphasic hierarchical extracellular matrix scaffold for osteochondral defect regeneration. Osteoarthritis Cartilage. 2018;26(3):433-444. doi: 10.1016/j.joca.2017.12.001.
24. Mikos AG, McIntire LV, Anderson JM, Babensee JE. Host response to tissue engineered devices. Adv Drug Deliv Rev. 1998;33(1-2):111-139. doi: 10.1016/s0169-409x(98)00023-4.
25. Braniste T, Cobzac V, Ababii P, Plesco I, Raevschi S, Didencu A, Maniuc M, Nacu V, Ababii I, Tiginianu I. Mesenchymal stem cells proliferation and remote manipulation upon exposure to magnetic semiconductor nanoparticles. Biotechnology Reports. 2020;25:e00435. https://doi.org/10.1016/j.btre.2020.e0043.
26. Orth P, Madry H. Complex and elementary histological scoring systems for articular cartilage repair. Histol Histopathol. 2015;30(8):911-9. doi: 10.14670/HH-11-620.
27. Madry H, van Dijk CN, Mueller-Gerbl M. The basic science of the subchondral bone. Knee Surg Sports Traumatol Arthrosc. 2010;18(4):419-33. doi: 10.1007/s00167-010-1054-z.
28. Rowland R, Colello M, Wyland DJ. Osteochondral autograft transfer procedure: arthroscopic technique and technical pearls. Arthrosc Tech. 2019;8(7):e713-e719. doi: 10.1016/j.eats.2019.03.006.

Authors' ORCID iDs and academic degrees
Vitalie Cobzac, MD, PhD Applicant – https://orcid.org/0000-0002-5010-1163
Mariana Jian, BioD, PhD Applicant – https://orcid.org/0000-0001-9352-5866
Tatiana Globa, MD, PhD, Assistant Professor – https://orcid.org/0000-0002-5317-2776
Viorel Nacu, MD, PhD, MPH, Professor – https://orcid.org/0000-0003-2274-9912

Authors' contributions
VC – conducted literature review, obtained raw data, created the unified histological score of regenerated cartilage and wrote the manuscript; MJ – interpreted the data and drafted the manuscript; TG - created the objective evaluation score of histological samples; VN – conceptualized the idea, designed the research and monitored the experiment. All the authors approved the final version of the manuscript.

Funding
The study was supported by the State Program Project 2020-2023: "GaN-based nanoarchitectures and three-dimensional matrices from biological materials for applications in microfluidics and tissue engineering", No 20.80009.5007.20. The trial was the authors' initiative, they are independent and take responsibility for the integrity of the data and accuracy of the data analysis.

Ethics approval and consent to participate
The research project was approved by Ethics Committee of *Nicolae Testemitanu* State University of Medicine and Pharmacy (Protocol No 31, 14.12.2016).

Conflict of interests
No competing interests were disclosed.

https://doi.org/10.52418/moldovan-med-j.65-2.22.04
UDC: 611.013.8

Morphological evaluation of the amniotic membrane decellularization

*[1,2,3]Olga Ignatov, [2]Adrian Cociug, [3]Oleg Pascal, [1,2]Viorel Nacu

[1]Laboratory of Tissue Engineering and Cell Cultures, *Nicolae Testemitanu* State University of Medicine and Pharmacy
[2]Human Tissue Bank, Orthopedic and Traumatological Hospital
[3]Department of Rehabilitation, *Nicolae Testemitanu* State University of Medicine and Pharmacy
Chisinau, the Republic of Moldova

Authors' ORCID iDs, academic degrees and contributions are available at the end of the article

*Corresponding author – Olga Ignatov, e-mail: olga.ignatov@usmf.md
Manuscript received October 03, 2022; revised manuscript November 24, 2022; published online December 20, 2022

Abstract

Background: Biological materials derived from decellularized tissues could be a good basis for progress in regenerative medicine while maintaining the main components of the extracellular matrix. A promising scaffold for tissue-engineered is the human amniotic membrane. It is one of the oldest biomaterials used for scaffolds.
Material and methods: 3 placentas were obtained through Human Tissue Bank. Under sterile condition human amniotic membrane was collected. The human amniotic membrane was treated with 0.5% of sodium dodecyl sulphate (SDS), 1% Triton for 24 and 5 hours. Amniotic membrane decellularization was also carried out in combination with ultrasound bath for 20 minutes 3 times. For morphological and structure evaluation of human amniotic membrane the scanning electron microscopy of native amniotic membrane and histology of decellularized and native amniotic membrane were performed.
Results: The human amniotic membrane decellularization process with 0.5% SDS solution and 1% Triton solution showed that decellularization for 24 hours is too aggressive for human amniotic membrane structure. The decellularization for 5h with 1% Triton solution was incomplete.
Conclusions: The method of decellularization with 0.5% SDS solution is more suitable for amniotic membrane decellularization and can be performed in only 5 hours. The use of ultrasound bath did not have a significant effect on the obtained results.
Key words: amniotic membrane, decellularization, morphology.

Cite this article
Ignatov O, Cociug A, Pascal O, Nacu V. Morphological evaluation of the amniotic membrane decellularization. *Mold Med J*. 2022;65(2):30-35. https://doi.org/10.52418/moldovan-med-j.65-2.22.04.

Introduction

Tissue engineering aims at replacing or regenerating human tissues or organs in order to restore or establish normal function [1]. The tissue engineering triad consists of three main factors: the cells, signaling molecules, and scaffold, which support and rely upon one another. The scaffold, together with integrated signaling molecules, provides structural, biochemical, and biomechanical cues to guide and regulate cell behavior and tissue development [2].

Scaffolds can be prepared through synthetic or natural materials. Synthetic scaffolds are beneficial in that their structure and mechanical properties can be manipulated and controlled with the goal of producing an optimal environment for a particular cell type or cell set. Among these properties, matrix stiffness and topography show profound influences on cell growth and differentiation [2].

Biomaterials have important roles as mimicking the natural environment and providing the physical and biological helpers to the attached cells during the *in vivo* and *in vitro* cultivation [3]. Cellular adhesion is one of the most undesirable properties for biomaterials. There are many studies in progress about surface modification of biomaterials [4]. Furthermore, optimal biomaterials should degrade without toxicity and must control degradation rate [5] and have excellent swelling and biodegradation behaviors [6]. Ideal scaffolds for tissue engineering should provide such properties as:

- Biocompatibility
- Biodegradability (tissue and damaged based)
- Support cell adhesion
- Non-immunogenicity
- Non-toxicity
- Easy obtainable
- Controllable porosity
- Provide vasculature for oxygen and nutrients delivery
- Provide microenvironment and promote cells growth
- Possess proper biomechanical strength [7].

Because many challenges are associated with preparing synthetic scaffolds that recapitulate the complexity of the cell microenvironment, there has been increasing interest in utilizing naturally derived extracellular matrix (ECM)

itself. This biologic scaffold is obtained through the process of decellularization. The ultimate goal of decellularization is to rid the ECM of native cells and genetic materials such as DNA while maintaining its structural, biochemical, and biomechanical cues [2]. The decellularized ECM can then be repopulated with a patient's own cells to produce a personalized tissue and be used to improve, maintain or restore damaged tissues or whole organs. The rationale for decellularization is related to the adverse response that cell waste may induce when tissue-derived material is used for implantation procedures, including immune reaction and inflammation, leading to implant rejection. Therefore, decellularized ECM is usually obtained by different decellularization methods, developed to eliminate the cells and their waste, mainly DNA [8]. As for all biological scaffolds, gentle but complete decellularization is a critical step in removing allogenous cells, and various methods have been described [9].

Various natural structures have the required therapeutic potential to be used as a tissue-engineered structure. Among them are the inner body membranes. Membranes actually consist of thin layers of cells or tissues that envelope the body, its internal organs, and cavities. Amniotic membrane, mesentery, omentum, pericardium, peritoneum, and pleura are all examples of these membranes with therapeutic applications [10].

A promising scaffold for tissue-engineered is the human amniotic membrane. It is one of the oldest biomaterials used for scaffolds and it has many characteristics that make it attractive as a biomaterial [11]. Human amniotic membrane is a thin semitransparent membrane normally 20 μm to 500 μm in thickness. It is tough and is devoid of blood vessels, lymphatics, and nerves [9, 12]. Amniotic membrane lines the amniotic cavity; its apical surface is bathed in amniotic fluid, whereas the basal surface lies on top of the chorion [13]. The amnion basement membrane is largely composed of collagen I, collagen III, collagen IV, laminin, and fibronectin. It is inexpensive and easily takes, and its availability is virtually unlimited, negating the need for mass tissue banking [11].

The human amniotic membrane has been widely used in tissue engineering and regenerative medicine not only due to its favorable biological and mechanical properties but also as its usage has low ethical problems. In general, for amniotic membrane clinical applications or its preservation in tissue banks, it is crucial to perform donor screening and selection, procure the membrane, wash it, and perform additional processing steps. It is common to treat the amniotic membrane chemically or with antibiotic substrates, preserve, sterilize, package, and store it [14]. The reasons for epithelial layer removal, amniotic membrane sterilization, and its preservation are, respectively, to reduce graft rejection, minimize the risk of disease transmission, and store it more quickly for a more extended period [15]. Elasticity, stiffness and other biomechanical properties also make it possible to use the amniotic membrane for various medical purposes. Amniotic membrane is almost always considered as discarded substance; it satisfies most of the criteria of an ideal biological tissue and shows almost zero rejection phenomenon [16].

This paper aim is to evaluate the morphology and structure of decellularized human amniotic membrane by different methods.

Material and methods

Human amniotic membrane collection

Human placentas were obtained through Human Tissue Bank, the Republic of Moldova. After written informed consent was obtained, 3 placentas were obtained after caesarean section. The research was approved 15.03.2019 No 14, by Ethical Committee of Research at *Nicolae Testemitanu* State Medical and Pharmaceutical University of the Republic of Moldova, Chisinau. According to Standard Operating Procedure (SOP) the screening to exclude any risk of transmissible infections, such as human immunodeficiency virus, hepatitis virus types B and C, and syphilis was done. Under sterile conditions the placentas were decontaminated to remove pathogens by rinsing several times with sterile saline solution, and finally, the amnion and chorion were separated manually and rinsed with the saline solution containing antibiotics and antimycotics. A part of human amniotic membrane was decellularized.

Decellularization of human amniotic membrane

Sodium dodecyl sulphate (SDS) decellularization. Human amniotic membrane was treated with 0.5% SDS solution for 24h and 5h at room temperature. To help remove cells from the substrate additional mechanical scraping was applied. After the decellularization process human amniotic membrane was washed three times with phosphate buffered saline (PBS) solution (pH 7.4) for 15 min each with gentle agitation.

Triton X-100 decellularization. The tissue was placed in a solution of 1% Triton X-100 for 24h and 5h at room temperature. The scraping for cell removal was performed, followed by a final wash using sterile PBS (pH 7.4) for 15 min each with gentle agitation.

Ultrasound bath decellularization. The amniotic membrane placed in tubes with 1% Triton and 0.5% SDS solutions was additionally placed in ultrasound bath for 20 minutes 3 times. After that, the solutions with human amniotic membrane were left for 24 and 5 hours at room temperature. After the decellularization process the mechanical scraping was applied and amniotic membrane was washed three times with PBS solution (pH 7.4) with gentle agitation for 15 min each.

Morphological characterization of human amniotic membrane

Scanning electron microscopy analysis

The samples were fixed in 2.5% glutaraldehyde in 0.1 M sodium phosphate buffer for 24 hours and post-fixed in 1% osmium tetroxide for 1 h, dehydrated with a series

of ethanol solutions of increasing concentrations (30%, 50%, 70%, 90%, and 100%) for 10 min each and critical point dried. For SEM, the amniotic membrane (AM) was further dried with carbon dioxide in a critical point dryer and coated with gold in a sputter coater. Then, the samples were subjected to scanning electron microscopy Zeiss EM 900 (MHH, Hannover).

Histological analysis

Native and decellularized human amniotic membranes were fixed in 10% formalin, dehydrated with an increasing series of ethanol solutions and embedded in paraffin wax. The samples were sectioned with each section having a thickness of 4 μm. The native amniotic membrane was stained with hematoxylin and eosin (H&E) and Van Gieson staining. Decellularized amniotic membrane was stained with H&E staining. Samples (n=3) were viewed by microscope (Leica S 80/0.30).

Results and discussion

Human amniotic membrane is one of the thickest membranes in the human body. It consists of a thin epithelial layer, a thick basement membrane and avascular stroma consisting mainly of collagen [17].

SEM was performed to study the surface morphology of the outer and inner layers of native amniotic membrane (fig.1). The cuboidal epithelial cells with irregular shape were observed on the outer layer of the amniotic membrane (fig. 1(a)). It was possible to see the direction of collagen fibers, which are an indicator of mechanical properties of the human amniotic membrane. Collagen fibers directed unregularly were clearly visible on the inner layer of human amniotic membrane (fig. 1(b)).

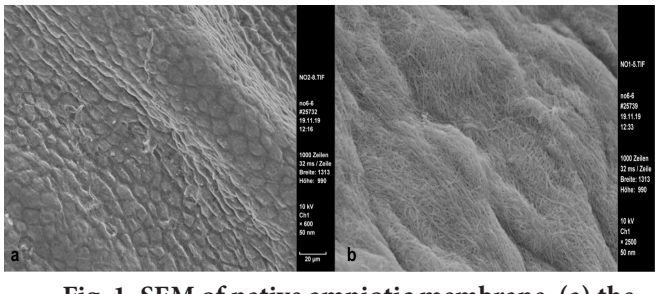

Fig. 1. SEM of native amniotic membrane. (a) the outer layer of amniotic membrane consists of epithelial cells, (b) collagen fibers on the inner layer of the amniotic membrane

Different direction of collagen fibers suggests that human amniotic membrane has good mechanical properties that allow using it in various fields of medicine and especially in tissue engineering.

Epithelium is a monolayer of metabolically active cuboidal cells with microvilli present on its apical surface [17] and uniformly arranged on the basement membrane. *Basement membrane* is made up of type IV, V and VI collagen in addition to fibronectin and laminin [18]. *Stroma* is further divided into three contiguous but distinct layers: the inner compact layer which is in contact with the basement membrane and contributes to the tensile strength of the membrane, middle fibroblast layer which is thick and made up of a loose fibroblast network and the outermost spongy layer [17].

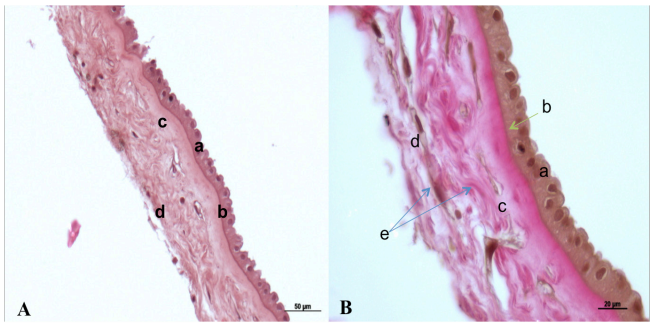

Fig. 2. (A) H&E stained histological image of native amniotic membrane: uniform epithelial layer (a), intact basement membrane (b), unmodified compact layer (c), preserved fibroblastic layer (d). H-E, × 100.

(B) Van Gieson stained histological image of native hAM: uniform epithelial layer (a), intact basement membrane (b), unmodified compact layer (c), preserved fibroblastic layer (d), collagen fibers (e). Picrofuxin, × 400

On histological examination of native human amniotic membrane (fig. 2) all the layers were found: uniform epithelial layer, basement membrane, compact layer and fibroblastic layer. In Van Gieson-stained slides the collagen fibers can be clearly seen (fig. 2A).

Figure 3 shows the histology of decellularized human amniotic membrane. The human amniotic membrane decellularization process with 0.5% SDS solution and 1% Triton solution showed that decellularization for 24 hours is too aggressive. The amniotic membrane structure was damaged with many gaps. In samples were used 1% Triton solution fig. 3 (A) could be seen disappearance of the epithelium (a); continuous basement membrane (b); disorganization of the fiber architecture of the compact layer (c); cellular debris (d). The decellularization in 0.5% SDS solution for 24 hours shows the disappearance of the epithelium (a); continuous basement membrane (b); disorganization of the architecture of the compact layer (c); cellular debris (d). The decellularization in the same solutions in complex with the ultrasound bath showed the same results (fig. 3 (C), (D)), which means that ultrasound had no significant effect on the amniotic membrane decellularization procedure. Decellularization with 1% Triton solution with ultrasound (fig. 3 (C)) shows some fragments of epithelial cells (a); continuous basement membrane (b); disorganized compact layer (c); cellularity (d). 0.5% SDS solution with ultrasound (fig. 3 (D)) shows the disappearance of the epithelium (a); basement membrane discontinuity (b); disorganized compact layer with fragmentation (c); and acellularity (d).

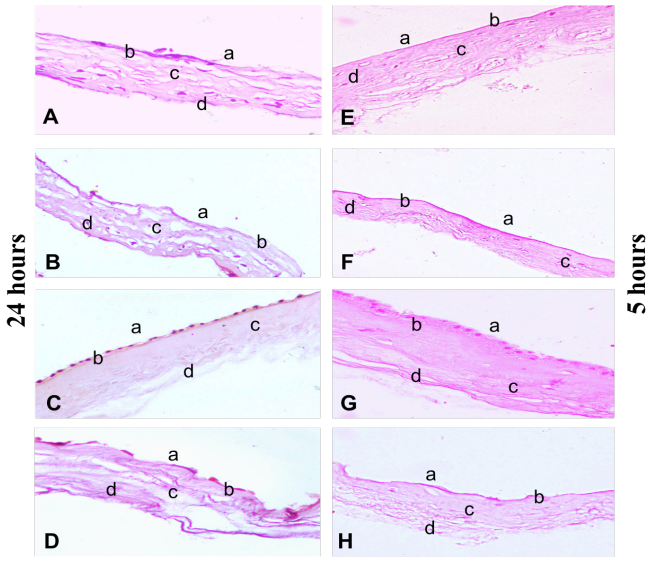

Fig. 3. Histological staining of decellularized amniotic membrane in:

(A) 1% Triton solution for 24h. H-E, × 100,
(B) 0.5% SDS solution for 24h. H-E, × 100,
(C) 1% Triton solution with ultrasound for 24h. H-E, × 100,
(D) 0.5% SDS solution with ultrasound for 24h. H-E, × 100,
(E) 1% Triton solution for 5h. H-E, × 100,
(F) 0.5% SDS solution for 5h. H-E, × 100,
(G) 1% Triton solution with ultrasound for 5h. H-E, × 100.
(H) 0.5% SDS solution with ultrasound for 5h. H-E, × 100.

The treatment of human amniotic membrane with 1% Triton solution for 5 hours (fig. 3 (E)) was incomplete with some visible cells. The histology shows the disappearance of epithelium (a); contoured basement membrane (b); compact layer preserved (c) and solitary cellular debris (d). Decellularization with 0.5% SDS solution of human amniotic membrane for 5 hours showed better results (fig. 3 (F)). The tissue remained undamaged with no visible cells. The histology shows the disappearance of the epithelium (a); continuous basement membrane (b); disorganized compact layer (c) and acellularity (d).

1% Triton solution ultrasound decellularization (fig. 3 (G)) shows the atrophy with disappearance of the epithelium (a); disappearance of the basement membrane (b); disorganized compact layer (c) and cellular debris (d). The same procedure of decellularization with 0.5% SDS solution and ultrasound bath (fig. 3 (H)) shows the disappearance of the epithelium (a); continuous basement membrane (b); disorganized compact layer (c) and acellularity (d). Based on the decellularization results, it can be assumed that the best decellularization method is with 0.5% SDS solution for 5 hours.

Tissue decellularization is a promising method for the preparation of bio-scaffolds for regenerative medicine. Removing cellular components from tissue or organs produces an ECM consisting of active structural proteins that can be used in tissue engineering. The most effective method of tissue and organ decellularization depends on many factors, such as cell (tissue) type, cell density, tissue's thickness, and lipid content [19]. Different decellularization protocols describe combinatorial and sequential use of different physical, chemical, and enzymatic techniques (tab. 1).

Table 1. Known used decellularization methods [7]

Chemical	Biological	Physical
*Alkaline-acid treatment *Non-ionic detergents *Ionic detergents *Zwitterionic detergents *Tri(n-buyl) phosphate *Hypotonic and hypertonic treatments *Chelating agents	*Protease inhibitors *Calcium chelating agents *Nucleases *Antibiotics	*Freezing & Thawing *Mechanical force *Sonication *Mechanical Agitation *Hydrostatic pressure

In general, chemical and enzymatic techniques are mainly responsible for successful decellularization in commonly used protocols. Physical techniques are generally used to complement chemical and biological techniques and therefore increase the decellularization effects. Physical techniques can produce damage in the matrix, while chemical techniques can produce reactions that change the chemical composition of the ECM [8, 20, 21].

Detergents are chemical agents used to solubilize cell membranes and to dissociate their inner structure. Among them, Triton X-100 is the most commonly used detergent in decellularization processes. It targets the lipid–lipid and lipid–protein interactions, but it leaves the protein–protein interaction intact [22, 23]. It is a very useful agent in those tissues where the key matrix components are primarily proteins. It is an effective detergent to eliminate cells from many tissues, but it is generally avoided in tissues with glycosaminoglycans as a key component in their matrix. Side by side with the Triton X-100, SDS is the other most commonly used detergent in decellularization procedures. SDS solubilizes both the external and nuclear membranes, but also tends to denature proteins and may alter the native structure of the matrix [24, 25]. For these reasons, short time SDS treatment is the most common, aiming to minimize the possible damage to proteins and the overall matrix structure. Nevertheless, it is very efficient in removing nuclear and cytoplasmic waste [26].

As previously mentioned, physical techniques are not enough to decellularize the tissue, but they can help in combination with chemical and enzymatic processes. For example, when big tissue pieces or whole organs are the target of decellularization, perfusion is recommended in order to better reach all tissue areas [27].

Superficial cells of a tissue can be effectively eliminated by physical scraping with a sharp tool or abrasive accompanied by enzymes or salt solution. Physical removal of the extra layers initially helps to make the decellularization regimen more efficient. However, the amount of force required must

be precise because the underlying structure and membrane attachment are vulnerable to any kind of direct mechanical stress [9, 21].

Mechanical agitation and sonication are useful in combination with a chemical treatment to assist in cell lysis and the removal of cellular debris [28, 29]. Mechanical agitation can be applied by using a magnetic stir plate, an orbital shaker, or a low-profile roller. There are no studies to determine the optimal magnitude or frequency of sonication for the disruption of cells. However, the standard ultrasonic cleaner appears to be as effective at removing cellular material as the movement of an orbital shaker. In all of these procedures, the optimal speed, the volume of reagent, and the length of mechanical agitation are dependent on the composition, volume, and density of the tissue [30]. In Forouzesh F. et al. study [31], direct and indirect ultrasonic waves were accompanied by SDS with 0.1% and 1% concentrations as chemical agents to decellularize cartilage tissue. The decellularization process was investigated by nucleus staining with H&E, and by glycosaminoglycans and collagen staining. Results of this study showed that H&E staining indicated that 1% SDS, in addition to ultrasonic bath for 5 h, significantly decreased the cell nucleus remnant to the lacuna ratio by 66%. It is declared that ultrasonic bath helps to a better infiltration of decellularization agents, moreover, it is mentioned that the process time has decreased due to this method and no significant defect has been seen on the structure of the tissue.

In order to select the appropriate decellularization method, the structure of the tissue must be taken into account. These decellularization methods must be carefully selected and tested. If it is necessary to keep the tissue structure intact, the chemical methods must be carefully selected in order not to damage the ECM.

Conclusions

Based on the SEM of the human amniotic membrane, it is possible to assume that the collagen fibers arranged in different directions are an indication that the human amniotic membrane has good mechanical and tensile properties.

The histological examination showed that the membrane consists of three main layers, such as epithelium, basement membrane and stroma, which were previously described in the literature.

The human amniotic membrane decellularization process with 0.5% SDS solution and 1% Triton solution showed that decellularization for 24 hours is too aggressive for the amniotic membrane structure. It shows the disappearance of the epithelium, obliterated basement membrane and disorganization of the architecture of the compact layer. The decellularization methods with 1% Triton solution for 5 hours show incomplete decellularization with some visible cells.

The method of decellularization with 0.5% SDS solution is more suitable for amniotic membrane decellularization and can be performed in only 5 hours.

The use of ultrasound during one hour did not have a significant effect on the decellularization procedure. Based on these results and literature data, it is possible that ultrasound should be used more time in combination with chemical decellularization.

References

1. Mason C, Dunnill P. A brief definition of regenerative medicine. Regen Med. 2008 Jan;3(1):1-5. doi: 10.2217/17460751.3.1.1.
2. Gilpin A, Yang Y. Decellularization strategies for regenerative medicine: from processing techniques to applications. BioMed Res Int. 2017;2017:9831534. doi: 10.1155/2017/9831534.
3. Sarig U, Machluf M. Engineering cell platforms for myocardial regeneration. Expert Opin Biol Ther. 2011;11(8):1055-77. doi: 10.1517/14712598.2011.578574.
4. Cannizzaro SM, Padera RF, Langer R, et al. A novel biotinylated degradable polymer for cell-interactive applications. Biotechnol Bioeng. 1998;58(5):529-535.
5. Davis ME, Hsieh PC, Grodzinsky AJ, Lee RT. Custom design of the cardiac microenvironment with biomaterials. Circ Res. 2005;97(1):8-15. doi: 10.1161/01.RES.0000173376.39447.01
6. Ignatov O, Pascal O, Nacu V. Acupoint embedding therapy. Mold Med J. 2020;63(1):52-58. doi: 10.5281/zenodo.3685665.
7. Akbay E, Onur MA. Scaffold technologies: using a natural platform for stem cell therapy. Medeniyet Med J (Ankara). 2016;31(3):205-212 doi: 10.5222/MMJ.2016.205.
8. Crapo PM, Gilbert TW, Badylak SF. An overview of tissue and whole organ decellularization processes. Biomaterials. 2011;32:3233-43. doi: 10.1016/j.biomaterials.2011.01.057.
9. Gilbert TW. Strategies for tissue and organ decellularization. J Cell Biochem. 2012 Jul;113(7):2217-22. doi: 10.1002/jcb.24130.
10. Inci I, Norouz Dizaji A, Ozel C, Morali U, Dogan Guzel F, Avci H. Decellularized inner body membranes for tissue engineering: a review. J Biomater Sci Polym Ed. 2020;31(10):1287-1368. doi: 10.1080/09205063.2020.1751523.
11. Niknejad H, Peirovi H, Jorjani M, Ahmadiani A, Ghanavi J, Seifalian AM. Properties of the amniotic membrane for potential use in tissue engineering. Eur Cell Mater. 2008 Apr 29;15:88-99. doi: 10.22203/ecm.v015a07.
12. Bourne GL. The microscopic anatomy of the human amnion and chorion. Am J Obstet Gynecol. 1960 Jun;79:1070-3. doi: 10.1016/0002-9378(60)90512-3.
13. van Herendael BJ, Oberti C, Brosens I. Microanatomy of the human amniotic membranes. A light microscopic, transmission, and scanning electron microscopic study. Am J Obstet Gynecol. 1978;131(8):872-80. doi: 10.1016/s0002-9378(16)33135-0.
14. Mamede AC, Carvalho MJ, Abrantes AM, Laranjo M, Maia CJ, Botelho MF. Amniotic membrane: from structure and functions to clinical applications. Cell. 2012;349(2):447-458. doi: 10.1007/s00441-012-1424-6.
15. Gholipourmalekabadi M, Farhadihosseinabadi B, Faraji M, Nourani MR. How preparation and preservation procedures affect the properties of amniotic membrane? How safe are the procedures? Burns. 2020;46(6):1254-71. doi: 10.1016/j.burns.2019.07.005.
16. Ignatov O, Melnic A, Procopciuc V, Mihaluța V, Pascal O, Nacu V. Could human amniotic membrane be a source for acupoint thread embedding therapy? Mold Med J. 2021;64(6):41-48. https://doi.org/10.52418/moldovan-med-j.64-6.21.08.
17. Malhotra C, Jain AK. Human amniotic membrane transplantation: different modalities of its use in ophthalmology. World J Transplant. 2014 Jun 24;4(2):111-21. doi: 10.5500/wjt.v4.i2.111.
18. Fukuda K, Chikama T, Nakamura M, Nishida T. Differential distribution of sub-chains of the basement membrane components type IV collagen and laminin among the amniotic membrane, cornea and conjunctiva. Cornea. 1999;18(1):73-79.

19. Rabbani M, Zakian N, Alimoradi N. Contribution of physical methods in decellularization of animal tissues. J Med Signals Sens. 2021 Jan 30;11(1):1-11. doi: 10.4103/jmss.JMSS_2_20.
20. White LJ, Taylor AJ, Faulk DM, Keane TJ, Saldin LT, Reing JE, Swinehart IT, Turner NJ, Ratner BD, Badylak SF. The impact of detergents on the tissue decellularization process: a ToF-SIMS study. Acta Biomater. 2017 Mar 1;50:207-219. doi: 10.1016/j.actbio.2016.12.033.
21. Keane TJ, Swinehart IT, Badylak SF. Methods of tissue decellularization used for preparation of biologic scaffolds and *in vivo* relevance. Methods. 2015 Aug;84:25-34. doi: 10.1016/j.ymeth.2015.03.005.
22. Woods T, Gratzer PF. Effectiveness of three extraction techniques in the development of a decellularized bone-anterior cruciate ligament-bone graft. Biomaterials. 2005 Dec;26(35):7339-49. doi: 10.1016/j.biomaterials.2005.05.066.
23. Cartmell JS, Dunn MG. Effect of chemical treatments on tendon cellularity and mechanical properties. J Biomed Mater Res. 2000;49(1):134-140. doi: 10.1002/(SICI)1097-4636(200001)49:1<134::AID-JBM17>3.0.CO;2-D.
24. Elder BD, Kim DH, Athanasiou KA. Developing an articular cartilage decellularization process toward facet joint cartilage replacement. Neurosurgery. 2010;66(4):722-727. doi: 10.1227/01.NEU.0000367616.49291.9F.
25. Chen RN, Ho HO, Tsai YT, Sheu MT. Process development of an acellular dermal matrix (ADM) for biomedical applications. Biomaterials. 2004 Jun;25(13):2679-86. doi: 10.1016/j.biomaterials.2003.09.070.
26. Tavassoli A, Matin MM, Niaki MA, Mahdavi-Shahri N, Shahabipour F. Mesenchymal stem cells can survive on the extracellular matrix-derived decellularized bovine articular cartilage scaffold. Iran J Basic Med Sci. 2015 Dec;18(12):1221-7.
27. Ott HC, Matthiesen TS, Goh S, Black LD, Kren SM, Netoff TI, Taylor DA. Perfusion-decellularized matrix: using nature' s platform to engineer a bioartificial heart. Nat Med. 2008;14:213-221 doi: 10.1038/nm1684.
28. Starnecker F, König F, Hagl C, Thierfelder N. Tissue-engineering acellular scaffolds – the significant influence of physical and procedural decellularization factors. J Biomed Mater Res B Appl Biomater. 2018;106(1):153-162. doi: 10.1002/jbm.b.33816.
29. Azhim A, Ono T, Fukui Y, Morimoto Y, Furukawa K, Ushida T. Preparation of decellularized meniscal scaffolds using sonication treatment for tissue engineering. Annu Int Conf IEEE Eng Med Biol Soc. 2013;2013:6953-6. doi: 10.1109/EMBC.2013.6611157.
30. Mendibil U, Ruiz-Hernandez R, Retegi-Carrion S, Garcia-Urquia N, Olalde-Graells B, Abarrategi A. Tissue-specific decellularization methods: rationale and strategies to achieve regenerative compounds. Int J Mol Sci. 2020;21(15):5447. doi: 10.3390/ijms21155447.
31. Forouzesh F, Rabbani M, Bonakdar S. A comparison between ultrasonic bath and direct sonicator on osteochondral tissue decellularization. J Med Signals Sens. 2019 Oct 24;9(4):227-233. doi: 10.4103/jmss.JMSS_64_18.

Authors' ORCID iDs and academic degrees
Olga Ignatov, MD, Scientific Researcher – https://orcid.org/0000-0003-2911-3239
Adrian Cociug, MD, PhD – https://orcid.org/0000-0001-5878-0239
Oleg Pascal, MD, PhD, MPH, Professor – https://orcid.org/0000-0002-4870-2293
Viorel Nacu, MD, PhD, MPH, Professor – https://orcid.org/0000-0003-2274-9912

Authors' contributions
OI conducted literature review, obtained the necessary data and wrote the manuscript; AC monitored the experiment and critically revised the manuscript; OP interpreted the data and drafted the manuscript; VN revised the manuscript critically. All the authors revised and approved the final version of the manuscript.

Funding
The study was supported by the State Program Project 2020-2023: "GaN-based nanoarchitectures and three-dimensional matrices from biological materials for applications in microfluidics and tissue engineering". No 20.80009.5007.20. The trial was the authors' initiative, they are independent and take responsibility for the integrity of the data and accuracy of the data analysis.

Ethics approval and consent to participate
The project was approved by the Research Ethics Committee of *Nicolae Testemitanu* State University of Medicine and Pharmacy (Protocol No14, 15.03.2019).

Conflict of interests
No competing interests were disclosed.

https://doi.org/10.52418/moldovan-med-j.65-2.22.05
UDC: 616.5-089.843-74:576.5

Structural and physical characteristics of the dermal decellularized structures evaluation

[1]Olga Macagonova, [2]Adrian Cociug, [3]Tudor Braniste, [1,2]Viorel Nacu

[1]Laboratory of Tissue Engineering and Cell Cultures, *Nicolae Testemitanu* State University of Medicine and Pharmacy
[2]Human Tissue Bank, Orthopedic and Traumatological Hospital
[3]Technical University of Moldova, Chisinau, the Republic of Moldova

Authors' ORCID iDs, academic degrees and contributions are available at the end of the article

*Corresponding author – Olga Macagonova, e-mail: olga.macagonova@usmf.md
Manuscript received October 03, 2022; revised manuscript December 02, 2022; published online December 20, 2022

Abstract

Introduction: Decellularized biomaterials derived from the biological tissues are ideal for tissue engineering applications because they mimic the biochemical composition of the native tissue. The physical and structural properties of the scaffold are important in the fields of tissue engineering and regenerative medicine.
Material and methods: Study material was 20 decellularized dermal grafts. 10 samples were obtained from piglets slaughtered in the slaughterhouse. Other tissues (n=10) were received from the donor from the Human Tissue and Cell Bank of the Republic of Moldova. Extracellular matrices were obtained by decellularization with 0.5% sodium dodecyl sulfate/0.1% EDTA solution. The evaluation of the structural characteristics was carried out by the histological examination with hematoxylin and eosin, scanning electron microscopy and the quantification of the amount of deoxyribonucleic acids. Assessment of the physical characteristics included analysis of extracellular matrix volume porosity, density, and swelling rate.
Results: Histological examination revealed fewer cells in decellularized tissues compared to non-decellularized ones. More than 80.5% of nucleic acids were removed from porcine matrix and 82.5% of genetic material – from decellularized human dermal structures. A mean correlation and inverse dependence of -0.43 was shown between porosity and swelling rate of decellularized dermis.
Conclusions: The decellularization process significantly ($P<0.05$) removed the cellular components while preserving the connective three-dimensional structure of the dermal matrices clearly shown by quantification of the amount of DNA and microscopic examination of the structures.
Key words: dermis, decellularization, tissue engineering, dermal grafts.

Cite this article
Macagonova O, Cociug A, Braniste T, Nacu V. Structural and physical characteristics of the dermal decellularized structures evaluation. *Mold Med J*. 2022;65(2):36-40. https://doi.org/10.52418/moldovan-med-j.65-2.22.05.

Introduction

The application of human skin allograft for the wound coverage is widely used worldwide [1]. However, complications have been reported in the use of allogeneic skin associated with the immunogenicity of the graft due to major histocompatibility complex antigens [2], the thickness and availability of the grafted skin, which will prolong the duration of the wound healing and increase the risk of graft failure, scar formation in the donor and transplanted region [3].

Decellularized biomaterials derived from biological tissues are ideal for the tissue engineering applications because they mimic the biochemical composition of native tissue [4]. The extracellular matrix (ECM) is composed of structural and regulatory proteins and polysaccharides and is generated and maintained by cells.

Many cellular functions, such as proliferation, migration or differentiation are controlled by the extracellular matrix [5]. Each organ and tissue is composed of an extracellular matrix distinct in its biochemical composition and structural organization. The physical and structural properties of the scaffold are important in the fields of tissue engineering and regenerative medicine. These materials can be used as films, sponges, hydrogels for the encapsulation, delivery of cells and medicinal agents, being transplanted directly into the wound as a biological dressing [6]. The antigenic individuality of the graft recipient requires tissue engineers to follow rules in choosing decellularization agents and techniques to create a valid biomaterial [7].

The methods used for tissue decellularization must contribute to the preservation of the ECM and avoid disruption of the ultrastructure, which may cause an immunogenic response. Preservation of native structural and biomechanical cues is required. The antigenicity of the biomaterial has the effect on the immune response in terms of the interaction between the decellularized extracellular matrix and macrophages with the subsequent influence on the activation of T cells and the occurrence of graft rejection [7]. Modified skin substitutes are developed

from the acellular materials or can be synthesized from autologous, allogeneic, xenogeneic, or synthetic grafts. Each of these engineered skin substitutes have their pros and cons. However, a fully functional skin substitute is not available, and research continues to develop a skin substitute product that can rapidly vascularize.

There is also a need to redesign currently available substitutes to make them user-friendly, commercially accessible and viable with a longer shelf life [2]. The present study focuses on the evaluation of structural and physical characteristics of decellularized dermal structures. The use of decellularized grafts is a way to help the body recover its damaged skin in cases where the healing process is impossible, such as severe wounds [8].

Material and methods

Skin preparation. To achieve the goal, were studied 20 decellularized dermal grafts. 10 samples were obtained from the piglet weighing up to 10 kg euthanized by blunt trauma. Other tissues (n=10) were received from a 40-year-old male donor, obtained from the Human Tissue and Cell Bank of the Republic of Moldova following the recommendations of the university ethics committee. As a result, were obtained 20 samples with an average surface area of 3.06±0.05 cm2 and a weight of 929±0.09 mg.

Separation method. By treating the tissues with 0.3% trypsin solution at 37° C, was obtained the dermal-epidermal separation of the grafts, according to the protocol [9].

Decellularization method. Tissue decellularization was performed by processing the grafts with a 0.5% sodium dodecyl sulfate solution in a 1:4 ratio with 0.1% EDTA for 72 hours. Renewal of the decellularizing solution was done every 24 hours [10].

Evaluation of the structural characteristics. The morphological assessment of the decellularized grafts was performed by histological examination with hematoxylin and eosin, scanning electron microscopy of freeze-dried tissues. Three representative tissue samples were used to determine total DNA content.

Evaluation of the physical characteristics. The analysis of the porosity of the grafts was performed by the method of moving 96% ethanol through the tissue:

$$Porosity\ (\%) = \frac{V_1 - V_3}{V_2 - V_3} \times 100$$

where, V_1 – the known volume of ethanol in which the graft was immersed, V_2 – the volume of ethanol and liquid-soaked tissue, V_3 – the volume of liquid when the soaked tissue was removed [11-14].

The swelling rate (%) of the decellularized tissues was estimated by the ratio of the difference of the final weight of the extracellular matrix soaked in phosphate buffer solution (Ws) and the initial weight of the dry-to-immersion structure (Wd) to the weight of the dry tissue scaffold (Wd) [15]:

$$SR\ (\%) = \frac{W - W}{W_d^s} \times 100$$

The analysis of the density of decellularized grafts was performed according to the equation:

$$d = W/(V2 - V3)$$

where W – weight of fluid-soaked graft, V2 – volume of fluid and fluid-soaked tissue, V3 – volume of fluid when the soaked tissue was removed, (V2 – V3) was the total volume of the scaffold. A minimum of three samples were analyzed for each tissue [16, 17].

Statistical evaluation. Material collection and data estimation were done in Microsoft Excel Worksheet using basic concepts and statistical methods. The interdependence of decellularized tissue characteristics was estimated by Bravais-Pearson correlation. Values of $p<0.05$ were considered statistically significant.

Results

As a result of the decellularization of human and porcine dermis (fig. 1) with sodium dodecyl sulfate 0.5% / EDTA 0.1% solution, were obtained acellular structures.

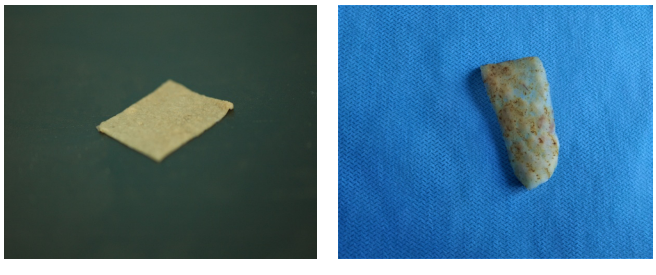

Fig. 1. Native human (a) and porcine dermis (b)

Histologically, in structures decellularized with 0.5% sodium dodecyl sulfate / 0.1% EDTA solution, fewer cells were determined in treated human and porcine dermis compared to non-decellularized structures (fig. 2, 3)

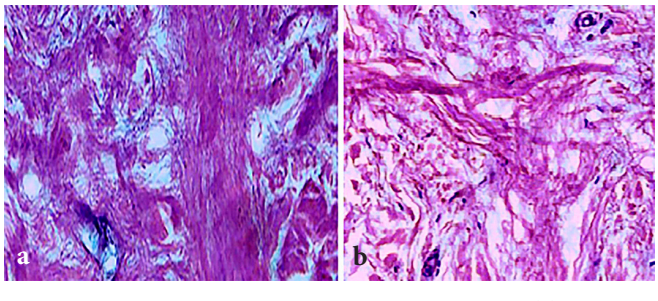

Fig. 2. Histological image of decellularized (a) and intact human dermis (b)

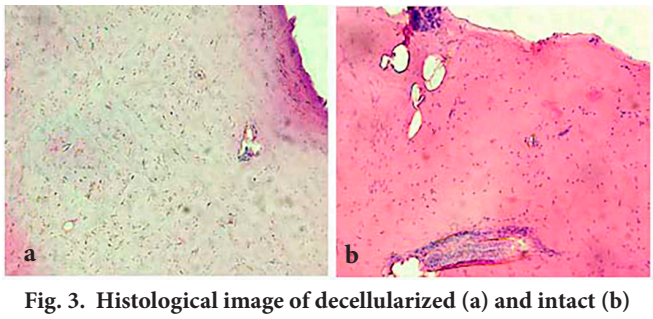

Fig. 3. Histological image of decellularized (a) and intact (b) porcine dermis

Scanning electron microscopy (SEM) shows the three-dimensional (3D) porous image of the human dermis (fig. 4)

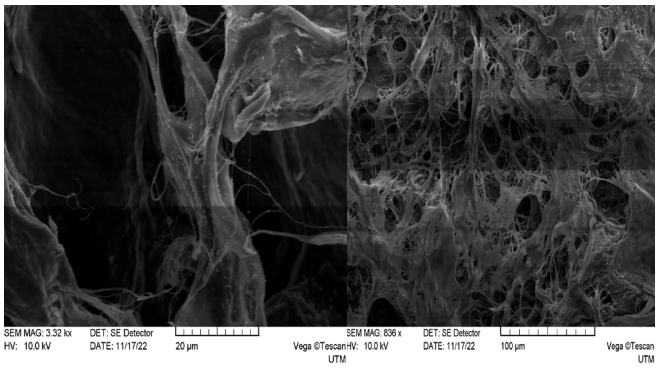

Fig. 4. SEM image shows reticular acellular human dermis

Through the spectrophotometric method, it was determined that in the human dermis decellularized with sodium dodecyl sulfate 0.5%, the amount of deoxyribonucleic acids was 1 ± 0.35 ng/µl compared to the non-cellularized human tissue 13.9 ± 0.4 ng/µl. As a result, it became possible to remove 82.5% of genetic material from human dermal structures. Respectively, 2.43 ± 0.5 ng/µl was determined in the porcine dermis compared to 17.43 ± 3.4 ng/µl in the intact sample, thus 80.5% of the nucleic acids were removed from the porcine matrix.

Evaluating the physical properties of the grafts (surface, volume, density, porosity, swelling rate), were collected the average values of the characteristics (fig. 5, tab. 1).

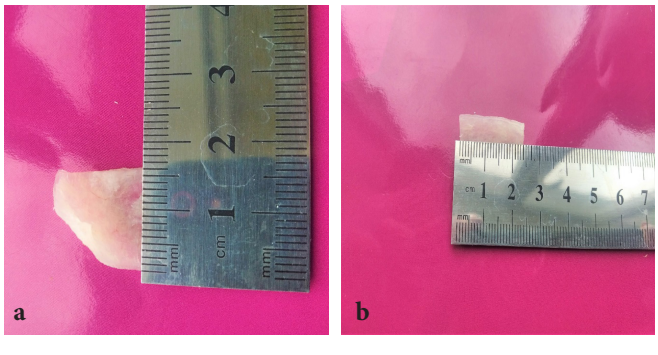

Fig. 5. Estimation of the surface and volume changes of the decellularized porcine dermis following the passage of liquids through the tissue (a, b)

Table 1. Distribution of the physical characteristics of decellularized structures

Characteristics	Human dermis (n=10)	Porcine dermis (n=10)
Surface (cm^2)	3.3±0.1	3.06±0.05
Volume (ml)	4.56±0.05	1.05±0.05
Density (mg/ml)	360±0.83	379.9±0.83
Porosity (%)	35±0.003	53±0.031
Swelling rate (%)	320.4±0.052	650.4±0.65

The significant difference ($P<0.05$) of the characteristics of decellularized dermal structures we observed. Calculating the Bravais-Pearson index showed a medium and weak direct and inverse correlation between density and swelling rate of decellularized porcine dermis 0.33, which means that tissues with significant swelling rate are more or less dense. A mean correlation and inverse dependence of -0.43 was shown between porosity and swelling rate of decellularized porcine dermis, indicating that increasing porosity will decrease the swelling rate of the sponge non-significantly ($P>0.05$).

Discussion

Grafts from xenogeneic dermal substitutes are often applied to extensive skin defects. Although human acellular dermal matrices (ADMs) have shown satisfactory effects in the treatment of large wounds when xenogeneic ADMs do not show immunogenicity due to major histocompatibility complex antigens [18]. An extensive list of animal ADM products is currently available, most of which are achieving success in clinical use. Since the 1960s, pigs have served as primary donors for xenografts in the United States due to their accessibility and histological structural similarities to human skin [19].

Several reports have attested to the benefits of using pigskin in the treatment of extensive wounds. These advantages include reduced healing rates for partial-thickness wounds and granular wounds [19]. Currently available acellular porcine dermal matrices include Permacol (Tissue Sciences Laboratories), Strattice (LifeCell Corp.), Collamend (Bard), Xenoderm (mbp), and XenMatrix (Davol, Inc.) [20]. Researchers have developed protocols for the decellularization of various native tissues [21]. Sodium dodecyl sulfate is the most powerful detergent used to decellularize biological tissues. It is ionic and disrupts all interactions between biomacromolecules. This agent is the most reported in decellularization protocols, and numerous teams have used it to process human skin [22]. SDS treatment is usually performed by immersing the tissue in a 0.5% w/v solution (range of concentrations reported in the literature: 0.1–1%) and takes hours. Thick and complex tissues containing a dense connective layer or a multilayered epithelium, such as the skin, are processed from 12 to 24 hours. All decellularization studies including SDS in concentrations > 0.1% in their protocols reported total removal of cells and cellular debris from native tissue and low levels of remaining DNA [23].

During the given study were found similar results. Porcine skin was decellularized with sodium dodecyl sulfate with the technique used according to the protocol having the amount of DNA of 1 ± 0.35 µg/µl. Sodium dodecyl sulfate is considered an excellent agent for tissue decellularization, but ECM damage has been frequently reported. Loss of ECM density as well as glycosaminoglycan content and collagen network damage have been observed

especially in the matrix produced from fibrillar sheets [24] or in complex tissues such as human skin [25]. Increasing SDS concentration from 0.05% to 0.5% on fibroblast sheets or exposure time from 6 to 12 h was directly correlated with amplification of ECM changes. Scanning electron microscopy studies also suggest rearrangements of ECM fibers and variations in scaffold porosity after SDS treatment. Different combinations of SDS and Triton X-100 were also tested on rat fasciocutaneous flaps, resulting in high DNA removal after perfusion of 1% SDS for 24 or 72 h, followed by Triton X-100 treatment of 1% [26]. Porosity measurement using SEM images is not an accurate method for the porosity analysis of scaffolds.

The ethanol displacement technique was also used by Nokoorani Y.D. et al. in 2021 [8]. Porosity greatly affects the biological and mechanical characteristics of a scaffold. It plays a vital role in cell migration and proliferation and can influence the exchange of gases and nutrients, especially when the vascular system is not functioning sufficiently. Porosity of chitosan and gelatin scaffolds obtained by Nokoorani Y.D. et al. in 2021 was between 27 and 32% using the ethanol displacement technique, which is comparable to the obtained results of 35% ± 0.003 for human tissue and 52% ± 0.031 for porcine tissue. Swellability is an essential property of scaffolds and is also a factor that determines the usability of biomaterials *in vivo* [27]. Traditional dressings are used to keep the wound dry and to defend the body against microorganisms. Therefore, an ideal skin scaffold should absorb wound exudates and keep the wound moist [28, 29]. In the study by Nokoorani Y.D. et al. in 2021 the average swelling rate being 292–377% in the first 15 minutes of the experiment is comparable to the obtained results 320.4±0.052 for human dermis and 650.4±0.65 for porcine matrix [8].

Conclusions

The decellularization process significantly ($P<0.05$) removed the cellular components while preserving the connective three-dimensional structure of the dermal matrices clearly shown by quantification of the amount of deoxyribonucleic acids and microscopic examination of the decellularized dermal structures. Decellularization of the dermis led to the change in density, volume and swelling rate significantly ($P<0.05$). Increasing the porosity of the decellularized dermal structures resulted in a non-significant ($P>0.05$) decrease in the swelling rate of the sponge. Decellularized dermal tissue shows value for regenerative medicine by being readily available without the use of complex chemical syntheses and complicated manufacturing processes.

References

1. Megahed MA, Elkashity SA, Talaab AA, et al. The impact of human skin allograft as a temporary substitute for early coverage of major burn wounds on clinical outcomes and mortality. Ann Burns Fire Disasters. 2021;34(1):67-74.
2. Vig K, Chaudhari A, Tripathi S, et al. Advances in skin regeneration using tissue engineering. Int J Mol Sci. 2017;18(4):789. doi: 10.3390/ijms18040789.
3. Dixit S, Baganizi DR, Sahu R, et al. Immunological challenges associated with artificial skin grafts: available solutions and stem cells in future design of synthetic skin. J Biol Eng. 2017;11:49. https://doi.org/10.1186/s13036-017-0089-9.
4. Fernández-Pérez J, Ahearne M. The impact of decellularization methods on extracellular matrix derived hydrogels. Sci Rep. 2019;9(1):1-12. doi: 10.1038/s41598-019-49575-2.
5. Frantz C, Kathleen MS, Weave VM. The extracellular matrix at a glance. J Cell Sci. 2010;123(24):4195-4200. doi: 10.1242/jcs.023820.
6. Sivaraj D, Chen K, Chattopadhyay A, et al. Hydrogel scaffolds to deliver cell therapies for wound healing. Front Bioeng Biotechnol. 2021;9:660145. doi: 10.3389/fbioe.2021.660145.
7. Chakraborty J, Roy S, Ghosh S. Regulation of decellularized matrix mediated immune response. Biomater Sci. 2020;8(5):1194-1215. doi: 10.1039/c9bm01780a.
8. Nokoorani YD, Shamloo A, Bahadoran M, et al. Fabrication and characterization of scaffolds containing different amounts of allantoin for skin tissue engineering. Sci Rep. 2021;11(1):16164. https://doi.org/10.1038/s41598-021-95763-4.
9. Wilkinson DI, Walsh JT. Effect of various methods of epidermal-dermal separation on the distribution of 14C-acetate-labeled polyunsaturated fatty acids in skin compartments. J Invest Dermatol. 1974;62(5):517-521. doi: 10.1111/1523-1747.ep12681061.
10. Böer U, Lohrenz A, Klingenberg M, et al. The effect of detergent-based decellularization procedures on cellular proteins and immunogenicity in equine carotid artery grafts. Biomaterials. 2011;32(36):9730-9737. doi: 10.1016/j.biomaterials.2011.09.015.
11. Hu Y, Grainger DW, Winn SR, Hollinger JO. Fabrication of poly (α-hydroxy acid) foam scaffolds using multiple solvent systems. J Biomed Mater Res. 2002;59(3):563-572. doi: 10.1002/jbm.1269.
12. Maspero FA, Ruffieux K, Müller B. Wintermantel E. Resorbable defect analog PLGA scaffolds using CO_2 as solvent: structural characterization. J Biomed Mater Res. 2002;62(1):89-98. doi: 10.1002/jbm.10212.
13. Kim HW, Knowles JC, Kim HE. Hydroxyapatite/poly(ε-caprolactone) composite coatings on hydroxyapatite porous bone scaffold for drug delivery. Biomaterials. 2004;25(7-8):1279-1287. doi: 10.1016/j.biomaterials.2003.07.003.
14. Guarino V, Causa F, Taddei P, et al. Polylactic acid fibre-reinforced polycaprolactone scaffolds for bone tissue engineering. Biomaterials. 2008;29(27):3662-3670. doi: 10.1016/j.biomaterials.2008.05.024.
15. Malagón-Escandón A, Hautefeuille M, Jimenez-Díaz E, et al. Three-dimensional porous scaffolds derived from bovine cancellous bone matrix promote osteoinduction, osteoconduction, and osteogenesis. Polymers. 2021;13(24):1-26. doi: 10.3390/polym13244390.
16. Loh QL, Choong C. Three-dimensional scaffolds for tissue engineering applications: role of porosity and pore size. Tissue Eng Part B Rev. 2013;19(6):485-502. doi: 10.1089/ten.TEB.2012.0437.
17. Tziveleka LA, Sapalidis A, Kikionis S, et al. Hybrid sponge-like scaffolds based on ulvan and gelatin: design, characterization and evaluation of their potential use in bone tissue engineering. Materials (Basel). 2020;13(7):1763. doi: 10.3390/ma13071763.
18. Yu G, Ye L, Tan W, et al. A novel dermal matrix generated from burned skin as a promising substitute for deep-degree burns therapy. Mol Med Rep. 2016;13(3):2570-2582. doi: 10.3892/mmr.2016.4866.
19. Imahara SD, Klein MB. Skin grafts. In: Orgill DP, Blanco C, editors. Biomaterials for treating skin loss. Cambridge, UK: CRC; 2009. p. 58-79.
20. Yamamoto T, Iwase H, King T, et al. Skin xenotransplantation: historical review and clinical potential. Burns. 2018;44(7):1738-1749. doi: 10.1016/j.burns.2018.02.029.
21. Dussoyer M, Michopoulou A, Rousselle P. Decellularized scaffolds for skin repair and regeneration. Appl Sci. 2020;10(10):3435. doi: 10.3390/app10103435.
22. Qu J, Van Hogezand RM, Zhao C, et al. Decellularization of a fasciocutaneous flap for use as a perfusable scaffold. Ann Plast Surg. 2015;75(1):112-116. doi: 10.1097/SAP.0000000000000157.

23. Chien PN, Zhang XR, Nilsu D, et al. *In vivo* comparison of three human acellular dermal matrices for breast reconstruction. *In Vivo*. 2021 Sep-Oct;35(5):2719-2728. doi: 10.21873/invivo.12556.
24. Xing Q, Yates K, Tahtinen M, et al. Decellularization of fibroblast cell sheets for natural extracellular matrix scaffold preparation. Tissue Eng Part C Methods. 2014;21(1):77-87. doi: 10.1089/ten.tec.2013.0666.
25. Carruthers CA, Dearth C, Reing J. Histologic characterization of acellular dermal matrices in a porcine model of tissue expander breast reconstruction. Tissue Eng Part A. 2014;21(1-2):35-44. doi: 10.1089/ten.TEA.2014.0095.
26. Cui H, Chai Y, Yu Y. Progress in developing decellularized bioscaffolds for enhancing skin construction. J Biomed Mater Res Part A. 2019;107(8):1849-59. doi: 10.1002/jbm.a.36688.
27. Rousselle P, Montmasson M, Garnier C. Extracellular matrix contribution to skin wound re-epithelialization. Matrix Biol. 2019;75-76:12-26. doi: 10.1016/j.matbio.2018.01.002.
28. Hu S, Bi S, Yan D, et al. Preparation of composite hydroxybutyl chitosan sponge and its role in promoting wound healing. Carbohydr Polym. 2018;184:154-63. doi: 10.1016/j.carbpol.2017.12.033.
29. Porzionato A, Stocco E, Barbon S, et al. Tissue-engineered grafts from human decellularized extracellular matrices: a systematic review and future perspectives. Int J Mol Sci. 2018;19(12):4117. doi: 10.3390/ijms19124117.

Authors' ORCID iDs and academic degrees
Olga Macagonova, MD, PhD, Scientific Researcher – https://orcid.org/0000-0003-4414-3196
Adrian Cociug, MD, PhD, Scientific Researcher – https://orcid.org/0000-0001-5878-0239
Tudor Braniste, TechD, Math PhD, Scientific Researcher – https://orcid.org/0000-0001-6043-4642
Viorel Nacu, MD, PhD, MPH, Professor – https://orcid.org/0000-0003-2274-9912

Authors' contributions
OM proposed the concept and design of research, selected the literature and contributed to the elaboration and writing of the manuscript. AC and TB performed microscopic images and helped draft the manuscript. VN conceptualized the idea, designed the research and monitored the experiment. All the authors approved the final version of the manuscript.

Funding
The study was supported by the State Program Project 2020-2023: "GaN-based nanoarchitectures and three-dimensional matrices from biological materials for applications in microfluidics and tissue engineering". No 20.80009.5007.20. The trial was the authors' initiative; they are independent and take responsibility for the integrity of the data and accuracy of the data analysis.

Ethics approval and consent to participate
The project was approved by the Research Ethics Committee of *Nicolae Testemitanu* State University of Medicine and Pharmacy (Protocol No 31, 14.12.2016).

Conflict of interests
No competing interests were disclosed.

https://doi.org/10.52418/moldovan-med-j.65-2.22.06
UDC: 615.322:582.949.27(478)

Polyphenolic content and antioxidant activity of *Hyssopus officinalis* L. from the Republic of Moldova

[1,3]Anna Benea,*[2,3]Cristina Ciobanu, [2,3]Nicolae Ciobanu, [3]Irina Pompus, [1,3]Maria Cojocaru-Toma

[1]Department of Pharmacognosy and Pharmaceutical Botany, [2]Department of Drug Technology
[3]Scientific Practical Centre in the Field of Medicinal Plants
Nicolae Testemitanu State University of Medicine and Pharmacy, Chisinau, the Republic of Moldova

Authors' ORCID iDs, academic degrees and contributions are available at the end of the article

*Corresponding author – Cristina Ciobanu, e-mail: cristina.ciobanu@usmf.md

Manuscript received November 07, 2022; revised manuscript December 02, 2022; published online December 20, 2022

Abstract

Background: *Hyssopus officinalis* L. (hyssop), a species native to the Caspian Sea region, has been cultivated in the Republic of Moldova as aromatic plant and has been used in folk medicine as antitussive, expectorant, carminative, digestive and sedative remedy.
Material and methods: The aerial parts of *H. officinalis* L., with pink, white and blue flowers, were collected from the collection of the Scientific Practical Center in the Field of Medicinal Plants during flowering phase. The extracts were obtained with 70% ethanol by maceration with stirring. The concetration of the extracts was done with the rotative evaporator Laborota 4011. Identification of phenolic compounds in dried extracts from hyssop herb was carried out by thin-layer chromatography. The total content of hydrocyanamic acids was measured in plant products and dried ethanolic extracts, by spectrophotometric method, with Arnow's reagent. Quantitative analysis of total phenolic content was carried out by UV-spectrophotometry analysis, using a Metertech UV/VIS SP 8001 spectrophotometer.
Results: The chlorogenic (Rf 0.47) and caffeic (Rf 0.93) acids were identified in the three genotypes of *Hyssop herba,* with pink, white and blue flowers. The total of hydroxycinnamic acids, expressed in caffeic acid, for both, aerial parts and dry extract, was the highest in *H. officinalis* L. with white flowers (1.484 mg/g; 3.014 mg/g respectively), followed by *H. officinalis* L. with pink flowers (1.190 mg/g; 2.915 mg/g) and *H. officinalis* L. with blue flowers (1.015 mg/g; 2.851 mg/g).
The highest polyphenol content, expressed in gallic acid equivalent (GAE), was found in the dry extract of *H. officinalis* L. with blue flowers (39.056 mgGAE/g dry extract).
Conclusions: This study showed that the extract of the *Hyssopus officinalis* L. containing phenolic compounds, can be used as a natural antioxidant in pharmaceutical and cosmetic industries.
Key words: *Hyssopus officinalis* L, phenolic compounds, antioxidant activity.

Cite this article
Benea A, Ciobanu C, Ciobanu N, Pompus I, Cojocaru-Toma M. Polyphenolic content and antioxidant activity of *Hyssopus officinalis* L. from the Republic of Moldova. *Mold Med J.* 2022;65(2):41-46. https://doi.org/10.52418/moldovan-med-j.65-2.22.06.

Introduction

Phenolic compounds are members of the largest group of plant secondary metabolites and have the main function to protect the plants against ultraviolet radiation or invasion by pathogens [1]. They can be divided into four distinct classes based on the number of phenol rings and structural fragments connecting them, namely phenolic acids, flavonoids, stilbenes and lignans [2]. The first class generally involves the phenolic compounds possessing a carboxylic acid as the main functional group [3], thus being named as phenolic acids, which are further split into two groups, namely hydroxybenzoic and hydroxycinnamic acids [4].

Hydroxycinnamic acid derivatives comprise a large group of simple phenolic acids, are abundant in fruits, vegetables and cereals and seeds of fruits. Ferulic acid, caffeic acid, p-coumaric acid, chlorgenic acid, sinapic acid, curcumin and rosmarinic acid belong to this important phenolic acid group [3].

Hyssopus officinalis L. (hyssop) belonging to the family Lamiaceae, is a perennial herbaceous plant from Southern Europe and some temperate regions of Asia. Hyssop, which is one of the most important pharmaceutical herbs, is extensively cultivated in central and South European countries, such as Spain, France and Italy [4]. Hyssop has thick ramified roots and several 20-60 cm high wooden stems. This plant has small, paired, pointed and very fragrant leaves and purplish darkblue, white and occasionally red flowers [5-7].

Hyssop has been exploited for many uses. It is well known for its aromatic scent, and as an ornamental and bee attracting plant. The aerial parts are used in the food industry as a condiment and spice or as a minty flavor. In traditional medicine, the plant has long been used as

a carminative, tonic, antiseptic, expectorant and cough reliever [8].

The aerial shoots of this herbaceous perennial are useful for the treatment of respiratory diseases, including asthma, bronchitis and cough, as they contain chemicals, such as terpenes, flavonoids, volatile oils, tannins and resins [5]. In *H. officinalis* L., from flavonoids group, apigenin, quercetin, diosmin, luteolin and their glucosides, and from other phenolic compounds – chlorogenic, protocatechuic, ferulic, syringic, p-hydroxybenzoic and caffeic acids are present. Reports on the essential oils extracted from aerial parts of *H. officinalis* L. revealed several principal components, including terpenoids pinocamphone, isopinocamphone and β-pinene [9].

The extracts and the essential oil isolated from hyssop showed moderate antioxidant and antimicrobial activity together with antifungal and insecticidal antiviral properties, *in vitro*. The ethanol extract of hyssop has been recently reported to present protective properties for the gastric tract based on the adhesive stomach mucosal compounds, and also significant anticoagulant and antioxidant properties through reducing the production of free radicals [5]. Animal model studies indicated myorelaxant, antiplatelet, and α-glucosidase inhibitory activities for this plant. The essential oil is mainly used for flavouring and food preservation and for phytotherapeutic uses [10]. Research suggests that hyssop essence has special antimicrobial effects on bacteria, such as *Streptococcus pyogenes*, *Staphylococcus aureus, Escherichia coli* and *Candida albicans* [5].

The purpose of this study was to investigate the content of the secondary metabolites accumulated in the aerial parts of hyssop cultivated in the Republic of Moldova, comparison of 3 genotypes with distinctive morphological characters highlighted by the colour of flowers (blue, pink and white) and evaluation of polyphenolic content and antioxidant capacity of the extractive products of the plant.

Material and methods

As plant material, the aerial parts of 3 genotypes of *Hyssopus officinalis* L. – hyssop with blue flowers, hyssop with pink and white flowers, collected from the Scientific Practical Center in the Field of Medicinal Plants of *Nicolae Testemitanu* State University of Medicine and Pharmacy, were used. The product was sampled during July 2022.

Obtaining the dry extract by the fractional maceration method

The method of fractional maceration with stirring was used for the extraction. 10 g of chopped plant product (*Hyssopi officinalis herba*) were treated with 5 portions of 200 ml ethanol 70% each, in a ratio of 1:10. All extraction phases lasted 60 min, with the separation of the extractive liquid from the vegetable residue. Fractions of extractive solutions stayed in the refrigerator for 5-6 hours at +50°C, then they were filtered through Whatman filter paper No 2, using the Buchner funnel. The Laborota 4011 digital rotary evaporator was used to concentrate the extractive solutions. The alcohol was evaporated at 40°C. The stirring was carried out with a magnetic stirrer at room temperature [11, 12].

Qualitative analysis by Thin Layer *chromatography* (TLC)

The qualitative evaluation of the alcoholic plant extractions was carried out on a silica TLC plate. The time of extraction was 60 min. Test solution: 0.05 g of dry extract was dissolved in 70% ethanol in a 25 ml volumetric flask. Reference solution: 0.1% solutions of rutin, hyperoside, isoquercetin, quercetol, apigenin, luteolin, gallic acid, chlorogenic acid, caffeic acid. Stationary phase: silica gel plates. Mobile phase: ethyl acetate: formic acid: water (6:9:90). Migration: 12.4 (extraction duration 1 hour) – 12.5 (extraction duration 15 min) cm. Plate drying: 100-105°C for 10 min. Detection: The plate was sprayed with a 3% solution of $AlCl_3$. After 30 min the plate was examined under UV light at a wavelength of 366 nm [12].

Determination of total hydroxycinnamic acids

The preparation of the stock solution from aerial plant products was performed with 80 ml of 50% ethyl alcohol mixed with 0.2 g of crushed plant product, boiled on a water bath under reflux condenser for 30 minutes, then cooled and filtered into a volumetric flask with 100 ml capacity. The entire volume was adjusted to the mark with 50% ethanol. Stock solution of dry extracts: 0.01 g of dry extract was dissolved with 80% ethanol, brought up to level in a 10 ml volumetric flask with the same solvent. The test solution: 1 ml of stock solution, 2 ml of 0.5 M hydrochloric acid, 2 ml of Arnow's reagent (prepared by dissolving 10 g of sodium nitrite and 10 g of sodium molybdate in 100 ml of water), 2 ml of 8.5% sodium hydroxide solution, adjusted up to the mark of 10 ml with purified water. The whole mixture was stirred. Blank solution: 1 ml of the stock solution adjusted up to 10 ml with distilled water. The absorbance of the test solution was immediately measured at 518 nm [13].

Determination of total polyphenol content

The quantitative analysis of the polyphenols, in the plant products of hyssop and in the dry extracts, was carried out by the spectrophotometric method with the Folin-Ciocalteu reagent, using gallic acid as standard. The samples from the dried hyssop extracts were prepared as 1 mg/ml with 70% ethyl alcohol. From each solution obtained, an aliquot of 1 ml, 5 ml of Folin-Ciocalteu reagent (1:10) was added, and stirred for one minute. After that 4 ml of 4% sodium carbonate solution were added. After stirring the mixture was left for 2 hours at room temperature in a dark place. The absorbance on Metertech UV/VIS SP8001 spectrophotometer at a wavelength of 765 nm was measured. Total polyphenolic content was expressed in mg gallic acid equivalent/g absolute dry mass of hyssop extract. The total polyphenol in the analyzed samples was

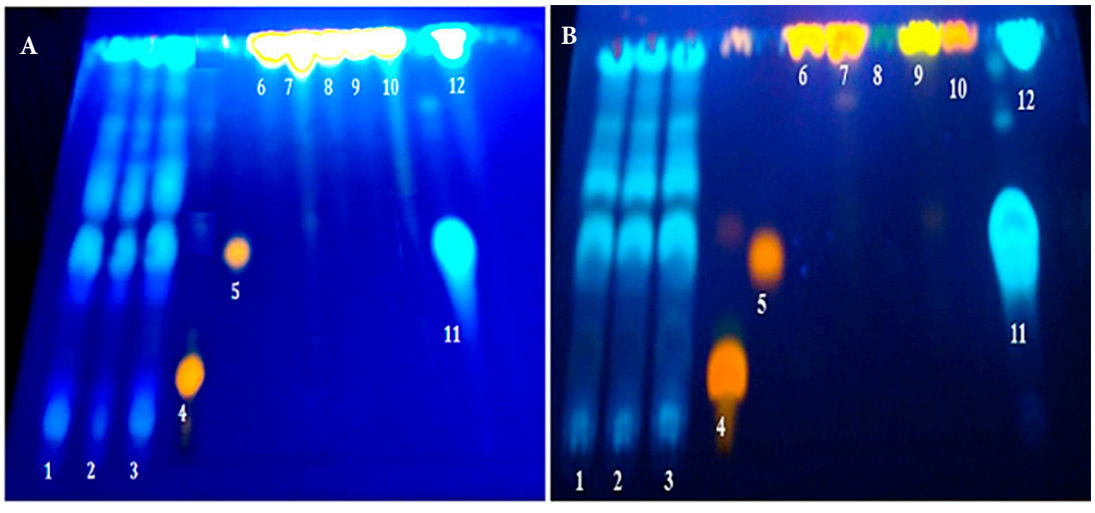

Fig. 1. Chromatogram of plant products (A) and dried extracts (B) of *Hyssopus officinalis* L. under UV light 366 nm

Samples from aerial parts with: 1 – white flowers, 2 – pink flowers, 3 – blue flowers. Standard substances: 4 – rutin, 5 – hyperoxide, 6 – isoquercetol, 7 – quercetol, 8 – apigenin, 9 – luteolin, 10 – myricetol, 11 – chlorogenic acid, 12 – caffeic acid

calculated using the calibration curve established under the same conditions as the analyzed solutions. All measurements were performed 3 times [14].

Determination of the antioxidant activity by the DPPH method

Stock solution: in a 100 ml volumetric flask, 20 mg of 1,1-diphenyl-2-picrylhydrazyl (DPPH) were added and adjusted up to the mark with 96% ethyl alcohol (concentration 200 mg/l). The given solution was kept at +4°C, in aluminum foil, for no more than a week. 5 ml of stock solution were withdrawn to a 50 ml volumetric flask and adjusted up to the mark with 96% ethanol (concentration 1 mg/ml). From this solution, the dilutions for the calibration curve (200, 100, 75, 50, 25, 10, 5 μg/ml) were prepared. The test solution: 1.5 ml of ethanolic solution was added to 3 ml of DPPH solution (20 mg/l). Absorbance was measured at a wavelength of 517 nm, 96% ethyl alcohol was used as blank solution [15-17].

All chemicals used were of analytical grade. Gallic acid, rutin, hyperoside, isoquercetin, quercetol, apigenin, luteolin, chlorogenic acid, caffeic acid, sodium hydroxide, sodium nitrite, Trolox, DPPH and Folin-Ciocalteu reagent all were obtained from Sigma Aldrich Corporation.

The experiments were carried out in triplicates and statistical analysis was performed by Excel 2020 using $p< 0.05$ significance level.

Results and discussion

Identification of flavonoids by TLC was performed to identify flavonoids in plant products and dry extracts. The extracts were dissolved in 70% ethanol. The analyzed samples and the controls were applied to the chromatographic plate (20x20 cm). After the development, the yellow color predominated, but the shades were different. The spots were analyzed with an ultraviolet lamp (fig. 1). To identify the substances, the Rf value and fluorescence of the spots obtained with the sample solution and the Rf value and fluorescence of the spots obtained with the reference solution were compared.

Thus, after analyzing the chromatogram in UV light at λ = 366 nm it was observed that in all the three genotypes of *Hyssopus officinalis* L. (white, pink and blue flowers), the blue spots corresponding to numbers 8 and 9 could be clearly observed, which denotes the presence of caffeic and chlorogenic acids. Also, in addition to the identified substances, a number of substances were separated on the plate, which demonstrates the diversity of compounds from the aerial parts of hyssop. The qualitative analysis by TLC demonstrated the presence, in plant products, along with the dry extracts, obtained from the 3 genotypes of *H. officinalis* L., of chemical compounds from flavonoid group: rutin (Rf = 0.21), caffeic acid (Rf = 0.93) and chlorogenic acid (Rf = 0.47), the chromatograms of the genotypes being practically identical.

Quantitative determination of total hydroxycinnamic acids

The European Pharmacopoeia method, for determining the total hydroxycinnamic acids (THA), describes the determination of the THA in the aerial parts of the plant and in its dry extract, using the Arnow's reagent (10% aqueous solution of sodium nitrite and sodium molybdate, 2 ml). Analysis of each sample was performed in triplicate. Following the experience, it was observed that the leader among the genotypes with the highest content of THA expressed in caffeic acid was the *H. officinalis* L. with white flowers (1.484±0.620 mg/g) as shown in fig. 2; the lowest content of THA was determined in *H. officinalis* L. with blue flowers (1.015±0.024 mg/g).

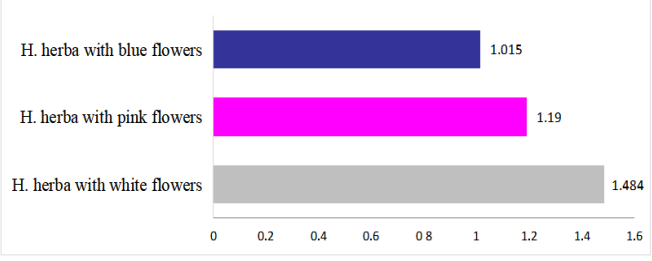

Fig. 2. The total content of hydroxycinnamic acids in plant products from the aerial parts of *Hyssopus officinalis* L. (mg/g)

The evaluation of THA in the hyssop dry extracts, revealed that the richest content was present in the dried extract of *H. officinalis* L. with white flowers (3.014±0.114 mg/g) followed by *H. officinalis* L. with pink flowers (2.915±0.126 mg/g) and *H. officinalis* L. with blue flowers (2.851±0.103 mg/g).

Quantitative determination of total polyphenols in plant products and dry extracts from the aerial parts of *Hyssopus officinalis* L. was identified by the spectrophotometric method in recalculation to gallic acid. The absorbance was read on a UV-VIS spectrophotometer over 90 min at a wavelength of 765 nm. The calibration curve was prepared in the following concentrations: 0.01; 0.02; 0.03; 0.06; 0.08 mg/ml (fig. 3) in methanol from standard 1 solution of gallic acid.

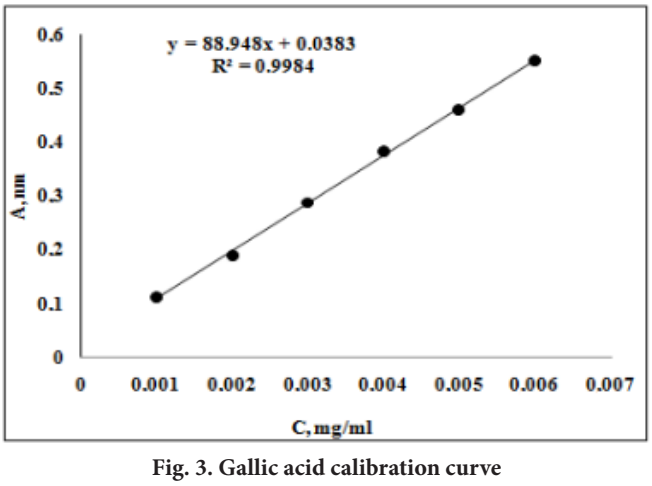

Fig. 3. Gallic acid calibration curve

The total polyphenol content (TPC) was ca culated according to the following formula: x=(y+0.0383)×250) /88.948 in gallic acid equivalent mg/g dry mass. The highest amount of phenolic componds was determined in aerial parts of hyssop with blue flowers (12.256±0.120 mg-GAE/g) and the lowest content in aerial parts of hyssop with white flowers (8.012±0.059 mgGAE/g), as shown in fig. 4.

The spectrophotometric dosage of TPC in dry extracts, demonstrated that the highest content was found in *H. officinalis* L. with blue flowers (39.056±0.894 mg/g dry extract), followed by the dry extract of *H. officinalis* L. with white flowers (36.111±0.314 mg/g) and the dry extract of *H. officinalis* L. with pink flowers (33.078±0.620 mg/g). The obtained results demonstrated the advantage of concentration of liquid extractive products and solvent evaporation, thus increasing the content of phenolic compounds.

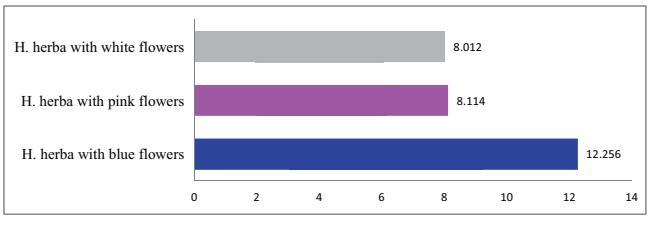

Fig. 4 The content of total polyphenols in plant products from the aerial parts of *Hyssopus officinalis* L. (mgGAE/g)

There are only few reports on the polyphenolic content of hyssop and no comparisons of different accessions of the species. Németh-Zámbori E. et al. reported significant difference in the total phenolic content among genotypes, that ranged from 443.64 mg/g DW ('Erfurter Ysop') and 329.32 mg/g DW ('Hyzop lekarsky') calculated as gallic acid. The effect of the year was not significant, although, detected a significant variety in year interaction for the species cultivated in Hungary [18].

Determination of the antioxidant activity by the DPPH method

The 1,1-diphenyl-2-picrylhydrazyl (DPPH) radical is a stable radical with a maximum absorption at 517 nm that can readily undergo reduction by an antioxidant. Because of the ease and convenience of this reaction it now has widespread use in the free radical-scavenging activity assessment [19]. Determination of the antioxidant action using the DPPH test (tab. 1), revealed that all three studied hyssop genotypes, *H. officinalis* L. with blue flowers (IC_{50}=38.091 mg/ml), *H. officinalis* L. with pink flowers (IC_{50}=34.172 mg/ml) as well as *H. officinalis* L. with white flowers (IC_{50}=34.774 mg/ml) possess high antioxidant properties, compared to the standard substance Trolox (IC_{50}=3.15 mg/ml).

Table 1. Total phenolic content and antioxidant activity of dry extracts from aerial parts of different *Hyssopus officinalis* L. genotypes

Hyssop samples	TPC mg GAE/g	THA mg CA/g	IC_{50}, mg/ml M±SD
Dry extract of *H. herba* with white flowers	36.111±0.314	3.014±0.114	34.774±1.954
Dry extract of *H. herba* with pink flowers	33.078±0.620	2.915±0.126	34.172±0.682
Dry extract of *H. herba* with blue flowers	39.056±0.894	2.851±0.103	38.091±0.288
Trolox			3.15±0.147

Each value is the mean ± SD of three independent measurements

Fathiazad F. et al. demonstrated the total phenolic content in the n-butanol and ethylacetate extracts of the aerial parts of *H. officinalis* L. from Iran was found to be

246 mg gallic acid equivalent GAE/g and 51 mg GAE/g [20]. Comparing the polyphenolic content, the methanolic extract obtained from Iranian *H. officinalis* L. var. *angustifolius* was richer than the ethanolic extract obtained from Romanian hyssop (90 mg/g and 77.72 mg/g, respectively) [10]. The antioxidant activity of ethanolic extract of *H. officinalis* L. (IC_{50}=125.44±4.70 μg/ml), native to Romania, was evaluated by DPPH radical scavenging, with Trolox as a positive control (IC_{50} = 11.20±0.20 μg/ml) [10].

The contents of total polyphenols in six samples of *H. officinalis* L. were collected from five localities on the territory of Montenegro, ranged between 64.1 and 112.0 mg GAE/g. The content of chlorogenic acid was in the range between 23.35 and 33.46 mg/g, whereas rosmarinic acid was present in lower amounts (3.53–17.98 mg/g). The sample richest in chlorogenic and rosmarinic acids was also the richest in total polyphenols. The methanol extracts expressed moderate to weak antioxidant activity (DPPH IC_{50} = 56.04-199.89 μg/ml), compared to the rutin methanolic solution [21].

Ethanolic extracts of *H. officinalis* L. var. angustifolius stems, leaves, and flowers showed good antioxidant activity. Inhibitory concentration (IC_{50}) for DPPH scavenging was found to be 148.8±4.31 μg/ml for flowers, 208.2±6.45 μg/ml for leaves and 79.9±2.63 μg/ml for stems [22].

Conclusions

The experimental findings show that dry extracts of hyssop cultivated in the Republic of Moldova, contain considerable amounts of hydroxycinnamic acids and polyphenols due to which, the free radical scavenging power, determined with DPPH method is comparable with Trolox standard. The findings of this study specify the importance of *Hyssopus officinalis* L. as a readily available source of antioxidants in order to prevent the occurrence of neurosis and hyper-excitability, liver dysfunction, inflammatory diseases for which free radicals are considered important contributing factors.

References

1. Sova M, Saso L. Natural sources, pharmacokinetics, biological activities and health benefits of hydroxycinnamic acids and their metabolites. Nutrients. 2020;12(8):2190. doi: 10.3390/nu12082190.
2. Manach C, Scalbert A, Morand C, Rémésy C, Jimenez L. Polyphenols: food sources and bioavailability. Am J Clin Nutr. 2004;79(5):727-47. doi: org/10.1093/ajcn/79.5.727.
3. Kizil S, Haşimi N, Tolan V, Kilinç E, Karataş H. Chemical composition, antimicrobial and antioxidant activities of hyssop (*Hyssopus officinalis* L.) essential oil. Notulae Botanicae Horti Agrobotanici Cluj-Napoca. 2010;38(3):99-103. doi: 10.15835/nbha3834788.
4. Figueredo G, Özcan MM, Chalchat JC, Bagci Y, Chalard P. Chemical composition of essential oil of *Hyssopus officinalis* L. and *Origanum acutidens*. J Essent Oil Bear Plants. 2012;15(2):300-306. doi: 10.1080/0972060X.2012.10644051.
5. Moulodi F, Khezerlou A, Zolfaghari H, et al. Chemical composition and antioxidant and antimicrobial properties of the essential oil of *Hyssopus officinalis* L. J Kermanshah Univ Med Sci. 2018;22(4):e85256. doi: 10.5812/jkums.85256.
6. Goncearuc M. Genotipuri de *Hyssopus officinalis* L. cu conținut și componență diferită a uleiului esențial [*Hyssopus officinalis L.* genotypes with different essential oil content and composition]. [Bul Acad Sci Moldova. Life Sci]. 2013;1(319):86-96. Romanian.
7. Ciobanu N, Cojocaru-Toma M, Pompuș I, Chiru T, Ciobanu C, Benea A. Plante din colecția Centrului Științific de cultivare a Plantelor medicinale USMF "Nicolae Testemițanu" [Plants from the collection of the Scientific Center for Cultivation of Medicinal Plants of *Nicolae Testemtanu* State University of Medicine and Pharmacy]. Chisinau; 2019. 214 p. ISBN 978-9975-56-660-5.
8. Venditti A, Bianco A, Frezza C, et al. Essential oil composition, polar compounds, glandular trichomes and biological activity of *Hyssopus officinalis* L. subspices *aristatus* (Godr.) Nyman from central Italy. Ind Crops Prod. 2015;77:353-363. https://doi.org/10.1016/j.indcrop.2015.09.002.
9. Fathiazad F, Hamedeyazdan S. A review on *Hyssopus officinalis* L.: composition and biological activities. Afr J Pharm Pharmacol. 2011;5(17):1959-1966. doi: 10.5897/AJPP11.527.
10. Vlase L, Benedec D, Hanganu D, et al. Evaluation of antioxidant and antimicrobial activities and phenolic profile for *Hyssopus officinalis*, *Ocimum basilicum* and *Teucrium chamaedrys*. Molecules. 2014;19(5):5490-507. doi: 10.3390/molecules19055490.
11. Popovici I, Lupuleasa D. Tehnologie farmaceutică [Pharmaceutical technology]. Vol. 1. Iași: Polirom; 1997. 605 p. Romanian.
12. Benea A. Conținutul polifenolic în extracte uscate de *Hypericum perforatum* L. din flora Republicii Moldova [The polyphenol content in dry extracts of Hypericum perforatum L. from the flora of the Republic of Moldova]. [Scientific Annals of *Nicolae Testemitanu* State University of Medicine and Pharmacy. 14th ed. Vol. 1]. Chisinau: Medicina; 2013. p. 411-416. Romanian.
13. Mahdavi H, Naderi MR, Esmaeili MH. Comparison of two spectrophotometric methods for quantifying total hydroxycinnamic acids in coneflower (*Echinacea purpurea*) preparations. J Herb Drugs. 2018;8(4):235-242. doi: 10.14196/JHD.2018.235.
14. Singleton VL, Orthofer R, Lamuela-Raventos RM. Analysis of the phenols and other oxidation substrates and antioxidants by means of Folin-Ciocalteu reagent. Methods Enzymology. 1999;299:152-177. https://doi.org/10.1016/S0076-6879(99)99017-1.
15. Flieger J, Flieger M. The [DPPH•/DPPH-H]-HPLC-DAD method on tracking the antioxidant activity of pure antioxidants and goutweed (*Aegopodium podagraria* L.) hydroalcoholic extracts. Molecules. 2020;25(24):1-17. doi: 10.3390/molecules25246005.
16. Osman AM. Multiple pathways of the reaction of 2,2-diphenyl-1-picrylhydrazyl radical (DPPH•) with (+)-catechin: evidence for the formation of a covalent adduct between (DPPH•) and the oxidized form of the polyphenol. Biochem Biophys Res Commun. 2011;412(3):473-478. doi: 10.1016/j.bbrc.2011.07.123.
17. Ciobanu N, Cojocaru-Toma M, Ciobanu C, Benea A. Evaluation of polyphenolic profile and antioxidant activity of some species cultivated in the Republic of Moldova. Eurasian J Anal Chem. 2019;3(13):441-447.
18. Németh-Zámbori É, Rajhárt P, Inotai K. Effect of genotype and age on essential oil and total phenolics in hyssop (*Hyssopus officinalis L.*) J Appl Bot Food Qual. 2017;90:25-30. doi: 10.5073/JABFQ.2017.090.005.
19. Lu Y, Yeap Foo L. Antioxidant activities of polyphenols from sage (*Salvia officinalis*). Food Chem. 2001;75(2):197-202. doi: 10.1016/S0308-8146(01)00198-4.
20. Fathiazad F, Mazandarani M, Hamedeyazdan S. Phytochemical analysis and antioxidant activity of *Hyssopus officinalis* L. from Iran. Adv Pharm Bull. 2011;1(2):63-67. doi: 10.5681/apb.2011.009.
21. Micović T, Topalović D, Živković L, et al. Antioxidant, antigenotoxic and cytotoxic activity of essential oils and methanol extracts of *Hyssopus officinalis L.* subspices *aristatus* (Godr.) Nyman (*Lamiaceae*). Plants. 2021;10(4):711. doi: 10.3390/ plants10040711.
22. Tahir M, Khushtar M, Fahad M, Rahman MA. Phytochemistry and pharmacological profile of traditionally used medicinal plant Hyssop (*Hyssopus officinalis* L.). J Appl Pharm Sci. 2018;8(07):132-140. doi: 10.7324/JAPS.2018.8721.

Authors' ORCID iDs and academic degrees
Anna Benea, PharmD, PhD Applicant – https://orcid.org/0000-0001-9670-5045
Cristina Ciobanu, PharmD, PhD, Associate Professor – https://orcid.org/0000-0001-6550-6932
Nicolae Ciobanu, PharmD, PhD, Associate Professor – https://orcid.org/0000-0002-2774-6668
Irina Pompus, BioD, Scientific Researcher – https://orcid.org/0000-0002-7429-4609
Maria Cojocaru-Toma, PharmD, PhD, Associate Professor – https://orcid.org/0000-0002-8255-9881

Authors' contributions
AB designed the study, performed the laboratory work and drafted the first manuscript; CC interpreted the data, revised the manuscript; IP introduced into culture the species *Hyssopus officinalis* L., NC conducted the laboratory work; MC-T revised the manuscript critically. All the authors revised and approved the final version of the manuscript.

Funding
The study was carried out with the support of project 20.80009.800724 "Biological and phytochemical study of medicinal plants with antioxidant, antimicrobial and hepatoprotective action" within the State Program (2020-2023), contracting authority: National Agency for Research and Development. The trial was the authors' initiative. The authors are independent and take responsibility for the integrity of the data and accuracy of the data analysis.

Ethics approval and consent to participate
No approval was required for this study.

Conflict of interests
No competing interests were disclosed.

REVIEW ARTICLES

https://doi.org/10.52418/moldovan-med-j.65-2.22.07
UDC: 616.391:577.161.21/.22+616.71-007.234

Vitamin D_2 versus vitamin D_3 as a risk factor in compromised bone health

***[1]Chiril Voloc, [2]Aliona Rotari, [3]Alexandru Voloc, [4]Eliane Kamgaing Kuissi, [5]Joel Fleury Djoba Siawaya, [4]Simon Jonas Ategbo**

[1]*Arsenie Gutan* Department of Oro-Maxillo-Facial Surgery and Oral Implantology,
[2]Municipal Clinical Hospital for Children No 1, Chisinau, the Republic of Moldova,
[3]Department of Pediatrics, *Nicolae Testemitanu* State University of Medicine and Pharmacy,
[4]Department of Pediatrics, University of Health Sciences, Libreville, Gabon,
[5]Mother-Child University Hospital Center Jeanne Ebori Foundation, Libreville, Gabon

Authors' ORCID iDs, academic degrees and contributions are available at the end of the article

*Corresponding author – Chiril Voloc, e-mail: chiril.voloc@gmail.com
Manuscript received September 15, 2022; revised manuscript November 30, 2022; published online December 20, 2022

Abstract

Background: Vitamin D plays an important role in the prevention of many diseases. More than 1 billion people worldwide suffer from vitamin D deficiency. Vitamin D deficiency can contribute to the development of 16 types of cancer (breast, colon, prostate, etc.), cardiovascular diseases, stroke, autoimmune diseases, periodontal pathologies, transplant failure in endo-alveolar surgery, etc. There are several risk factors that would prevent the achievement of treatment objectives. The national protocol for deficiency rickets prevention privileges vitamin D_2 versus vitamin D_3, which creates a medical risk factor compromising oral health in both children and adults. The article provides sufficient arguments in favour of vitamin D_3 vs vitamin D_2 prescription for prophylactic and treatment purposes.

Conclusions: Considering that vitamin D deficiency is currently a global public health problem, it can be proposed to declare vitamin D deficit/deficiency a priority public health problem at the national level. Vitamin D_3 should be elective in preventing deficit. Taking into account the multitude of acute and chronic diseases related to vitamin D deficiency, in order to improve the status of vitamin D in all population categories, it is necessary to include vitamin D_3 in the list of molecules fully subsidized by the state and distributed free of charge at least to children under the age of 5 years and adolescents in the period of intensive growth.

Key words: Vitamin D deficiency, osteoporosis, risk factor, oral health, rickets.

Cite this article
Voloc C, Rotari A, Voloc A, Kuissi EK, Djoba Siawaya JF, Ategbo SJ. Vitamin D_2 versus vitamin D_3 as a risk factor in compromised bone health. *Mold Med J*. 2022;65(2):47-50. https://doi.org/10.52418/moldovan-med-j.65-2.22.07.

Introduction

Vitamin D deficiency is a public health problem, affecting more than a billion children and adults worldwide [1]. There is a strong correlation between vitamin D deficiency and a range of acute and chronic diseases and conditions, such as hypocalcemia in newborns, rickets/osteomalacia in children and adolescents, obesity, osteoporosis, type 1 diabetes, asthma, juvenile arthritis, high blood pressure, premenstrual syndrome in teenage girls, depression, fibromyalgia, chronic asthenia syndrome, schizophrenia, neuro-degenerative diseases, including Alzheimer's disease, sarcopenia in adults. Vitamin D deficiency can contribute to the development of 16 types of cancer (breast, colon, prostate, etc.), cardiovascular diseases, stroke, autoimmune diseases, periodontal pathologies, transplant failure in endo-alveolar surgery, etc.

Analysis and discussion

Studies on the role and involvement of vitamin D in oral health are still too few and too recent, but some leads are emerging. Thus, hypovitaminosis D would be correlated with a higher risk of periodontitis particularly through an overexpression of RANK L, responsible for osteoclastogenesis [2, 3], also leading to a decrease in bone density [4]. The deficiency would also increase the rate of dental loss, again in correlation with bone metabolism [5] but also through a lower resistance to infection.

The link between caries risk in children and serum vitamin D levels has been demonstrated in some studies, but the results are still conflicting [6-8]. On the other hand, its role in MIH (Molar – Incisor – Hypomineralization) has been statistically demonstrated [9]. In terms of implantology, vitamin D is gradually emerging as a factor

favoring good osseointegration, administered systemically [10, 11] or topically [12], as well as a better defense against infections, especially during bone grafting.

For a successful promotion of national strategies for vitamin D deficiency correction, it is necessary to identify and prevent the risk factors that lead to the high maintenance of its metabolism disturbance. The number of risk factors for hypovitaminosis D varies from country to country. Their identification and correction would allow a much more effective prophylaxis of rickets and other conditions related to vitamin D deficiency, since its deficiency begins during pregnancy and is associated with a significant reduction in bone mineral density, which persists until the age of 9-10 years after birth and even until adulthood if it is not corrected in time [13]. The risks of developing a vitamin D deficiency are found in all corners of the world, regardless of the socio-economic level of the countries. Thus, official statistics from Africa, Australia, the Far East, Mongolia, New Zealand, Brazil, have documented a continuous increase in risk factors for vitamin D deficiency in both children and adults [14-16].

Putting aside the publications of the last 5 years from France, Canada and the USA, on the need to review the prophylactic doses used in vitamin D deficiency to increase them for all population categories that aim not only to strengthen bone health, but also extraosseous health (oral health, improvement of prognosis after surgery in endo-alveolar procedures, prophylaxis of 16 types of cancer, strengthening the immune and nutritional status, decreasing the incidence and prevalence of cardiovascular, rheumatic, renal, gastrointestinal, dermatological, neurological, neuro-psychological diseases, etc.), it is important to point out that in the national protocol for the prevention of deficiency rickets of the Ministry of Health, Labor and Social Protection No 105 of 04.06.2010, vitamins D_2 and D_3 are considered equivalent both in terms of dosage and action. The research in recent years has eloquently demonstrated that these vitamins, having different origins, are also very different in terms of effectiveness on the human body and phosphocalcic metabolism [11-13, 17-21], almost unanimously giving priority to vitamin D_3.

Thus, numerous randomized studies or meta-analysis have demonstrated that the use of Vitamin D_3 is still more effective in increasing the serum level of 25(OH)D3, compared to the administration of the same dose of Vit D2, especially in long-term treatment duration [22-24].

Vitamins D_2 and D_3 work as prohormones, therefore, do not have independent biological effects, a series of biochemical transformations in the human body being required for them to manifest the effect. These 2 molecules are of different origin – Vitamin D_2 – of vegetable origin, vitamin D_3 – of animal origin, differing at the biochemical level by the structure of the lateral chains, but having the sterol ring in common. To become active, both substances need two successive hydroxylations – the first in the liver – under the influence of 25-hydroxylase (with the involvement of microsomal cytochrome P450 2R1 and mitochondrial cytochrome P450 27A1), resulting in 25-hydroxyvitamin D (calcidiol). In the kidneys, a second hydroxylation occurs under the influence of the enzyme 1-alphahydroxylase (cytochrome P450 B1), resulting in 1,25-dihydroxyvitamin D_2/D_3. Hydroxylations are controlled by the level of parathormone, through homeostatic mechanisms. Although both vitamins eventually reach the active form of calcitriol, statistical data show that taking D_3 results in a more pronounced increase in 25(OH)D levels compared to D_2.

Scientists have established that vitamins D_2 and D_3 have different affinities for the vitamin D receptor (VDR), which in turn activates 24-hydroxylase – the enzyme responsible for the inactive metabolite calcitriol formation. Moreover, vitamin D_2 is inactivated faster by this enzyme than vitamin D_3, so it has a shorter half-life than vitamin D_3. It was found that 24(R),25-dihydroxyergocalciferol ($24,25\text{-}(OH)_2D_2$) has 1.7 times weaker affinity than 24(R),25 dihydroxycholecalciferol ($24,25\text{-}(OH)_2D_3$), the latter also having a much higher affinity to the plasma transport protein of vitamin D – DBP – resulting in a half-life 1.3 times longer than $1,25\text{-}(OH)_2D_2$ vis-à-vis VDR in the intestine. Scientists claim that this plays an important role in the difference in the action of vitamins D_2 and D_3. It should be noted that $1,24,25(OH)_2D_3$ is also an inactivated product, but already of cholecalciferol. Unlike $1,24,25(OH)_3D_2$, it maintains its affinity for VDR and requires one more oxidation to become completely inactive. Therefore, this additional step gives cholecalciferol (vitamin D_3) an increased potential for biological activity and maintenance of an adequate 25(OH)D status in the body [19, 25]. Vitamin D_3 is assumed to be the "preferred" substrate for the liver 25-hydroxylase, which in combination with the difference in VDR affinity of vitamins D_3 and D_2 and inactivation rate, respectively, only reinforces the importance of using vitamin D_3 prophylaxis.

According to a review by Houghton and Vieth in 2006 [24], the metabolic differences between vitamins D_2 and D_3 are due to the difference in the internal chain structure of the vitamins. Thus, ergocalciferol (vitamin D_2) still has a methyl group in position 24, which slows down the rate of conversion to 25(OH)D and respectively decreases the affinity towards the vitamin D binding protein (DBP). Armas et al. and Heaney et al. demonstrated that vitamin D_3 induces a faster and longer response in maintaining serum 25(OH)D levels. They also demonstrated that after a single bolus administration of 50000 IU of ergocalciferol (vit D_2), $25(OH)D_2$ values decrease much faster (on the 14th day) compared to $25(OH)D_3$ at the same dose of cholecalciferol (elevated values are maintained even on the 28th day) [19, 25]. Thus, 50 000 IU of D_3 and D_2 respectively were used in 2 distinct groups for 12 weeks. The values of the 25(OH)D growth curve were higher for $25(OH)D_3$ than for $25(OH)D_2$. Additionally, it was determined that 6 weeks after finishing the administration of bolus vitamins,

the degradation rate of serum 25(OH)D_2 was higher than for 25(OH)D_3, respectively the concentration of the latter being higher in the serum, and of ergocalciferol decreasing to the initial base values.

Therefore, the most plausible explanation for the better effect of vitamin D_3 supplementation is: a) the increased affinity of vitamin D_3 and its metabolites to VDR, DBP and liver 25-hydroxylase; b) the lack of liver's ability to directly hydroxylate position 24 of the internal chain of vit D_3 as opposed to vit D_2.

A 2011 Cochrane study highlighted the significant differences between the two vitamins and the death rate examined for people who supplemented their diet with vitamin D_2 compared to those who did so with vitamin D_3. Analysis of 50 randomized controlled trials, which included nearly 100000 participants, showed a relative risk reduction of 6% among those who used D_3 and an increase in relative risk of 2% among those who used D_2.

According to recent research, vitamin D_3 is about 85% better at increasing and maintaining vitamin D concentrations in the body and produces a storage of vitamin D 200-300% higher than vitamin D_2. It is repeatedly mentioned that any form needs to be converted by the body into a more active form, and vitamin D_3 is converted 500% faster than vitamin D_2. The latter has a shorter deposit life and binds poorly to blood proteins, further hindering their effectiveness.

Moreover, synthetic vitamin D_3 is produced as analog of the natural one by obtaining 7- dehydrocholesterol from cholesterol and then by UV irradiation it turns into D_3. Vitamin D_2, however, is synthesized from ergosterol which is obtained chemically from ergot extracted from molds (fungi). Thus, vitamin D_2, in addition to low biological activity, also has instability to temperature differences, humidity or even dependent on storage containers. Contrary to this, vitamin D_3 is stable. The instability and low purity of vitamin D_2 may also favor higher toxicity compared to D_3, which is more stable and much more purified [24].

Vitamin D_3 increases the total and free 25(OH)D level more than D_2 (25(OH)D concentration increases practically twice faster per week for vitamin D_3 versus vitamin D_2. Finally, another argument in favor of vitamin D_3 is that laboratories do not have kits to determine 25(OH)D_2, which can lead to errors in assessing the status of vitamin D in the body.

In conclusion it can be supposed that the determination of vitamin D status may also be necessary pre-operatively, pre-implant or before any bone grafting.

As several studies have shown, age should not be taken into account, as even young people and children can be deficient.

The elderly population is considered to be deficient, but a preliminary assessment of vit D status would enable better tailoring of supplementation.

Prevention in the field of oral health should be based on more frequent dosing of vitamin D: such test could be considered by its importance as equivalent to taking blood pressure when examined by a physician.

The elements that suggest a deficiency:

– Population groups: elderly, obese, pregnant women
– Clinical: nonspecific diffuse musculoskeletal pain; spontaneous fractures; chronic kidney disease; chronic generalized fatigue; alcoholism and smoking, depression
– Radiological: Decreased bone density
– Biological: increased parathyroid hormone (PTH), hypocalcemia.

Conclusions

Based on the above, the following course of action is proposed:

1. Daily intake of vitamin D is on average 2000 to 4000 IU [25]. The daily intake will therefore have to compensate for the latter.

2. In a healthy population, classical supplementation is around 800 to 1200 IU/day without any risk of toxicity, or 50000 IU/month [25]. People at risk should logically receive a higher dose.

Supplementation can be done in several ways:

- Droplets (Uvedose) 1 million IU percent: 6 to 12 drops per day
- Vials (Uvedose) 100000 IU, 3 to 4 times a year
- Tablets (200, 400, 800 or 1000 IU per tablet depending on the deficiency, 1 tablet per day).

3. For an attack treatment (stoss method), supplementation is done in 2 to 4 doses of 100000 IU, 15 days apart, depending on the severity of hypovitaminosis D.

4. There is a proposal that the currently existing national protocol on deficiency rickets be adapted according to the presented information, favoring the fractional or stoss prescription of vitamin D_3.

5. Based on the fact that vitamin D deficiency is currently a global public health problem, it is necessary to declare the deficit/deficiency of vitamin D as a priority public health problem at the national level.

6. Taking into account the multitude of acute and chronic diseases related to vitamin D deficiency, in order to improve the status of vitamin D in all population categories, it would be useful to include vitamin D_3 in the list of molecules fully subsidized by the state and distributed free of charge at least to children under the age of 5 years and adolescents in the period of intensive growth.

References

1. Holick MF. Vitamin D deficiency. N Engl J Med. 2007 Jul 19;357(3):266-81. doi: 10.1056/NEJMra070553.
2. Kull M Jr, Kallikorm R, Tamm A, et al. Seasonal variance of 25-(OH) vitamin D in the general population of Estonia, a Northern European country. BMC Public Health. 2009; 9:22. doi: 10.1186/1471-2458-9-22.
3. Joseph R, Nagrale AV, Joseraj MG, et al. Low levels of serum Vitamin D in chronic periodontitis patients with type 2 diabetes mellitus: a hospital-based cross-sectional clinical study. Indian Soc Periodontol. 2015 Sep-Oct;19(5):501-6. doi: 10.4103/0972-124X.167162.

4. Martelli FS, Martelli M, Rosati C, et al. Vitamin D: relevance in dental practice. Clin Cases Miner Bone Metab. 2014 Jan;11(1):15-91.
5. Nakamichi Y, Takahashi N. Current topics on Vitamin D. The role of active forms of vitamin D in regulation of bone remodeling. Clin Calcium. 2015 Mar;25(3):395-402.
6. Zhan Y, Samietz S, Holtfreter B, et al. Prospective study of serum 25-hydroxy Vitamin D and tooth loss. J Dent Res. 2014 May 14;93(7):639-644. doi: 10.1177/0022034514534985.
7. Schroth RJ, Rabbani R, Loewen G, et al. Vitamin D and dental caries in children. Dent Res. 2016 Feb;95(2):173-9. doi: 10.1177/0022034515616335.
8. Schroth RJ, Levi JA, Sellers EA, et al. Vitamin D status of children with severe early childhood caries: a case-control study. BMC Pediatr. 2013;13:174. doi: 10.1186/1471-2431-13-174.
9. Schroth RJ, Lavelle C, Tate R, et al. Prenatal vitamin D and dental caries in infants. Pediatrics. 2014;133(5):e1277-84. doi: 10.1542/peds.2013-2215.
10. Kühnisch J, Thiering E, Kratzsch J, et al. Elevated serum 25(OH)-vitamin D levels are negatively correlated with molar-incisor hypomineralization. J Dent Res. 2015;94(2):381-7. doi: 10.1177/0022034514561657.
11. Dvorak G, Fügl A, Watzek G, et al. Impact of dietary vitamin D on osseointegration in the ovariectomized rat. Clin Oral Implants Res. 2012 Nov;23(11):1308-13.
12. Golden KE, Vergnaud S. Vitamin D2: what you should know [Internet]. Santa Monica: GoodRx, Inc; ©2011-2022. [cited 2022 June 12]. Available from: https://www.goodrx.com/well-being/supplements-herbs/vitamin-d2-vs-vitamin-d3-whats-the-difference
13. Holick, MF. High prevalence of vitamin D inadequacy and implications for health. Mayo Clinic Proceedings. 2006;81(3):353-373. doi: 10.4065/81.3.353.
14. Holick MF, Binkley NC, Bischoff-Ferrari HA, Gordon CM, Hanley DA, Heaney RP, Murad MH, Weaver CM. Guidelines for preventing and treating vitamin D deficiency and insufficiency revisited. J Clin Endocrinol Metab. 2012 Apr;97(4):1153-8. doi: 10.1210/jc.2011-2601.
15. Rich-Edwards JW, Ganmaa D, Kleinman K, Sumberzul N, Holick MF, Lkhagvasuren T, Dulguun B, Burke A, Frazier AL. Randomized trial of fortified milk and supplements to raise 25-hydroxyvitamin D concentrations in schoolchildren in Mongolia. Am J Clin Nutr. 2011 Aug;94(2):578-84. doi: 10.3945/ajcn.110.008771.
16. Maeda SS, Kunii IS, Hayashi L, Lazaretti-Castro M. The effect of sun exposure on 25-hydroxyvitamin D concentrations in young healthy subjects living in the city of São Paulo, Brazil. Braz J Med Biol Res. 2007 Dec;40(12):1653-9. doi: 10.1590/s0100-879x2006005000162.
17. Arnarson A. Vitamin D2 vs. D3: what's the difference? 2018 March 4 [cited 2022 Mar 15]. In: Healthline [Internet]. Healthline Media; c2005-2022. Available from: https://www.healthline.com/nutrition/vitamin-d2-vsd3
18. Hiatt T. The (enormous) difference between vitamins D3 and D2 and why you should never take D2 [Internet]. [cited 2022 June 12] Available from: https://www.linkedin.com/pulse/enormous-difference-between-vitamins-d3-d2-why-you-thomas
19. Shieh A, Chun RF, Ma C, Witzel S, Meyer B, Rafison B, Swinkels L, Huijs T, Pepkowitz S, Holmquist B. Effects of high-dose Vitamin D2 versus D3 on total and free 25-Hydroxyvitamin D and markers of calcium balance. J Clin Endocrinol Metab. 2016;101(8):3070-8. doi: 10.1210/jc.2016-1871.
20. Tripkovic L, Lambert H, Hart K, Smith CP, Bucca G, Penson S, Chope G, Hyppönen E, Berry J, Vieth R. Comparison of vitamin D_2 and vitamin D_3 supplementation in raising serum 25-hydroxyvitamin D status: a systematic review and meta-analysis. Am J Clin Nutr. 2012;95(6):1357-64. doi: 10.3945/ajcn.111.031070.
21. Oliveri B, Mastaglia SR, Brito GM, et al. Vitamin D3 seems more appropriate than D2 to sustain adequate levels of 25OHD: a pharmacokinetic approach. Eur J Clin Nutr. 2015;69(6):697-702. doi: 10.1038/ejcn.2015.16.
22. Logan VF, Gray AR, Peddie MC, Harper MJ, Houghton LA. Long-term vitamin D3 supplementation is more effective than vitamin D2 in maintaining serum 25-hydroxyvitamin D status over the winter months. Br J Nutr. 2013;109(6):1082-8. doi: 10.1017/S0007114512002851.
23. Hammami MM, Yusuf A. Differential effects of vitamin D2 and D3 supplements on 25-hydroxyvitamin D level are dose, sex, and time dependent: a randomized controlled trial. BMC Endocr Disord. 2017;17:12. https://doi.org/10.1186/s12902-017-0163-9.
24. Houghton LA, Vieth R. The case against ergocalciferol (vitamin D-2) as a vitamin supplement. Am J Clin Nutr. 2006;84(4):694-7. doi: 10.1093/ajcn/84.4.694.
25. Benhamou CL, Souberbielle JC, Cortet B, Fardellone P, Gauvain JB, Thomas T; Group of Research and Information on Osteoporosis (GRIO). The vitamin D in adults: GRIO guidelines. Presse Med. 2011;40:673-82.

Authors' ORCID iDs

Chiril Voloc, MD, PhD Student – https://orcid.org/0000-0002-3428-9880
Aliona Rotari, MD – https://orcid.org/0000-0002-3214-846X
Alexandru Voloc, MD, PhD, Professor – https://orcid.org/0000-0001-8882-3164
Eliane Kamgaing Kuissi, MD, PhD, Professor – https://orcid.org/0000-0002-4594-2582
Joel Fleury Djoba Siawaya, MD, PhD, Professor – https://orcid.org/0000-0002-0369-0153
Simon Jonas Ategbo, MD, PhD, Professor – https://orcid.org/0000-0002-4069-3791

Authors' contributions

CV designed the study and wrote the manuscript; AR collected the data; AV revised the manuscript critically; EKK collected and carried out the analysis of the literary sources; JFDS collected and conducted the analyses of the literary sources; SJA collected and effected the analysis of the literary sources. All the authors revised and approved the final version of the manuscript.

Ethics approval and consent to participate

No approval was required for this study.

Conflict of interests

The authors have no conflict of interests to declare.

https://doi.org/10.52418/moldovan-med-j.65-2.22.08
UDC: 616.98:578.834.1

Factors to consider when assessing the severity of COVID-19

*[1,2]Ivan Civirjic, [1,2]Serghei Sandru, [1,3]Oleg Arnaut, [1,2]Natalia Cernei, [2]Victoria Moghildea

[1]*Valeriu Ghereg* Department of Anaesthesiology and Reanimatology No 1
Nicolae Testemitanu State University of Medicine and Pharmacy
[2]Department of Anaesthesia and Intensive Care, Institute of Emergency Medicine,
[3]Department of f Human Physiology and Biophysics, *Nicolae Testemitanu* State University of Medicine and Pharmacy
Chisinau, Republic of Moldova.

Authors' ORCID iDs, academic degrees and contributions are available at the end of the article

*Corresponding author – Ivan Civirjic, e-mail: civirjic.ivan@gmail.com
Manuscript received September 26, 2022; revised manuscript November 23, 2022; published online December 20, 2022

Abstract

Background: Analysis and evaluation of the multitude of parameters that impact and mirror clinical evolution of COVID-19 infection. Narrative literature review type of study. Bibliographic search of the PubMed database, applying the keywords: "SARS-CoV-2", "COVID-19", "risk score", "laboratory parameters", "pathophysiology", "cytokine storm", "imaging evaluation", "outcomes", "clinical evolution", which were combined with each other. There were selected English-language publications, in extenso, published in recognized journals from March 2020. Priority in the analysis was given to articles of critical synthesis of literature, randomized studies, those with large samples of patients. One of the clinically important symptoms that reflects severe or critical clinical evolution is persistent fever during the time. The presence of comorbidities, especially associated with obesity, represents a high risk of severe evolution. Proinflammatory, prothrombotic and systemic endothelial damage processes are represented by changes in platelet count, lymphocytes, neutrophil / lymphocyte ratio, C-reactive protein, D-dimers, fibrinogen, procalcitonin, urea, creatinine, ALS, AST, interleukin-6 and serum ferritin. Bacterial and fungal infections negatively influence clinical evolution. Common prediction scores have low value in COVID-19 patients and need adaptation. Imaging evaluation identifies the type of lung injury and correlates with the severity degree and outcome.
Conclusions: COVID-19 disease caused by SARS-CoV-2 virus includes a multitude of pathophysiological changes that through its mechanism represent a systemic nosology. The complete analysis of all the factors and parameters that can influence its clinical evolution is a basic component of the decision-making steps and treatment approach.
Key words: severity predictors, COVID-19, laboratory parameters, risk score, SARS-CoV-2.

Cite this article
Civirjic I, Sandru S, Arnaut O, Cernei N, Moghildea V. Factors to consider when assessing the severity of COVID-19. *Mold Med J*. 2022;65(2):51-58. https://doi.org/10.52418/moldovan-med-j.65-2.22.08.

Introduction

COVID-19 disease is an infectious pathology, transmitted by infected aerosol droplets or direct contact with surfaces contaminated by them [1], caused by the SARS-CoV-2 virus, first identified in December 2019 in Wuhan, Hubei Province, China. During the 3 months since the first identification, due to the high contagiousness, this infection had a global spread, which made in March 2020, the World Health Organization declare "Pandemic State" in connection with the increased number of cases and the global spread of this viral infection. From the beginning of the pandemic until the present, over 515400000 cases of COVID-19 infection have been confirmed with 1% of currently mortality rate [2].

COVID-19 is a polymorphic disease with the predominant clinical presentation of viral interstitial pneumonia and secondary systemic hypoxemia. But, pathophysiologically, the viral infection COVID-19, through the mechanism of viral penetration, the lesions caused at the systemic vascular level and the secondary immune response represents a systemic pathology, mirrored by the pulmonary vascular lesions. The clinical evolution is highly dependent on the secondary immune response and the detailed analysis of each stage of the disease, the predisposing factors towards an unfavourable evolution and the changes occurring in the lung and at laboratory level can guide us about disease course, the risks of adverse events and the necessity for close monitoring. During the pandemic different clinical and laboratory parameters that impact and are associated with negative outcome and mortality, but with different informativity, were highlighted. Also were applied and developed specific scores for evaluation and prognosis of clinical course.

The goal of this review is analysis and evaluation of impact and predictability of the multitude of parameters and prognostic scores that mirror clinical evolution of

COVID-19 infection. In order to realize the goal of the study was realized bibliographic search of the PubMed database, applying the keywords: "SARS-CoV-2", "COVID-19", "risk score", "laboratory parameters", "pathophysiology", "cytokine storm", "imaging evaluation", "outcomes", "clinical evolution", which were combined with each other. There were selected English-language publications, in extenso, published in recognized journals from March 2020. Priority in the analysis was given to articles of critical synthesis of literature, randomized studies, those with large samples of patients. The final bibliography included 76 references.

Discussion

1. Pathophysiology

1.1. *Cell penetration and immune reponse*

The SARS-CoV-2 virus is enveloped with a single-stranded positive sense 30 kb RNA virus, which is part of the Coronaviridae family along with the viruses HCoV-229E, HCoV-OC43, SARS-CoV, HCoV-NL63, HCoV-HKU1 and MERS-CoV [3]. The SARS-CoV-2 virus consists of 4 structural proteins: spike (S), membrane glycoprotein (M) with the role of stabilizing the viral structure, forming the envelope and releasing the viral; envelope (E) responsible for virulence and activation of the body's immunopathological response; nucleocapsid (N) that binds to viral RNA and participates in viral replication [4].

The S protein is composed of 2 subunits: S1 – responsible for binding to the host cell receptor and S2 – responsible for the fusion of viral and cell membranes. The Angiotensin-Converting Enzyme 2 receptor (ACE2) has been identified as a functional receptor for the structural protein S of SARS-COV-2 virus. The Type II transmembrane Serine Protease (TMPRSS2), which is present in the host cell, promotes viral uptake by cleavage with the ACE2 receptor and the S protein of the virus and its entry into the cell [5].

The life cycle of the virus consists of five periods: attachment, penetration, biosynthesis, maturation and release [6]. Being an RNA virus, it directly begins the production of its own protein and new genomes after penetrating the cell by attaching to ribosomes of the host cell. The ribosomes of the host cell transcribe RNA into RNA polymerase, which is then used to produce new virions in the Golgi apparatus. Newly formed virions are released from the cell by exocytosis by excretory vesicles. The release of the virus from the cell is associated with its deformation and injury. At the same time, the SARS-CoV-2 virus interferes with direct cell damage by promoting cell apoptosis [7].

The virions spread systemically, affecting the target organs that contain the high expression of ACE2 receptors and TMPRSS2 protein, which include: lungs (through type II alveolar cells), heart (through myocardial cells), arterial vascular system (through cells endothelial), kidneys (through proximal tubule cells), ileum and oesophagus (through epithelial cells), bladder (through urothelial cells) [8]. This localization of ACE2 receptors explains the clinical polymorphism of COVID-19 disease and the susceptibility or predisposition of certain population groups to the development of certain complications as well as to the evolution of the disease in severe and critical form.

The pathophysiology and clinical course of COVID-19 disease is the consequence of the T-cells mediated immune response, which produce interferon-gamma (INF-gamma) and interleukins like response to the cell invasion of the virus. Also, the damage of infected cells (especially alveolar), is the result of pro-inflammatory mediators, cytokines, interferons and other intracellular elements release. Alveolar macrophages identify cell damage and the secretion of cytokines, responding with proper secretion of cytokines and chemokines. Tumor necrosis factor (TNF), secreted by macrophages along with other proinflammatory cytokines, increases vascular permeability and cell adhesion, that induces the recruitment of other immune cells, such as neutrophils and monocytes. Neutrophils incorporate viruses and other elements from the affected area. This process is accompanied by the secretion of chemokines that leads to affect the surrounding tissues. Leukopenia associated with lymphopenia is the result of the consumption of immune cells involved in a large number in the process of immune and inflammatory response as well as the secretion of interferon [9].

1.2. *Cytokine storm*

The multitude of immune elements, cytokines and proinflammatory mediators activated by the SARS-CoV-2 invasion and cell destruction potentiate the phenomenon of "Cytokine storm", which is increasingly discussed in the context of COVID-19 disease.

Cytokine storm or Cytokine storm syndrome, is a cascade of activations and auto-amplification processes of pro-inflammatory cytokines production followed by exaggerated and dysregulated immune response of the host to various triggers (infection, rheumatic diseases, malignancies) [10].

Immune hyperactivity in cytokine storm is the result of the imbalance between the activity of pro- and anti-inflammatory processes with the predominance of proinflammatory ones. This is caused by excessive immune cell activation, pathogenic overload (e.g. sepsis), uncontrolled infections and prolonged immune activation. All this leads to the failure of the negative feedback mechanism, whose role is to control and avoid or prevent the hyperinflammatory phenomenon [11]. The clinical phenotype of the cytokine storm is largely manifested by elements of systemic inflammation, acute lung injury associated with acute respiratory distress syndrome and multiple organ dysfunction [11].

1.3. *Covid coagulopathy*

Endothelial injury caused by the virus and the immune response, which involves cytokines and leads to compliment activation, plays an important role in the association

of COVID-19 coagulopathy [12]. In this context, the involvement of neutrophils and monocytes in the "thromboinflammatory" or "immunothrombosis" process is evaluated.

The role of monocytes consists in the formation and activation of thrombo-monocyte aggregates, whose activation degree correlates with the severity of the disease and with the values of the reactive "C" protein [13].

Neutrophils are also involved in the process of micro- and macrothrombosis by forming neutrophil extracellular traps (NETs) [14]. Elevated levels of NETs closely correlate with disease severity and oxygenation disorders [15]. The presence of extracellular neutrophil traps was identified in the lungs, liver and kidneys of patients who died from COVID-19 disease [16]. Along with the mentioned immune cells, hypoxia, like a result of the multitude of proinflammatory processes in the lung capillaries, promotes thrombotic processes in patients with COVID-19 disease [17].

Hypoxia acts in 2 ways: first, the direct pathway of immunomodulin suppression and reduction of fibrinolytic potential and the second, by the formation of HIF-1a and HIF-2 transcription factors. These factors potentiate the thrombosis process by involving the inhibitor of plasminogen activation and blocking tissue factor (TF) inhibitor [18]. Therefore, in severe forms of COVID-19 disease, the hypercoagulant phenotype, with the fibrin polymerization and the resulting thrombosis, predominates over that of consumption coagulopathy [19].

The events resulting from the viral invasion on the host have a self-amplifying character, where each involved element represents a trigger and stimulates the development of a vicious pathophysiologic circle. This circle induces "cytokine storm" with prothrombotic and hypercoagulant status and the development of acute lung injury, ventilation/perfusion mismatch, pulmonary oedema, hypoxia similar to acute respiratory distress syndrome (ARDS) and promotes the development of multiple organs damage [20].

2. Severity degrees and characteristics of clinical evolution

In the clinical course of COVID-19 disease can be evident the following forms of severity [21]:

1. Asymptomatic – with positive SARS-CoV-2 test, no symptoms;

2. Mild illness – accompanied by fever, cough, anosmia and loss in taste, no dyspnea;

3. Moderate illness – with clinical or radiographic evidence of pathological changes in the lower airways and lungs, but with the maintenance of peripheral oxygen saturation (SpO2)> 94%, without oxygen support;

4. Severe illness – presence of lung infiltrates more than 50% of the total surface, SpO2 <93% without oxygen support, tachypnoea more than 30 breaths/min and signs of respiratory distress;

5. Critical illness – defined by the criteria of acute respiratory distress syndrome, sepsis, septic shock and multiple organs dysfunction.

From the total number of cases, those with asymptomatic, mild and moderate manifestations represent approximately 80% and the rest of them get severe and critical forms. The rate of Intensive Care Unit (ICU) admission of COVID-19 patients is 11% of the total number of confirmed cases [22].

There are several clinical stages in the evolution of the disease. The transition from one stage to another is not mandatory for all those infected with the SARS-CoV-2 virus.

These are:

– Incubation period – lasts on average 5.3 days;

– Early stage of disease evolution – manifested by the signs and symptoms of a seasonal viral infection (fever, myalgia, cough, fatigue, diarrhoea, anorexia) – is observed during the first 5-8 days after the symptoms onset;

– Pulmonary phase – is characterized by the appearance of dyspnea, signs of hypoxia, the appearance of opacity on lung radiography and computed tomography – develops at day 8-11 of illness;

– Hyperinflammatory phase characterized by "cytokine storm", acute respiratory distress syndrome, sepsis and septic shock – starting from day 11-15 of illness [22–25].

The factors that contribute to the progression of the disease in another phase are not fully elucidated at the moment [24]. It is assumed, that the unfavourable evolution of the disease dependents on the individual over-response of the immune system to the SARS-CoV-2 infection and on the presence of comorbidities that represent the risk factors for a severe evolution.

Management and treatment approach differs from the disease evolution stage and the patient's treatment response determins the regression of the disease or its transition to a more advanced phase [26].

In COVID-19 patients, the average time from the first symptoms onset until the admission in intensive care unit (ICU) is 9.84 days. The overall ICU mortality rate is 35.5% and the average duration from the onset of the first symptoms until death is 15.93 days [25, 27].

3. Severity predictors, evolution particularities and clinical outcome

3.1. *Demographics*

The severity of COVID-19 disease and the final outcome of survivor or non-survivor is determined by several factors and comorbidities, including: age, male gender, diabetes, chronic heart disease, cerebrovascular disease, pulmonary, renal and hepatic diseases, immunosuppression and malignancy [22]. Furthermore, obesity is one of the unfavourable predictors, and the presence of Body Mass Index (BMI) more than 30 in association with one of the factors mentioned above substantially increases the risk of disease severity [28].

The fever with values more than 38.0 and resistance to antipyretic treatment is one of the independent factors of severity and prognosis of the disease, especially in the first 5 days after the symptoms onset. Its rate is approx. 80% in symptomatic patients COVID-19 and is the common symptom in approx. 90% of patients requiring hospitalization [22, 29].

3.2. *Association of bacterial and fungal infection*

Bacterial co-infection. The pooled prevalence of bacterial co-infection identified in patients with COVID-19 disease reaches 21%. The respiratory co-infection has pooled prevalence of 5.2% and gastrointestinal 4.8% [30]. In hospitalized patients, this varies from 5.9 to 7%, with a double value of 8-14% in ICU patients. The most frequently cultivated pathogens are Mycoplasma pneumoniae (42%), Pseudomonas aeruginosa (12%) and Haemophilus influenzae (12%) [31].

Bacterial superinfection rate reaches a value of 24% in patients with COVID-19 disease, and 41% in cases of ICU patients. The most often cultivated are: Acinetobacter spp. (22.0%), Pseudomonas (10.8%), and Escherichia coli (6.9%) [32].

Ventilator Associated Pneumonia (VAP) is most common manifestation of healthcare associated bacterial superinfection in COVID-19 with rate of 50%. Bloodstream infection represents 34% of total cases and venous catheter-associated bloodstream infections – 10% [33]. The development of VAP in COVID-19 patients during mechanical ventilation serves as an aggravating factor of disease clinical course, with the mortality rate of 42.7%. These mortality values are triple higher in comparation with non-Covid-19 patients [34, 35].

Fungal infection – has a rate of 8% in COVID-19, with the predominance of Candida species (18.8%) [32].

The presence of co-infection and especially a bacterial superinfection in COVID-19 patients is an unfavourable prognostic factor, associated with an increased risk of mortality, mainly among ICU patients [31, 32].

3.3. *The laboratory predictors*

In COVID-19 clinical course can be highlighted following laboratory parameters with prognostic value of evolution, assessment of disease severity and risk or rate of adverse events (mechanical ventilation, acute kidney injury, septic shock, need in vasopressors, PE, AMI or others) [19, 36]:

- Lymphopenia – indicates severe evolution of the disease, due to increased viremia and the increased consumption of immune cells. In its case the lymphocytes number is inversely proportional to the severity of the disease [37].
- Neutrophil-lymphocyte ratio – it is a marker of stress and systemic inflammation in critically ill patients. Its value higher than 9.8 in COVID-19 patients correlates with the higher rate of ARDS and the need for non-invasive or invasive ventilatory support [38].
- Platelets count – values less than 150, are a negative prognostic factor [39]. The value less than 50 indicates very high, up to 92%, risk of death [40]. At the same time, the increase in the platelets number (which is below the normal range), during hospitalization, indicates a positive evolution and an increase in the chances of survival [41].
- Fibrinogen is a protein of acute phase which is synthesized in the liver under the interleukin-6 (IL-6) induction, like a response to a systemic inflammatory process [42]. Fibrinogen participates in the coagulation cascade and its decrease is associated with increased mortality in sepsis [43]. However, in patients with COVID-19, attention is given to high fibrinogen levels, which indicate an unfavourable outcome and a severe course of the disease [44].
- ALT / AST are liver enzymes whose values increase as a result of hepatocyte damage. In COVID-19 patients, the systemic inflammatory process or administered hepatotoxic medication can be factors that contribute to liver injury and their elevation. The amount of these enzymes guides the prognosis, and their increased values at admission are associated with an increased risk of ICU admission, the need for vasopressor support, non-invasive or mechanical ventilation and acute kidney injury [45].
- Albumin – hypoalbuminemia is a negative prognosis factor in both general groups of patients and in COVID-19 and is an independent indicator of mortality [19, 46].
- Lactate dehydrogenase (LDH) – is the enzyme that participates in the formation of energy by converting lactate to pyruvate and is present in several cells in the body. Its increase has been recorded in acute or chronic lung diseases and interstitial diseases [47]. Elevated LDH levels are an indicator of illness severity and are associated with a 6-fold higher risk of adverse outcome and respiratory worsening at values more than 450 U/l [39, 47].
- Creatinine is a marker of kidney function, which closely correlates with COVID-19 severity. Values higher than 130 mmol / l indicate a 2.6-fold increased risk of negative outcome [39]. Also, the rate of acute renal injury (AKI) in COVID-19 patients is approx. 20%, with a mortality rate of approx. 55% in case of its association [48].
- Urea values higher than 6.5 mmol/l registered at admission indicate negative evolution, poor prognosis and the greater risk of developing the severe and critical form of the illness [49].

Biomarkers

- Interleukin 6 (IL6) is a protein produced by activated monocites, macrophages and other cells. Interaction with specific receptors on responsive cells, IL-6 promotes antiviral effect, release of acute-phase reactant from hepatocytes [42]. In COVID-19, IL-6 is a reliable predictor of desease severity and ventilatory support,

where the IL- 6 levels exceeding 210 pg/mL were 100% associated with respiratory failure [50, 51]. Also, the IL-6 level recorded in ICU patient is 52% higher in comparation with non-ICU [52], and each increase in the IL-6 level of 1 pg/mL significantly increased the risk of mortality of COVID-19 patients [53].

- Serum Ferritin is a shell protein that sequesters iron in its core. Its synthesis is regulated by various "oxidant and antioxidant stimuli" and represents "acute phase reactant" that mirrors the degree of both chronic and acute inflammatory reaction inside the body [54]. A higher ferritin level indicates an activated monocyte-macrophage system, where the synthesis of ferritin is responsive to alteration in cytokine status [54]. High ferritin level is observed across a lot of inflammatory diseases and it serves as biomarker for different conditions like a rheumatologic and inflammatory disorders and cancer [54]. COVID-19 patients with severe and critical disease had higher ferritin level compared to patients with mild and moderate. Moreover, the same results were observed in non-survivors and survivors, also in ICU patients requiring mechanical ventilation and in those who didn't require ICU and did not require mechanical ventilation [54]. Additionally, higher ferritin levels correlate with presence of COVID-19 related thrombotic complications [54]. Increased ferritin value [median 1016 ng/mL (IQR 516–2534)] was reported in patients with COVID-19 related acute kidney injury compared to those without AKI [median value 680 ng/mL (IQR 315 to 1416)] [55].
- C-reactive protein (CRP) – is the inflammatory marker of the acute phase, and is produced by hepatocytes following stimulation by interleukin-6 and is used as an indicator of the severity of both inflammatory and infectious processes [56]. In the case of patients with COVID-19, it not only directly correlates with the degree and extent of pulmonary damage in the initial stage and the early pulmonary phase, but also suggests the possibility of poor prognosis and four time higher rate of negative outcome and respiratory worsening at values more than 10 mg/l [39, 47, 57, 58].

Coagulation disorders are often associated with COVID-19 infection and they are reflected by changes in coagulation tests like fibrinogen level, D-dimer, and total platelet counts. Severe forms with bad prognosis are correlated with elevated levels of D-dimers and fibrinogen and low levels of total platelet counts [44].

- D-dimers are fibrin degradation products which level indicates the increased quantity of thrombin and intense fibrinolysis process. Thromboembolic events have a high rate in patients with severe COVID-19 forms admitted in ICU. Rates of these are for venous thromboembolism – 31%, for deep vein thrombosis – 28% and for pulmonary thromboembolism – 19%, which rate is of 22% in post-mortem studies and the presence of these events is associated with 74% higher risk of mortality [59]. The high levels of D-dimers are directly proportional with the disease severity and show a 3-fold higher risk of adverse events, and the values more than 2 mcg / ml at admission predict a high risk of in-hospital mortality and are considered like an early marker of severity and therapeutic strategy. A double increase in mortality rate, from 32.8 to 52.4%, can be followed in those with D-dimer values higher than 3 mcg /ml [39, 44, 59, 60].
- Procalcitonin is a precursor of calcitonin that is normally synthesized in parafollicular C cells of the thyroid gland. In case of bacterial infection, under the action of high concentrations of TNFα and interleukins it can be synthesized by extrathyroidal tissues [61]. The synthesis of this biomarker is inhibited by interferon-(INF)-γ, which predominates in the early phase of the disease and, as a result, with the presence of normal values in non-severe evolution. The dynamical increase of this parameter levels indicates the negative evolution of the disease, the possible presence of bacterial superinfection and the 5 times increased risk of negative outcomes [62].

3.4. *Main prediction scores and their value*

In clinical practice, especially in ICU patients, different prediction scores are used for risk stratification, prognosis of clinical evolution and correction of treatment tactics.

In critical patients the most used and with a high predictive value are: APACHE II, SOFA, NEWS2, which at the beginning of the pandemic were used in COVID-19 diseases in order to stratify risks. However, it was later shown that the APACHE II score has the best predictive value in these patients, but it is significantly lower compared to non-covid patients [63]. At the same time, the use of the previously mentioned scores, which include a lot of complex parameters whose evaluation requires time, creates difficulties in the triage and analysis of patients in conditions of pandemic and overload of the medical system.

The decrease in the predictive values of nonspecific COVID-19 scores is argued by evaluating uncharacteristic for SARS-CoV-2 infection parameters of omitting others with high predictive value, such as the number of lymphocytes or D-dimers. For example, in this context, the A-DROP score, as a modification of the CURB-65, has a higher mortality predictive value than the Pneumonia Severity Index (PSI), CURB-65, CRB-65, SMART-COP, qSOFA and NEWS2 in the case of patients hospitalized with Community Acquired Pneumonia, as well as, in the case of COVID-19 patients [63,64]. Additionally, the MEWS score being one of the simplest and fastest, with a satisfactory degree of prediction [65].

The applicability of the CURB 65, NEWS-2 and qSOFA scores remains debatable in the context of the moderate prognostic level and underestimation of the mortality rate in patients with COVID-19 disease [66].

3.5. *COVID-19 prediction scores*

During the pandemic, many factors associated with the increased mortality were identified and were adapted several prediction models. The common parameters that were included in most of them are: lymphocytes number, D-dimers, CRP, platelet count, neutrophil-lymphocyte ratio, LDH, oxygen saturation and the presence of comorbidities. For example, Covichem score which includes 2 clinical and 5 biochemical parameters [67], COVID-19 Scoring System (CSS) which evaluates 4 parameters (procalcitonin, D-dimers, lymphocytes (%) and the presence of cardiovascular pathology) [68], ABC2-SPH mortality risk score that analyses 7 parameters (age, SpO2 / FiO2 ratio, platelet count, CRP values) [69].

In the list of the developed and validated for COVID-19 scores is also included the ISARIC score, which was evaluated in 75000 patients and was validated and applied in 9 regions of the United Kingdom [70]. This score evaluates 11 parameters at hospital admission or at first contact with a patient. This is the number of comorbidities, age, sex, presence of pulmonary infiltrates, urea level, respiratory rate, CRP, lymphocyte number, oxygen saturation. After introducing the required parameters depending on the score obtained, is stratified and assessed the risk of two evolutions – deterioration and mortality. The calculated risks are presented in percentage values. Unfortunately, the value of D-dimers was not included in the prediction parameters of this score, because it was present and analysed in a small number of participants included in the study [70].

3.6. *Scores for imaging evaluation and standardization*

Imaging assessment of the lung lesions severity plays an important role in the analysis and stratification of the COVID-19 evolution.

The gold standard in the imaging evaluation of the degree and type of lung modification, as well as of the evolutionary stage, is represented by Computed Tomography (CT-scan). The main changes that can be identified on CT are: vascular enlargement (84.8%), followed by ground-glass opacity (60.1%), air-bronchogram (47.8%) and lung consolidations (41.4%) [71]. Likewise, it can establish the location of the changes and the degree and extent of the spread. The CO-RADS score and the CT Severity Score (CSS) are used to standardize the severity of the lung damage. The CO-RADS score accuracy in estimating is slightly higher and both of them, closely correlate with the disease severity and changes in laboratory parameters with prediction of negative evolution [72, 73].

The overload of the medical system and the large flow of patients create impediments in imaging evaluation by computed tomography. Dynamical examination of lung infiltrates evolution requires transporting to the CT scan that is associated with certain risks, especially in severe or critically ill connected to non-invasive or mechanical ventilation. Like an alternative, the role in imaging evaluation in this situation was taken by the chest X-ray, which has a lower diagnostic value compared to computed tomography, but can be easier, faster and dynamically performed in ICU patient.

In March 2020, a group of Italian authors, based on radiological images of patients with COVID-19, developed a new system for grading the severity of lung damage, specific to the type and form of tissue damage encountered in SARS-CoV-2 infection, called Brixia Score [74]. Subsequent research has shown a close correlation of the Brixia Score with both the severity of the disease and the prognosis [75, 76]. This score includes two stages of analysis of the radiological image. In the first step, the lungs are divided into six zones on frontal chest projection (posteroanterior or anteroposterior projection according to the patient position). In the second step, a score (from 0 to 3) is assigned to each zone based on the lung abnormalities detected on frontal chest projection as follows [74]:

- *Score 0* no lung abnormalities,
- *Score 1* interstitial infiltrates,
- *Score 2* interstitial and alveolar infiltrates (interstitial predominance),
- *Score 3* interstitial and alveolar infiltrates (alveolar predominance).

The scores of the six lung zones are then added to obtain an overall "CXR SCORE" ranging from 0 to 18.

The application of this score standardized the analysis and calculation of the degree of lung damage in COVID-19 patients by radiologists giving it diagnostic severity and prognostic value [75].

Conclusions

COVID-19 disease caused by SARS-COV-2 virus includes a multitude of pathophysiological changes that through its mechanism represent a systemic nosology. The complete analysis of all the factors and parameters that can influence its clinical evolution, especially in patients at risk groups, is a basic component of the decision-making steps, management tactics and treatment approach.

References

1. European Centre for Disease Prevention and Control. Transmission of COVID-19 [Internet]. Stockholm: ECDC; 2022- [cited 2022 May 5]. Available from: https://www.ecdc.europa.eu/en/covid-19/latest-evidence/transmission
2. Worldometers.info. COVID Live - Coronavirus Statistics [Internet]. Dover, USA; 2022- [cited 2022 May 5]. Available from: https://www.worldometers.info/coronavirus/
3. Rabi FA, Al Zoubi MS, Al-Nasser AD, Kasasbeh GA, Salameh DM. SARS-CoV-2 and Coronavirus Disease 2019: what we know so far. Pathogens. 2020;9(3):231. doi: 10.3390/PATHOGENS9030231.
4. Satarker S, Nampoothiri M. Structural proteins in Severe Acute Respiratory Syndrome Coronavirus-2. Arch Med Res. 2020;51(6):482. doi: 10.1016/J.ARCMED.2020.05.012.
5. Hoffmann M, Kleine-Weber H, Schroeder S, et al. SARS-CoV-2 cell entry depends on ACE2 and TMPRSS2 and is blocked by a clinically proven protease inhibitor. Cell. 2020;181(2):271-280.e8. doi:10.1016/J.CELL.2020.02.052.
6. Yuki K, Fujiogi M, Koutsogiannaki S. COVID-19 pathophysiology: A review. Clin Immunol. 2020;215:108427. doi: 10.1016/J.CLIM.2020.108427.

7. Astuti I, Ysrafil. Severe Acute Respiratory Syndrome Coronavirus 2 (SARS-CoV-2): an overview of viral structure and host response. Diabetes Metab Syndr Clin Res Rev. 2020;14(4):407-412. doi: 10.1016/J.DSX.2020.04.020.
8. Zou X, Chen K, Zou J, Han P, Hao J, Han Z. Single-cell RNA-seq data analysis on the receptor ACE2 expression reveals the potential risk of different human organs vulnerable to 2019-nCoV infection. Front Med. 2020;14(2):185-192. doi: 10.1007/S11684-020-0754-0.
9. Rahman S, Montero MTV, Rowe K, Kirton R, Kunik F. Epidemiology, pathogenesis, clinical presentations, diagnosis and treatment of COVID-19: a review of current evidence. Expert Rev Clin Pharmacol. 2021;14(5):1. doi: 10.1080/17512433.2021.1902303.
10. Tang Y, Liu J, Zhang D, Xu Z, Ji J, Wen C. Cytokine storm in COVID-19: the current evidence and treatment strategies. Front Immunol. 2020;11:1708. doi: 10.3389/FIMMU.2020.01708/FULL.
11. Fajgenbaum DC, June CH. Cytokine storm. N Engl J Med. 2020;383(23):2255-2273. doi: 10.1056/NEJMra2026131.
12. Goswami J, MacArthur TA, Sridharan M, et al. A review of pathophysiology, clinical features, and management options of COVID-19 associated coagulopathy. Shock. 2021;55(6):700. doi: 10.1097/SHK.0000000000001680.
13. Hottz ED, Azevedo-Quintanilha IG, Palhinha L, et al. Platelet activation and platelet-monocyte aggregate formation trigger tissue factor expression in patients with severe COVID-19. Blood. 2020;136(11):1330. doi: 10.1182/BLOOD.2020007252.
14. Fuchs TA, Brill A, Wagner DD. Neutrophil extracellular trap (NET) impact on deep vein thrombosis. Arterioscler Thromb Vasc Biol. 2012;32(8):1777-1783. doi: 10.1161/ATVBAHA.111.242859.
15. Zuo Y, Yalavarthi S, Shi H, et al. Neutrophil extracellular traps in COVID-19. JCI Insight. 2020;5(11). doi: 10.1172/JCI.INSIGHT.138999.
16. Middleton EA, He XY, Denorme F, et al. Neutrophil extracellular traps contribute to immunothrombosis in COVID-19 acute respiratory distress syndrome. Blood. 2020;136(10):1169-1179. doi: 10.1182/BLOOD.2020007008.
17. Thachil J. Hypoxia – an overlooked trigger for thrombosis in COVID-19 and other critically ill patients. J Thromb Haemost. 2020;18(11):3109-3110. doi: 10.1111/JTH.15029.
18. Gupta N, Zhao YY, Evans CE. The stimulation of thrombosis by hypoxia. Thromb Res. 2019;181:77-83. doi: 10.1016/J.THROMRES.2019.07.013.
19. Gallo Marin B, Aghagoli G, Lavine K, et al. Predictors of COVID-19 severity: a literature review. Rev Med Virol. 2021;31(1):1-10. doi: 10.1002/RMV.2146.
20. Liu J, Zheng X, Tong Q, et al. Overlapping and discrete aspects of the pathology and pathogenesis of the emerging human pathogenic coronaviruses SARS-CoV, MERS-CoV, and 2019-nCoV. J Med Virol. 2020;92(5):491-494. doi: 10.1002/JMV.25709.
21. World Health Organization. Living guidance for clinical management of COVID-19. Geneva: WHO; 2021 [cited 2022 May 5]. Available from: https://www.who.int/publications/i/item/WHO-2019-nCoV-clinical-2021-2
22. Li J, Huang DQ, Zou B, et al. Epidemiology of COVID-19: a systematic review and meta-analysis of clinical characteristics, risk factors, and outcomes. J Med Virol. 2021;93(3):1449-1458. doi: 10.1002/JMV.26424.
23. Xie Y, Wang Z, Liao H, Marley G, Wu D, Tang W. Epidemiologic, clinical, and laboratory findings of the COVID-19 in the current pandemic: systematic review and meta-analysis. BMC Infect Dis. 2020;20(1):1-12. doi: 10.1186/S12879-020-05371-2/FIGURES/3.
24. dos Santos WG. Natural history of COVID-19 and current knowledge on treatment therapeutic options. Biomed Pharmacother. 2020;129:110493. doi: 10.1016/J.BIOPHA.2020.110493.
25. Khalili M, Karamouzian M, Nasiri N, Javadi S, Mirzazadeh A, Sharifi H. Epidemiological characteristics of COVID-19: a systematic review and meta-analysis. Epidemiol Infect. 2020;148. doi: 10.1017/S0950268820001430.
26. Gandhi RT. The multidimensional challenge of treating coronavirus disease 2019 (COVID-19): remdesivir is a foot in the door. Clin Infect Dis. 2021;73(11):e4175-e4178. doi: 10.1093/CID/CIAA1132.
27. Armstrong RA, Kane AD, Kursumovic E, Oglesby FC, Cook TM. Mortality in patients admitted to intensive care with COVID-19: an updated systematic review and meta-analysis of observational studies. Anaesthesia. 2021;76(4):537-548. doi: 10.1111/ANAE.15425.
28. Hernández-Garduño E. Obesity is the comorbidity more strongly associated for Covid-19 in Mexico. A case-control study. Obes Res Clin Pract. 2020;14(4):375-379. doi: 10.1016/J.ORCP.2020.06.001.
29. Chew NW, Ngiam JN, Tham SM, et al. Fever as a predictor of adverse outcomes in COVID-19. QJM An Int J Med. 2021;114(10):706-714. doi: 10.1093/QJMED/HCAB023.
30. Soltani S, Faramarzi S, Zandi M, et al. Bacterial coinfection among coronavirus disease 2019 patient groups: an updated systematic review and meta-analysis. New Microbes New Infect. 2021;43:100910. doi: 10.1016/J.NMNI.2021.100910.
31. Lansbury L, Lim B, Baskaran V, Lim WS. Co-infections in people with COVID-19: a systematic review and meta-analysis. J Infect. 2020;81(2):266-275. doi: 10.1016/J.JINF.2020.05.046.
32. Musuuza JS, Watson L, Parmasad V, Putman-Buehler N, Christensen L, Safdar N. Prevalence and outcomes of co-infection and superinfection with SARS-CoV-2 and other pathogens: a systematic review and meta-analysis. PLoS One. 2021;16(5):e0251170. doi: 10.1371/JOURNAL.PONE.0251170.
33. da Silva Ramos FJ, de Freitas FGR, Machado FR. Sepsis in patients hospitalized with coronavirus disease 2019: how often and how severe? Curr Opin Crit Care. 2021;27(5):474-479. doi: 10.1097/MCC.0000000000000861.
34. Ippolito M, Misseri G, Catalisano G, et al. Ventilator-associated pneumonia in patients with covid-19: a systematic review and meta-analysis. Antibiotics. 2021;10(5):545. doi: 10.3390/ANTIBIOTICS10050545/S1.
35. Maes M, Higginson E, Pereira-Dias J, et al. Ventilator-associated pneumonia in critically ill patients with COVID-19. Crit Care. 2021;25(1):1-11. doi: 10.1186/S13054-021-03460-5/FIGURES/4.
36. Ou M, Zhu J, Ji P, et al. Risk factors of severe cases with COVID-19: a meta-analysis. Epidemiol Infect. 2020;148. doi: 10.1017/S095026882000179X.
37. Tan L, Wang Q, Zhang D, et al. Lymphopenia predicts disease severity of COVID-19: a descriptive and predictive study. Signal Transduct Target Ther. 2020;5(1):1-3. doi: 10.1038/s41392-020-0148-4.
38. Ma A, Cheng J, Yang J, Dong M, Liao X, Kang Y. Neutrophil-to-lymphocyte ratio as a predictive biomarker for moderate-severe ARDS in severe COVID-19 patients. Crit Care. 2020;24(1):288. doi: 10.1186/S13054-020-03007-0.
39. Malik P, Patel U, Mehta D, et al. Biomarkers and outcomes of COVID-19 hospitalisations: systematic review and meta-analysis. BMJ Evidence-Based Med. 2021;26(3):107-108. doi: 10.1136/BMJEBM-2020-111536.
40. Yang X, Yang Q, Wang Y, et al. Thrombocytopenia and its association with mortality in patients with COVID-19. J Thromb Haemost. 2020;18(6):1469-1472. doi: 10.1111/JTH.14848.
41. Chen R, Sang L, Jiang M, et al. Longitudinal hematologic and immunologic variations associated with the progression of COVID-19 patients in China. J Allergy Clin Immunol. 2020;146(1):89-100. doi: 10.1016/J.JACI.2020.05.003.
42. Kerr R, Stirling D, Ludlam CA. Interleukin 6 and haemostasis. Br J Haematol. 2001;115(1):3-12. doi: 10.1046/J.1365-2141.2001.03061.X.
43. Matsubara T, Yamakawa K, Umemura Y, et al. Significance of plasma fibrinogen level and antithrombin activity in sepsis: a multicenter cohort study using a cubic spline model. Thromb Res. 2019;181:17-23. doi: 10.1016/J.THROMRES.2019.07.002.
44. Lin J, Yan H, Chen H, et al. COVID-19 and coagulation dysfunction in adults: a systematic review and meta-analysis. J Med Virol. 2021;93(2):934-944. doi: 10.1002/JMV.26346.
45. Piano S, Dalbeni A, Vettore E, et al. Abnormal liver function tests predict transfer to intensive care unit and death in COVID-19. Liver Int. 2020;40(10):2394-2406. doi: 10.1111/LIV.14565.
46. Huang J, Cheng A, Kumar R, et al. Hypoalbuminemia predicts the outcome of COVID-19 independent of age and co-morbidity. J Med Virol. 2020;92(10):2152-2158. doi: 10.1002/JMV.26003.
47. Poggiali E, Zaino D, Immovilli P, et al. Lactate dehydrogenase and C-reactive protein as predictors of respiratory failure in CoVID-19 patients. Clin Chim Acta. 2020;509:135-138. doi: 10.1016/J.CCA.2020.06.012.
48. Raina R, Mahajan ZA, Vasistha P, et al. Incidence and outcomes of acute kidney injury in COVID-19: a systematic review. Blood Purif. 2022;51(3):199-212. doi: 10.1159/000514940.
49. Hachim MY, Hachim IY, Naeem K Bin, Hannawi H, Salmi I Al, Hannawi S. D-dimer, troponin, and urea level at presentation with

COVID-19 can predict ICU admission: a single centered study. Front Med. 2020;7:949. doi: 10.3389/FMED.2020.585003/BIBTEX.
50. Liu X, Wang H, Shi S, Xiao J. Association between IL-6 and severe disease and mortality in COVID-19 disease: a systematic review and meta-analysis. Postgrad Med J. 2021;98(1165):871-879. doi: 10.1136/POSTGRADMEDJ-2021-139939.
51. Herold T, Jurinovic V, Arnreich C, et al. Elevated levels of IL-6 and CRP predict the need for mechanical ventilation in COVID-19. J Allergy Clin Immunol. 2020;146(1):128-136.e4. doi: 10.1016/J.JACI.2020.05.008.
52. Prompetchara E, Ketloy C, Palaga T. Allergy and Immunology Immune responses in COVID-19 and potential vaccines: lessons learned from SARS and MERS epidemic. Asian Pac J Allergy Immunol. 2020;38(1):1-9. doi: 10.12932/AP-200220-0772.
53. Halim C, Mirza AF, Sari MI. The association between TNF-α, IL-6, and Vitamin D levels and COVID-19 severity and mortality: a systematic review and meta-analysis. Pathogens. 2022;11(2):195. doi: 10.3390/pathogens11020195.
54. Kaushal K, Kaur H, Sarma P, et al. Serum ferritin as a predictive biomarker in COVID-19. A systematic review, meta-analysis and meta-regression analysis. J Crit Care. 2022;67:172-181. doi: 10.1016/J.JCRC.2021.09.023.
55. Mohamed MMB, Lukitsch I, Torres-Ortiz AE, et al. Acute kidney injury associated with Coronavirus Disease 2019 in urban New Orleans. Kidney360. 2020;1(7):614. doi: 10.34067/KID.0002652020.
56. Wang L. C-reactive protein levels in the early stage of COVID-19. Médecine Mal Infect. 2020;50(4):332-334. doi: 10.1016/J.MEDMAL.2020.03.007.
57. Tan C, Huang Y, Shi F, et al. C-reactive protein correlates with computed tomographic findings and predicts severe COVID-19 early. J Med Virol. 2020;92(7):856-862. doi: 10.1002/JMV.25871.
58. Malas MB, Naazie IN, Elsayed N, Mathlouthi A, Marmor R, Clary B. Thromboembolism risk of COVID-19 is high and associated with a higher risk of mortality: a systematic review and meta-analysis. EClinicalMedicine. 2020;29-30:100639. doi: 10.1016/J.ECLINM.2020.100639.
59. Yin S, Huang M, Li D, Tang N. Difference of coagulation features between severe pneumonia induced by SARS-CoV2 and non-SARS-CoV2. J Thromb Thrombolysis. 2021;51(4):1107. doi: 10.1007/S11239-020-02105-8.
60. Zhang L, Yan X, Fan Q, et al. D-dimer levels on admission to predict in-hospital mortality in patients with Covid-19. J Thromb Haemost. 2020;18(6):1324-1329. doi: 10.1111/JTH.14859.
61. Lippi G, Cervellin G. Procalcitonin for diagnosing and monitoring bacterial infections: for or against? Clin Chem Lab Med. 2018;56(8):1193-1195. doi: 10.1515/CCLM-2018-0312/PDF.
62. Lippi G, Plebani M. Procalcitonin in patients with severe coronavirus disease 2019 (COVID-19): a meta-analysis. Clin Chim Acta. 2020;505:190. doi: 10.1016/J.CCA.2020.03.004.
63. Chu K, Alharahsheh B, Garg N, Guha P. Evaluating risk stratification scoring systems to predict mortality in patients with COVID-19. BMJ Health Care Informatics. 2021;28(1):100389. doi: 10.1136/BMJHCI-2021-100389.
64. Fan G, Tu C, Zhou F, et al. Comparison of severity scores for COVID-19 patients with pneumonia: a retrospective study. Eur Respir J. 2020;56(3). doi: 10.1183/13993003.02113-2020.
65. Wang L, Lv Q, Zhang X, et al. The utility of MEWS for predicting the mortality in the elderly adults with COVID-19: a retrospective cohort study with comparison to other predictive clinical scores. PeerJ. 2020;8:e10018. doi: 10.7717/PEERJ.10018/SUPP-5.
66. Bradley P, Frost F, Tharmaratnam K, Wootton DG. Utility of established prognostic scores in COVID-19 hospital admissions: multicentre prospective evaluation of CURB-65, NEWS2 and qSOFA. BMJ Open Respir Res. 2020;7(1):e000729. doi: 10.1136/BMJRESP-2020-000729.
67. Bats ML, Rucheton B, Fleur T, et al. Covichem: a biochemical severity risk score of COVID-19 upon hospital admission. PLoS One. 2021;16(5):e0250956. doi: 10.1371/JOURNAL.PONE.0250956.
68. Shang Y, Liu T, Wei Y, et al. Scoring systems for predicting mortality for severe patients with COVID-19. EClinicalMedicine. 2020;24:100426. doi: 10.1016/J.ECLINM.2020.100426.
69. Marcolino MS, Pires MC, Ramos LEF, et al. ABC2-SPH risk score for in-hospital mortality in COVID-19 patients: development, external validation and comparison with other available scores. Int J Infect Dis. 2021;110:281-308. doi: 10.1016/J.IJID.2021.07.049.
70. Gupta RK, Harrison EM, Ho A, et al. Development and validation of the ISARIC 4C. Deterioration model for adults hospitalised with COVID-19: a prospective cohort study. Lancet Respir Med. 2021;9(4):349-359. doi: 10.1016/S2213-2600(20)30559-2.
71. Ghayda RA, Lee KH, Kim JS, et al. Chest CT abnormalities in covid-19: a systematic review. Int J Med Sci. 2021;18(15):3395-3402. doi: 10.7150/IJMS.50568.
72. Zayed NE, Bessar MA, Lutfy S. CO-RADS versus CT-SS scores in predicting severe COVID-19 patients: retrospective comparative study. Egypt J Bronchol. 2021;15(1):1-10. doi: 10.1186/S43168-021-00060-3.
73. Canovi S, Besutti G, Bonelli E, et al. The association between clinical laboratory data and chest CT findings explains disease severity in a large Italian cohort of COVID-19 patients. BMC Infect Dis. 2021;21(1):1-9. doi: 10.1186/S12879-021-05855-9.
74. Borghesi A, Maroldi R. COVID-19 outbreak in Italy: experimental chest X-ray scoring system for quantifying and monitoring disease progression. Radiol Medica. 2020;125(5):509-513. doi: 10.1007/S11547-020-01200-3.
75. Maroldi R, Rondi P, Agazzi GM, Ravanelli M, Borghesi A, Farina D. Which is the role for chest X-ray score in predicting the outcome in COVID-19 pneumonia? Eur Radiol. 2021;31(6):4016-4022. doi: 10.1007/S00330-020-07504-2.
76. Borghesi A, Zigliani A, Golemi S, et al. Chest X-ray severity index as a predictor of in-hospital mortality in coronavirus disease 2019: a study of 302 patients from Italy. Int J Infect Dis. 2020;96:291-293. doi: 10.1016/J.IJID.2020.05.021.

Authors' ORCID iDs and academic degrees
Ivan Civirjic, MD, PhD Applicant, Assistant Professor – https://orcid.org/0000-0002-1360-5485
Serghei Sandru, MD, PhD, Professor – https://orcid.org/0000-0002-2973-9154
Oleg Arnaut, MD, PhD, Associate Professor – https://orcid.org/0000-0002-5483-8672
Natalia Cernei, MD, PhD Applicant, Assistant Professor – https://orcid.org/0000-0002-2031-5881
Victoria Moghildea, MD, PhD Applicant – https://orcid.org/0000-0002-5336-1470

Authors' contributions
IC conceptualized the idea, conducted literature review, and wrote the first manuscript; SS and AO revised critically the manuscript and completed the final text; CN and MV wrote the manuscript; CN and MV conducted literature review. All the authors approved the final version of the manuscript.

Funding
This research did not receive any specific grant from funding agencies in the public, commercial, or not-for-profit sectors.

Ethics approval and consent to participate. No approval was required for this study.

Conflict of interests . The authors have no conflict of interests to declare.

https://doi.org/10.52418/moldovan-med-j.65-2.22.09
UDC: 616.724

Temporomandibular joint dysfunction

***Daria Ribacova, Olga Cheptanaru, Diana Uncuta**

Pavel Godoroja Department of Dental Propaedeutics
Nicolae Testemitanu State University of Medicine and Pharmacy, Chisinau, the Republic of Moldova

Authors' ORCID iDs, academic degrees and contributions are available at the end of the article

*Corresponding author – Daria Ribacova, e-mail: daria.rybacova@gmail.com
Manuscript received June 07, 2022; revised manuscript November 18, 2022; published online December 20, 2022

Abstract

Background: The dysfunction of the temporomandibular joint (TMJ) becomes a significant and serious problem for modern society. TMJ disorder is the pathology of the stomatognathic system that is encountered more and more often every year, because the etiology is different and the pathogenesis is not well investigated. This disease is the result of the action of many factors that are constantly related to each other and over time can intensify and aggravate each other. A large number of studies have been done, articles and scientific papers have been published on the subject to establish the degree of prevalence and severity of this disease. Every year there are more and more patients with this pathology, which would mean that an effective solution in solving this problem has not yet been found and the topic remains relevant to this day. Insufficient knowledge of the mechanisms of this disease is one of the main reasons for the ineffectiveness of the treatment methods used. The objective of the work was to identify the clinical relevance of temporomandibular joint diseases.

Conclusions: TMJ dysfunction is a topic that does not lose its relevance, because it is still a problem to identify the causes of pathologies of the TMJ and their treatment. TMJ pathology can be caused by various factors, the identification of this problem should be approached with all seriousness, taking into account all diagnostic methods and a high-quality anamnesis taken from the patient.

Key words: temporomandibular joint dysfunction, pain, Costen's syndrome.

Cite this article
Ribacova D, Cheptanaru O, Uncuta D. Temporomandibular joint dysfunction. Mold Med J. 2022;65(2):59-63. https://doi.org/10.52418/moldovan-med-j.65-2.22.09.

Introduction

Dysfunctional temporomandibular joint (TMJ) pain (Costen's syndrome) was first described in 1934 by otolaryngologist James Costen and it is a complex of symptoms characterized by dull pain in the TMJ, headache, pain in the cervical spine, occiput and behind the auricle, which increases towards the end of the day, clicks in the TMJ during eating, hearing loss, tinnitus, heartburn in the throat and nose [1-3].

According to the source of 2019, pain in the face associated with the pathology of TMJ, occurs in 19-26% of the adult population [4]. In 2015, students of ninth – twelfth grades were examined, of which 33.3% suffered from TMJ dysfunction and 52.5% of them had TMJ pain. Without dolore symptoms – 31.03%; in orthodontic treatment – 17.24%; bruxism – 43.1% [5]. This study showed that this disease has a tendency to rejuvenate and therefore does not lose its relevance.

According to the 2004 source, the disease affected about 5-12% of the adult population and is the most common musculoskeletal disorder [6]. Analyzing different articles written in different years, it can be concluded that the problem of TMJ dysfunction is not solved and therefore continues to be current.

TMJ dysfunction is also a multifaceted and interdisciplinary problem that must be solved by doctors from various fields: dentist, neurologist, psychotherapist and others [7-9]. Maxillofacial surgeons restore the correct ratio of TMJ elements, the work of orthodontists is aimed at restoring adequate occlusal ratios, neurologists mainly use medical methods to combat tinnitus, and otorhinolaryngology doctors often identify and treat dysfunction of the Eustachian tube, which is associated with tinnitus and vertigo [10].

Numerous factors can contribute to TMJ dysfunction. Factors that increase the risk of TMJ dysfunction are called predisposing factors. Factors that cause the onset of TMJ are called initiation factors, and factors that interfere with healing or stop the progression of TMJ dysfunction are called perpetuating factors. In some cases, a single factor can perform one or all of these roles. These factors are: occlusal condition, trauma, emotional stress, severe pain intake and parafunctional activities [11].

Based on the main complaints of patients inherent in the syndrome of TMJ dysfunction the following can be highlighted:

- Accusations directly related to TMJ: pain, sound phenomena (clicks, squeaks, and crackles), limitation

of mouth opening, and blockage of the joint, deviation of the lower jaw to the side when opening the mouth.

- Accusations of occlusal disorders: abrasion of enamel, deformation and disruption of occlusion, dissatisfaction with the results of prosthetic and orthodontic treatment.
- Accusations related to pain: in the maxillofacial region, in the masticatory and facial muscles, tension in the facial muscles, frequent headaches, pain when yawning, wide opening of the mouth or mastication.
- Accusations of disorders of the psycho-emotional state: depression, irritability, vertigo, general weakness, general discomfort, decreased performance [12].

The most common clinical manifestations in TMJ dysfunction is the following triad of symptoms: sound phenomena in the joint, functional disorders and pain syndrome [13].

After analyzing a large number of bibliographic sources, four main causes of TMJ dysfunction can be highlighted:

1. Dysfunction of TMJ as a result of orthodontic treatment;
2. Dysfunction of TMJ as a result of partial or total edentation;
3. Dysfunction of TMJ as a result of pathological abrasion of teeth (occlusal pathologies);
4. Dysfunction of TMJ as a result of psycho-emotional stress.

Dysfunction of TMJ as a result of orthodontic treatment

Orthodontic treatment should begin with an examination of the temporomandibular joint, muscles, which are responsible for the movement of the lower jaw, since even in minor abnormalities of localization of a tooth or groups of teeth, the patient may have complaints and, accordingly, symptoms of TMJ dysfunction, which the doctor-orthodontist must take into account in the process of work. In 2012, a scientific research was carried out, which shows that at the stage of examination and preparation of patients for orthodontic treatment, symptoms of musculoskeletal dysfunction of TMJ were revealed, which in the first group of patients intensified in the treatment process, while in another group the symptoms barely appeared [14]. During orthodontic treatment premature contacts on the surface of the teeth may occur, and they are possible to develop disorders in the TMJ. In this case, a possible distal displacement of the articular condyles with dislocation of the anteromedial disc may occur. These changes in the mandibular kinematics and TMJ function lead to damage to the bilaminar zone, which is located behind the articular disc and carries out TMJ trophic. In this case, the formation of synovial fluid and nutrition of the cartilaginous structures of the joint will be disturbed. If the bilaminar zone is already intertwined, pain in the joint appears [9].

Dysfunction of TMJ as a result of partial or total edentation

TMJ dysfunction is detected in more than half (62.5%) of people with dentition defects [3]. Due to partial or total tooth loss, vertical occlusion size height and vertical resting size height change. Long change of these parameters leads to the development of irreversible consequences in the TMJ. Tooth loss leads to statistically significant changes in the parameters that characterize the mandibular fossa, articular tubercle and articular condyle of the mandible. Changes in the articular surfaces related to occlusion lead to severe dysfunction of the TMJ and stretching of its capsule [3]. Some authors mention that the most common cause of TMJ dysfunction is the partial absence of teeth or their destruction, which leads to a decrease in the vertical occlusion size [3].

As pointed out by N. A. Rabukhina et al., in the absence of teeth, the articular condyle of the mandible is displaced posteriorly, while there is a moment of compression in the joint to the retroarticular space, where the anatomical formations located in it are compressed [3]. In this regard, it can be assumed that the appearance of Costen's syndrome will be observed, because the anatomical formations and the bilaminar area, which are located posteriorly, are compressed and the patient feels some pain.

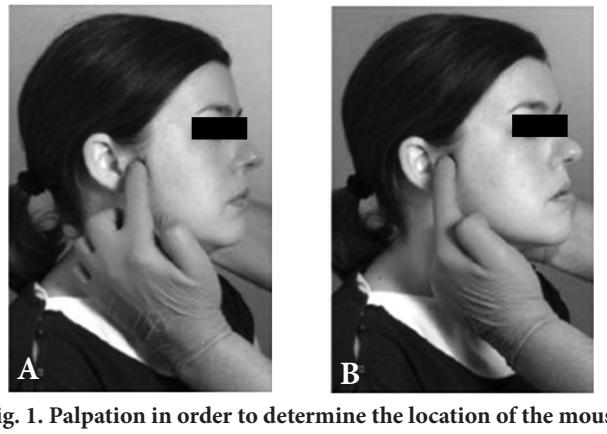

Fig. 1. Palpation in order to determine the location of the mouse process of the lower jaw. A – with a comfortable closing of the mouth, B – with protrusion of the lower jaw [9]

Fig. 2. Palpation of the masticatory muscle in order to determine the form of TMJ dysfunction. A – place of origin of muscle, B – body of muscle, C – muscle attachment area [9]

Dysfunction of TMJ as a result of pathological abrasion of the teeth (occlusal pathology)

For many years, the main cause of TMJ dysfunction was considered to be occlusal disorders, which lead to tension and hypertrophy of the masticatory muscles and TMJ pathology. However, in recent years this relationship has been called into question.

Fig. 3. Palpation of the temporal muscle in order to determine the form of TMJ dysfunction. A – anterior portion of muscle, B – middle portion of muscle, C – posterior portion of muscle [9] Dysfunction of TMJ as a result of pathological abrasion of teeth (occlusal pathology)

If occlusal factors are related to TMJ, then the medical dentist is the only professional who can provide adequate therapy. On the other hand, if occlusal factors are not related to TMJ, the medical dentist should refrain from treating TMJ with occlusal changes [4, 11].

There are many etiological factors of the occurrence of TMJ pathology, the main and most common of which is pathological occlusion [15]. The founder of this theory, the occlusal theory of temporomandibular disorders, is considered Costen J. [9]. In 1934, James Costen made the first systematic description of this group of diseases, indicating occlusal disorder as the main cause [16]. Occlusal pathology can involve several factors that can cause TMJ dysfunction, namely, the presence of premature contacts as a result of dental restorations and the presence of pathological abrasion of the teeth. Both factors will lead to the development of TMJ pathology. In the presence of occlusal pathologies, the patient will feel a constant tension of a certain muscle group, as a result of which the lower jaw will begin to move along the wrong path – pathological. If the pathogenic factor is not eliminated in time, the muscles will be in constant hypertonicity, which will soon lead to a spasm of the mimic and masticatory muscles [17]. These factors will contribute to a change in muscle tone and, as a consequence, the development of the pathological trajectory of the lower jaw will lead to changes in the joint itself, namely, deformation of the articular disc and a change in its position when opening and closing the mouth – the pathological position of the articular disc [9]. In correcting pathological occlusion, it is necessary to take into account the condition of the masticatory muscles; otherwise the treatment will not be effective. In such patients, during treatment to eliminate TMJ dysfunction resulting from occlusion disorders, physical therapy (myogymnastics) is prescribed [8].

It is considered, that TMJ and dental occlusion from a functional point of view are related not only to each other, but also to the musculoskeletal system. In this context it has been observed that if a patient with occlusion pathology begins orthodontic or prosthetic treatment without correcting the condition of the cervical spine, then the success of dental treatment is questioned. A scientific research, conducted in 2018, can show us that the complex rehabilitation tactics, which include muscle relaxation procedures, drug treatment, splint therapy, myogymnastic exercises for masticatory muscles according to an individual plan and correction of body posture, proved to be 12.49 and 2.18% more effective than traditional methods of treatment [18]. Occlusal pathologies include not only the presence of supracontacts, but also pathological abrasions, which can also be called bruxism [19, 20]. To best understand bruxism that occurs at night, the clinician should first have an appreciation of the sleep process. Sleep is investigated by monitoring the brain wave activity (electroencephalogram) of an individual during sleep. This monitoring is called a polysomnogram. Elements of bruxism seem to be associated with an etiology and identification of functional disorders in the masticatory system, during the transition from a deeper sleep to a lighter one [11]. Most often, the front group of teeth is prone to bruxism. This may not bother the patient for a long time; he will not notice a decrease in the function of the stomatognathic (dental) system [19, 20]. The only thing that will worry him will be the presence of an aesthetic defect. At the same time, the height of the vertical occlusion size decreases, the position of the lower jaw relative to the upper one may change, which entails the appearance of problems in the temporomandibular joint. The appearance of attrition of the hard tissues of the tooth, the narrowing of the clinical crown of the tooth, the lowering of the lower third of the face – all this will indicate bruxism [19].

Dysfunction of TMJ as a result of psycho-emotional stress

The emotional state of the patient is largely dependent on the psychological stress incurred. Stress is described by Selye as the "nonspecific response of the body to any request made on it" [11]. The etiopathogenetic basis of this factor, which is the cause of TMJ disorders, is based on the neuromuscular theory, proposed by B. Jankelson (1953). The main link of this theory is the statement that "TMJ only allows movement to be performed, and the very movement and, accordingly, the function is performed by the muscles" [21].

A common systemic phenomenon that can influence masticatory function is an increase in the level of emotional stress borne by the patient. The emotional centers of the

brain influence muscle function. The hypothalamus, the reticular system, and especially the limbic system are primarily responsible for the emotional state of the individual. These centers influence muscle activity in many ways, some of which are gamma – efferent pathways. Stress can affect the body by activating the hypothalamus, which in turn prepares the body to respond (the autonomic nervous system). By the hypothalamus, through the complex neural pathways, increases the activity of gamma efferents, which cause contraction of muscle fibers. This sensitizes the muscle shaft so that any slight stretching of the muscle will cause a reflex contraction. The overall effect is to increase the tonicity of the muscle. The therapist must understand and appreciate emotional stress, as it plays an important role in the development of TMJ dysfunction [11].

The masticatory muscles participate in raising the mandible (masticatory, temporal, masseter and medial pterygoid muscles) and lowering the lower jaw (milohyoid, geniohyoid, digastric venter anterior, lateral pterygoid muscle). These muscles are at rest when the mandible is in a state of physiological rest and contract when closing the mouth (i.e. raising the lower jaw) and closing the teeth in occlusion. In a stressful situation, the teeth will more often be placed in the position of centric occlusion, which means that the masticatory muscles will be in constant tension (there will be a constant contraction of muscle fibers). Such discoordination of the activity of the masticatory muscles will lead to disturbances in intraarticular relationships [21, 22]. Prolonged hypertonicity of the masticatory muscles, which can be examined using magnetic resonance imaging (MRI), can lead to structural changes in the muscles, i.e., TMJ dysfunction. MRI imaging allows obtaining multiplanar images, visualization of masticatory muscles throughout, evaluation of their symmetry and morphostructure [23].

Conclusions

Analyzing a large number of different sources and scientific articles, it is possible to make the conclusion, that TMJ dysfunction can be caused by different reasons.

1. The dentist must consciously examine patients with TMJ disorders, drawing special attention to the collection of anamnesis. To make an accurate diagnosis of the disease, additional instrumental methods of TMJ examination should also be used.

2. As reported, TMJ dysfunction has different etiologies, and for etiotropic treatment, the doctor must establish a causal relationship between the symptoms of TMJ dysfunction and the causes that caused it.

3. Treatment of TMJ dysfunction, as well as its study and examination, must be carried out by specialists from different fields of medicine. Surgical treatment does not give the desired effect and often entails various destructive and functional disorders in the postoperative period. The treatment of patients with TMJ dysfunction will be complex: therapeutic and preventive measures aimed at normalizing occlusal relations, restoring the functional state of the masticatory muscles, normalizing the psycho-emotional state of patients. Also it is recommended to exclude solid foods, limit the opening of the mouth, which increase strain and tension or cause a feeling of fatigue, stiffness and spasm in the TMJ region.

References

1. Lesco T, Mostovei M, Solomon O, et al. Utilizarea computer tomografiei cu fascicol conic în diagnosticarea disfuncției articulației temporo-mandibulare = The use of cone-beam computed tomography for diagnostic of tempormandibular disorders. J Stomatol Med. 2018;(4/49):37-41. Romanian, English.
2. Temurov F, Kozhambekova E, Ubaidullaev A, Tasybaev D. [Features of clinical manifestations of the syndrome of pain dysfunction of the temporomandibular joint]. In: Modern trends in the development of science and technology: 1st International scientific and practical conference. Belgorod, 2015. Russian.
3. Gaivoronskii I, Iordanishvili A, Voitiatskaia I, Gaivoronskaia M. [The peculiarities of petrotympanic fissure topography in Costen syndrome and possible causes of its development]. Morfologiia. 2014;145(2):58-62. Russian.
4. Latysheva N, Platonova A, Filatova E. [Temporomandibular disorder and cervicalgia: pathophysiology underlying the comorbidity with chronic migraine]. Zh Nevrol Psikhiatr S.S. Korsakova. 2019;119(1):17-22. Russian. https://doi.org/10.17116/jnevro201911901117.
5. Iovu G, Miron G. Disfuncțiile articulației temporo-mandibulare la elevii claselor IX-XII, liceul "Petre Ştefănucă", or. Ialoveni. Aspecte de diagnostic [Temporo-mandibular joint dysfunctions in pupils of classes IX-XII, lyceum "Petre Stefanuca", Ialoveni. Aspects of diagnostic]. In: *Nicolae Testemitanu* State University of Medicine and Pharmacy of the Republic of Moldova. Collection of scientific abstracts of students, residents and young researchers. Chisinau; 2015. p. 323. Romanian.
6. Nistor L. Aspecte etiologice şi patogenetice în disfuncția temporo-mandibulară: sinteză de literatură = Etiological and pathogenic aspects of the temporomandibular dysfunction. Mold J Health Sci. 2016;2(8):70-76. Romanian, English.
7. Şcerbatiuc D, Iovu G. Disfunctiile articulatiei temporo-mandibulare [Temporomandibular joint dysfunctions]. Med Stomatol. 2013;(4):18-23. Romanian.
8. Fadeev R, Parshin V. [Results of complex treatment of patients with diseases of the temporomandibular joint and parafunctions of masticatory muscles. Part 1]. Ortodontiia. 2018;(1):39-43. Russian.
9. Boian A. [Observation of the causes of temporomandibular joints (TMJ) disorders in patients with muscle-joint dysfunction, and the identification of the most common symptoms]. Med Stomatol. 2014;(4/33):7-12. Russian.
10. Tardov M, Stulin I, Drobysheva N, et al. [Comprehensive treatment of Costen syndrome]. Zh Nevrol Psikhiatr S.S. Korsakova. 2020;120(4):60-64. Russian. https://doi.org/10.17116/jnevro202012004160.
11. Okeson J. Management of temporomandibular disorders and occlusion. 6th ed. St. Louis: Mosby Elsevier; 2008. 631 p.
12. Strandstrem I. [Clinical and pathophysiological features of the temporomandibular joint dysfunction syndrome: clinic, diagnosis, treatment] [dissertation]. Moscow; 2004. 125 p. Russian.
13. Postnikov M, Andriianov D, Osadchaia E. [Diagnostics of morphofunctional state of the temporo-mandibular joint using sonography in patients with malocclusion]. Bul Acad Sci Mold. Sci Med. 2020;(2/66):206-214. Russian.
14. Naumenko Iu. [Muscular dysfunctional disorders of the temporomandibular joint in patients with anomalies of teeth and dentition during orthodontic treatment]. Ortodontiia. 2012;(1):83. Russian.
15. Bekreev V, Rabinovich S, Persin L, Gruzdeva T. [Reason of tactics of treatment of patients with dysfunctions of the temporomandibular joint]. Ortodontiia. 2012;(1):38-43. Russian.

16. Latysheva N, Filatova E, Osipova V. [Temporomandibular disorder as the most prevalent cause of facial pain: current evidence]. Zh Nevrol Psikhiatr S.S. Korsakova. 2017;117(10):106-113. Russian. https://doi.org/10.17116/jnevro2017117101106-113.
17. Klimova T, Nabiev N, Ivanenko T, et al. [Classification of the causes of disorders of the movement of the lower jaw]. Ortodontiia. 2019;(2/86):4-10. Russian.
18. Fadeev R, Parshin V. [Results of complex treatment of patients with diseases of the temporomandibular joint and parafunctions of masticatory muscles. Part 2]. Ortodontiia. 2018;(1):44-48. Russian.
19. Fala V, Lacusta V, Bordeniuc G, Golovin B, Romaniuc D. Bruxismul diurn și factorii cotidieni (studiu preliminar) [Awake bruxism and everyday factors (preliminary research)]. Med Stomatol. 2016;(3/40):9-14. Romanian.
20. Gray Robin JM, Al-Ani MZ. Temporomandibular disorders: a problem-based approach. Chichester, West Sussex: Wiley-Blackwell; 2011. 214 p.
21. Shipika D, Lian D, Drobyshev A. [Clinical assessment of the effectiveness of botulinum toxin A in the treatment of temporomandibular joint pain dysfunction syndrome]. Stomatologiia. 2021;100(1):44-51. Russian. https://doi.org/10.17116/stomat202110001144.
22. Shipika D, Ostashko A, Burenchev D, et al. [Clinical example of complex diagnostic and treatment of patient with temporomandibular joint internal derangements with arthroscopic surgery]. Stomatologiia. 2021;100(4):109-116. Russian. https://doi.org/10.17116/stomat2021100041109.
23. Silin A, Itskovich I, Butova A. [Magnetic resonance imaging in a comprehensive examination of masticatory muscles and monitoring the results of treatment of muscular-articular dysfunction of the temporomandibular joints]. Ortodontiia. 2018;(3):18-24. Russian.

Authors' ORCID iDs and academic degrees
Daria Ribacova, MD, Undergraduate Student – https://orcid.org/0000-0002-8487-9950
Olga Cheptanaru, MD, PhD, Associate Professor – https://orcid.org/0000-0003-3182-2691
Diana Uncuta, MD, PhD, Professor – https://orcid.org/0000-0001-8172-2854

Authors' contributions
DR collected data, wrote the first version of the manuscript; OC conceptualized the idea, completed the final text; DU revised critically the manuscript. All the authors approved the final version of the manuscript.

Funding
This study was supported by *Nicolae Testemitanu* State University of Medicine and Pharmacy of the Republic of Moldova. The review study was the authors' initiative. The authors are independent and take responsibility for the integrity of the data and accuracy of the data analysis.

Ethics approval and consent to participate
There is no need to approve this review.

Conflict of interests
The authors have no conflict of interests to declare.

https://doi.org/10.52418/moldovan-med-j.65-2.22.10
UDC: [617.735+617.731-007.23]-08:602.9

A new approach in the treatment of retinopathies and optic nerve atrophy using mesenchymal stem cells

***[1]Tatiana Taralunga, [2]Ala Paduca, [1]Viorel Nacu**

[1]Laboratory of Tissue Engineering and Cell Cultures, *Nicolae Testemitanu* State University of Medicine and Pharmacy
[2]Department of Ophthalmology, *Nicolae Testemitanu* State University of Medicine and Pharmacy
Chisinau, the Republic of Moldova

*Corresponding author – Tatiana Taralunga, e-mail: tatiana.taralunga@usmf.md
Manuscript received October 03, 2022; revised manuscript December 02, 2022; published online December 20, 2022

Abstract

Background: The tissue engineering is the evolving science that combines cells, biomaterials and biochemical factors aimed at restoring, maintaining and substituting different types of tissue. An important role is played by the use of the stem cells in various fields of medicine, including ophthalmology, namely in cases of retinopathies and optic nerve atrophy.
Conclusions: Current treatment of the optic nerve atrophy is based on the etiological causes or late complications. Considering the availability of advanced therapies, stem cell therapy offers a new approach in the treatment of the atrophy of the optic nerve. Being easy to harvest and cultivate, mesenchymal stem cells are most commonly used in regenerative medicine, they can be induced to differentiate into cartilage, tendons, adipose tissue and other cell lines. Mesenchymal stem cell harvesting has no ethical issues compared to embryonic stem cell harvesting. The major histocompatibility factor II is not expressed on the surface of mesenchymal stem cells, and this great advantage allows their use in autologous or allogenic form. Mesenchymal stem cells produce growth factors with paracrine action that are thought to activate endogenous repair mechanisms, due to these properties mesenchymal stem cells have been used in several clinical studies in optic nerve disorders where immunomodulatory and neuroprotective properties have been demonstrated. All of the properties mentioned above stand for the clinical use of mesenchymal stem cells in case of optic nerve atrophy.
Key words: stem cells, retinopathy, optic nerve atrophy.

Cite this article
Taralunga T, Paduca A, Nacu V. A new approach in the treatment of retinopathies and optic nerve atrophy using mesenchymal stem cells. *Mold Med J*. 2022;65(2):64-68. https://doi.org/10.52418/moldovan-med-j.65-2.22.10.

Introduction

The retinal diseases and the optic nerve atrophy are more frequent causes of decreased visual acuity and blindness [1]. There are multiple causes of the retinopathies and of the optic nerve atrophy: inflammatory and vascular pathologies of the optic nerve and retina, glaucoma, atherosclerosis of the vessels of the head and neck, pathologies of the central nervous system, intoxications of various etiology, hereditary diseases. Optic nerve atrophy is caused by the irreversible apoptosis of retinal neuronal cells. In the absence of curative treatment for these degenerative pathologies, current therapies focus mainly on the etiological cause or late complications. However, most treatments have low specificity. Given the availability of advanced therapies, stem cell-based therapies offer a new approach in the treatment of retinal and optic nerve pathologies [2].

Being easily harvested and cultured, mesenchymal stem cells are the most widely used stem cells in regenerative medicine [3]. Mesenchymal stem cells can be induced to differentiate into bone, cartilage, fat, tendon and other cell lineages, depending on conditions and growth factors [4, 5]. Mesenchymal stem cells are easy to isolate and expand rapidly after a short rest period [6].

The harvesting of mesenchymal stem cells is free of ethical problems, compared to the harvesting of embryonic stem cells [7]. It is also considered that mesenchymal stem cells are "immunoprivileged" because the Major Histocompatibility Factor II is not expressed on their surface [8], this great advantage allows the use of mesenchymal stem cells in autologous or allogeneic form [9].

Furthermore, mesenchymal stem cells produce several growth factors with paracrine action that are believed to activate endogenous repair mechanisms [10-14]. Due to these properties, mesenchymal stem cells have been used in several preclinical studies in optic nerve disorders and retinopathies, where immunomodulatory, neuroprotective and tissue repair properties have been demonstrated [15-17]. These properties support the clinical use of mesenchymal stem cells. In neurodegenerative disorders, the use of mesenchymal stem cells is an opportunity for tissue repair and regeneration [18].

This synthesis aims to review the published clinical studies on the indications, dosage and results of stem cell therapy in case of retinal pathology and in case of optic nerve pathology.

Results and discussion

The material was synthesized based on clinical studies in which mesenchymal stem cells were used in cases of retinopathies and optic nerve atrophy.

For the advanced selection of bibliographic sources, the following filters were applied: stem and eye, optic nerve atrophy, retina, the materials published from 2004 to 2022 were analyzed. After examining the titles of the articles found, only papers containing relevant information on the use of stem cells in retinopathies and optic nerve atrophy were considered. The information was systematized, highlighting both the contemporary aspects of the use of mesenchymal stem cells in retinal and optic nerve pathologies, as well as the results obtained following the performance of published clinical studies. In the analyzed clinical studies, autologous stem cells from bone marrow or adipose tissue were used, the main route of administration of mesenchymal stem cells was intravitreal injection, followed by intravenous administration.

As a result of analyzing the information identified by the Google Search engine, from the PubMed databases according to the search criteria, 127 articles and 24 clinical trials were found on clinicaltrials.gov that address the problem of retinopathies and optic nerve atrophy. After the primary review of the titles, 40 publications and 24 clinical trials were considered relevant and were included in this review article.

Retinitis pigmentosa is one of the main hereditary degenerative retinal diseases, affecting 1 in 4000 people. Retinitis pigmentosa is characterized by low arteriolar diameter and pallor of the papilla [19-20]. Stargardt disease is the most common form of hereditary juvenile macular degeneration. The worldwide prevalence is 1 in 10000 people [21].

Initially, patients present a decrease in central vision. The pathology is defined by the accumulation of lipofuscin in the apical area in the cells of the pigmented epithelium of the retina. The clinical manifestations are a decrease in visual acuity up to blindness, secondary choroidal neovascularization with a gradual bilateral decrease in vision [21].

There are currently 9 clinical studies using mesenchymal stem cells to treat this type of retinal dystrophy (6 for retinitis pigmentosa, 2 for Stargardt disease and retinitis pigmentosa, 1 for retinitis pigmentosa and other pathologies).

Although most clinical trials are in the recruitment phase, there are two completed trials that include retinitis pigmentosa. Both performed at Hospital das Clinicas, Sao Paolo. (NCT01068561 phase I, NCT01560715 phase II). Autologous MSCs harvested from the bone marrow were used, which were injected intravitreally containing 10x106 cells/0.1ml. MSCs were obtained by aspirating 10 ml of bone marrow tissue from the posterior iliac crest and were separated by Ficoll-Hypaque centrifugation.

In the NCT01068561 study (phase I) there is one reported case [22]. The patient presented macular edema associated with retinitis pigmentosa. The macular edema resolved within seven days after mesenchymal stem cells injection, and the result was maintained for one month, a fact demonstrated by optical coherence tomography. It was concluded that adult stem cells have the ability to restore the ocular blood barrier due to paracrine effects or through an osmotic gradient that allows the absorption of macular edema [22].

The NCT01560715 study (phase II) is completed, from the published results it was concluded that therapy with intravitreal administration of mesenchymal stem cells can improve the quality of life of patients with retinitis pigmentosa.

The results were evaluated with a test that assesses the quality of life related to sight (NEI VFG-25) before therapy, 3 and 12 months later. There was considerable improvement 3 months after treatment, while at 12 months there was no significant difference from baseline [23].

A phase I clinical trial with autologous mesenchymal stem cells from bone marrow in retinitis pigmentosa patients is underway at the Virgen Hospital in Arrixaca, Spain. This clinical trial continues to recruit patients.

There are some clinical studies involving patients with diabetic retinopathy and age-related macular degeneration. Diabetic retinopathy is a prevalent microvascular complication in diabetes and remains the main cause of blindness in able-bodied people (20-74 years). Approximately 30% of all patients with diabetes have signs of diabetic retinopathy, and 30% of them may have sight-threatening retinopathy (severe retinopathy or macular edema) [24, 25]. Current standard treatment for the management of these disorders is mainly based on laser therapy or antiangiogenic therapy, both of which are associated with unavoidable ocular and systemic effects [25]. Age-related macular degeneration is a chronic, progressive retinal pathology and a leading cause of vision loss worldwide in people older than 60 years [26]. The prevalence of this pathology is increasing as an exponential consequence of the aging of the population. Significant progress has been made in the management of age-related macular degeneration with the introduction of anti-angiogenesis therapy [27]. However, antiangiogenic treatment does not stop progression or treat age-related macular degeneration. Thus, new approaches in the treatment of age-related macular degeneration, such as stem cell therapy, are needed. The use of bone marrow-derived stem cell therapy in diabetic retinopathy has been evaluated [28, 29] and there are five ongoing clinical trials (NCT01518842, IRCT 201111291414N29, NCT01736059, ChiCTR-ONC-16008055 and NCT01920867), and in case of age-related macular degeneration there are four clinical trials (NCT02016508, NCT01920867, NCT01736059 and NCT01518127). Following the NCT01736059 study, results were published in patients with age-related macular degeneration [30]. In these clinical trials, bone marrow mesenchymal stem cells were collected from the patient's

iliac crest in an average volume of 50 ml. Then, mononucleated cells were separated by Ficoll gradient centrifugation. The dose of cells was between $2x10^4$-$1.8x10^8$ suspended in 0.1 ml of buffered saline. A clinical study using stem cells obtained from adipose tissue was withdrawn, the reasons were not elucidated (NCT02024269).

The results of stem cell treatment for diabetic retinopathy are limited to the report of two patients. A 43-year-old patient with advanced retinal and optic nerve atrophy caused by diabetic retinopathy, vision – limited to defective light perception. After treatment with mesenchymal stem cells the patient showed improvement and did not show side effects such as inflammation or infection [28]. In this study, a patient with macular edema associated with macular ischemia is included, after intravitreal injection of mesenchymal stem cells from the bone marrow, the decrease of macular edema and the improvement of retinal function were described [29]. Clinical results of mesenchymal stem cell therapy in age-related macular degeneration describe two patients with 20/200 visual acuity. After intravitreal injection of mesenchymal stem cells, visual acuity changed to 20/80 and 20/160. In the patient with visual acuity 20/80, the result was maintained for 6 months. In the case of the second patient with visual acuity 20/160, it returned to the initial values of 20/200. After performing fluorescein angiography, in the case of both patients, a slight increase in extrafoveal geographic atrophy was detected in both eyes, a fact that can be attributed to disease progression [24].

Optic neuropathies are characterized by the degeneration of the optic nerve and can be caused by pathologies, such as glaucoma, autoimmune diseases, infections, trauma, ischemia or infections. In adults, glaucoma is the most common cause of vision loss followed by nonarteritic anterior ischemic optic neuropathy [30-32]. Traumatic optic neuropathy is a cause of vision loss and currently has no reliable treatment [33]. Neuromyelitis optica or Devic's disease is an autoimmune demyelinating pathology that causes optic neuritis, prevalence 1-3 per 100000 [31, 34]. Currently, the treatment consists of administration of corticosteroids and immunosuppressive drugs [32, 35].

There are two phase I clinical trials using mesenchymal stem cells to treat glaucoma (NCT02330978 and NCT02144103). Both clinical trials are currently recruiting patients. One clinical trial is taking place at the University of Sao Paolo, Brazil (NCT02330978), and the other at the Burnasyan Federal Medical Center, Russian Federation (NCT02144103). In the clinical study carried out in Brazil, autologous mesenchymal stem cells, derived from the bone marrow, are injected intravitreally. In the clinical study carried out in the Russian Federation, autologous mesenchymal stem cells are introduced into the subtenon space. Mesenchymal stem cells are taken from the adipose tissue on the anterior abdominal wall. There are currently no published data from these studies. In the SCOTS clinical trial (NCT01920867), conducted at the John Hopkins Hospital, United States of America, a case of autoimmune optic neuropathy was reported [36]. The patient underwent vitrectomy and injection of autologous mesenchymal stem cells from the bone marrow in one eye, and injection of autologous mesenchymal stem cells from the retrobulbar, subtenon and intravitreal bone marrow was performed in the other eye. Thus, the improvement of visual acuity was noticed.

A case of idiopathic optic neuropathy was also included in this study. The patient, in the right eye, was injected with autologous MSCs from the bone marrow in the retrobulbar, subtenon and intravitreal space, and in the left eye vitrectomy was performed, followed by direct injection of autologous MSC cells from the bone marrow, followed by the intravenous injection of them. After this procedure, a considerable improvement in visual acuity was observed, and the result was maintained for 12 months postoperatively [36].

For neuromyelitis optica there is an active clinical trial at Foothills Medical Center, University of Calgary, Canada (NCT01339455), two patients recruited at Northwestern University, United States (NCT00787722), an ongoing clinical trial in Tianjin Medical University General Hospital, China (NCT02249676) and one with unknown status at the Affiliated Hospital of Nanjing University, China (NCT01364246). Most active and recruitment clinical trials use immunosuppressive treatment followed by autologous hematopoietic stem cell transplantation. Nanjing University uses human umbilical cord mesenchymal stem cell transplantation. In this clinical trial (NCT01364246), 5 patients were followed for 18 months, including assessment of the Extended Disability Status Scale (EDSS), clinical course, magnetic resonance imaging (MRI) features, and adverse events, and reported an improvement in symptoms and signs of neuromyelitis optica in four out of five treated patients [34]. There is another clinical trial for secondary progressive multiple sclerosis with evidence of optic nerve damage (NCT00395200), in which patients were treated with autologous bone marrow stem cell transplantation, which resulted in an increase in visual acuity [35]. Some individual cases of neuromyelitis optica treated with allogeneic hematopoietic stem cells have also been reported.

Traumatic optic neuropathy is being studied in a clinical trial in China by the Cellular Biotherapy Center, Daping Hospital, Third Military Medical University (ChiCTR-TRC-14005093). They are currently recruiting patients and will use human umbilical cord-derived mesenchymal stem cell transplantation. There are no results yet.

Advances in the knowledge of the neuroprotective, immunomodulatory and regenerative properties of MSC are continuously generated by several *in vitro* and *in vivo* preclinical studies on animal models with different neurodegenerative diseases, including optic nerve atrophy and retinopathies. This fact gave the possibility to carry out the translation of treatment approaches in clinical practice.

Since 2008, several steps have been taken, designing new treatment approaches, regarding the use of cell therapy in patients with degenerative pathologies of the optic nerve and retina. These are phase I or I/II clinical trials, whose main objective is to evaluate the safety of mesenchymal stem cells using different routes of administration, in which the main route used is intravitreal injection. However, of the 24 clinical trials registered on clinicaltrials.gov, there are only 2 completed clinical trials, 3 ongoing, 15 in patient recruitment, 3 in unknown status, and 1 clinical trial has been withdrawn without informing about the reasons for this decision. Most of the results published so far are reduced to 6 cases reported in various retinopathies and optic nerve atrophy, but the number of patients is small.

Moreover, most of these clinical trials use autologous cells, obtained by bone marrow aspirates, so that the final content to be administered is a concentrate of mononuclear cells, which contains a very small percentage of mesenchymal stem cells (0.1%) [15], only four clinical trials used a specific concentration of mesenchymal stem cells without adding another cell type. Surprisingly, although adipose tissue-derived MSCs are easier to obtain and in higher concentration [17], there are only 2 clinical trials using this type of cells and one of them was withdrawn without explanation. Regarding the use of allogeneic MSCs, it is limited to 2 clinical trials, using umbilical cord-derived MSCs, however, it is not known whether patients will receive immunosuppressive therapy. Regarding the cell dose used in different clinical trials, there is a large variation from one to another. There is no consensus regarding the calculation of cell dose for the use of these cells by intravitreal injection. In clinical trials using aspirated mononuclear cells, the doses are usually high (between 3×10^6 cells / 0.1 ml and 30×10^6 cells/0.1 ml), while in clinical trials using a purified concentrate of mesenchymal stem cells the doses are smaller (1×10^6cells/0.1 ml). However, the information collected by clinicaltrials.gov and the international clinical trial registration platform does not specify the cell dose calculation.

Conclusions

It is important to know the development of cell therapy in relation to its use in clinical practice. However, it is also important to recognize that there is still a long way to go to reach phase III-IV clinical trials. One of the factors needed to proceed is the establishment of unified criteria for the dose to be used, another important factor is the use of only CSM without the addition of other cells, mesenchymal stem cells are immunoprivileged cells. Therefore, it is necessary to continue preclinical and clinical studies to improve this new therapeutic tool.

References

1. Bunce C, Wormald R. Leading causes of certification for blindness and partial sight in England & Wales. BMC Public Health. 2006 Mar 8;6:58. doi: 10.1186/1471-2458-6-58.
2. Lamba DA, Karl MO, Reh TA. Strategies for retinal repair: cell replacement and regeneration. Prog Brain Res. 2009;175:23-31. doi: 10.1016/S0079-6123(09)17502-7.
3. Braniste T, Cobzac V, Ababii P, Plesco I, Raevschi S, Didencu A, Maniuc M, Nacu V, Ababii I, Tiginyanu I. Mesenchymal stem cells proliferation and remote manipulation upon exposure to magnetic semiconductor nanoparticles. Biotechnol Rep (Amst). 2020 Feb 11;25:e00435. doi: 10.1016/j.btre.2020.e00435.
4. Jian M, Cobzac V, Mostovei A, Nacu V. The procedure of bone cells obtaining, culture and identification. In: 4th International Conference on Nanotechnologies and Biomedical Engineering: IFMBE Proceedings. Chisinau; 2019. p. 595-599. doi.org/10.1007/978-3-030-31866-6_108.
5. Phinney DG, Isakova I. Plasticity and therapeutic potential of mesenchymal stem cells in the nervous system. Curr Pharm Des. 2005;11(10):1255-65. doi: 10.2174/1381612053507495.
6. Vega A, Martín-Ferrero MA, Del Canto F, Alberca M, García V, Munar A, Orozco L, Soler R, Fuertes JJ, Huguet M, Sánchez A, García-Sancho J. Treatment of knee osteoarthritis with allogeneic bone marrow mesenchymal stem cells: a randomized controlled trial. Transplantation. 2015 Aug;99(8):1681-90. doi: 10.1097/TP.0000000000000678.
7. McLaren A. Ethical and social considerations of stem cell research. Nature. 2001;414(6859):129-31. doi: 10.1038/35102194.
8. Ng TK, Fortino VR, Pelaez D, Cheung HS. Progress of mesenchymal stem cell therapy for neural and retinal diseases. World J Stem Cells. 2014 Apr 26;6(2):111-9. doi: 10.4252/wjsc.v6.i2.111.
9. Johnson TV, Bull ND, Hunt DP, Marina N, Tomarev SI, Martin KR. Neuroprotective effects of intravitreal mesenchymal stem cell transplantation in experimental glaucoma. Invest Ophthalmol Vis Sci. 2010;51(4):2051-9. doi: 10.1167/iovs.09-4509.
10. Li N, Li XR, Yuan JQ. Effects of bone-marrow mesenchymal stem cells transplanted into vitreous cavity of rat injured by ischemia/reperfusion. Graefes Arch Clin Exp Ophthalmol. 2009 Apr;247(4):503-14. doi: 10.1007/s00417-008-1009-y.
11. Otani A, Dorrell MI, Kinder K, Moreno SK, Nusinowitz S, Banin E, Heckenlively J, Friedlander M. Rescue of retinal degeneration by intravitreally injected adult bone marrow-derived lineage-negative hematopoietic stem cells. J Clin Invest. 2004 Sep;114(6):765-74. doi: 10.1172/JCI21686.
12. Zhang Y, Wang W. Effects of bone marrow mesenchymal stem cell transplantation on light-damaged retina. Invest Ophthalmol Vis Sci. 2010 Jul;51(7):3742-8. doi: 10.1167/iovs.08-3314.
13. Wexler SA, Donaldson C, Denning-Kendall P, Rice C, Bradley B, Hows JM. Adult bone marrow is a rich source of human mesenchymal 'stem' cells but umbilical cord and mobilized adult blood are not. Br J Haematol. 2003 Apr;121(2):368-74. doi: 10.1046/j.1365-2141.2003.04284.x.
14. Bieback K, Kern S, Klüter H, Eichler H. Critical parameters for the isolation of mesenchymal stem cells from umbilical cord blood. Stem Cells. 2004;22(4):625-34. doi: 10.1634/stemcells.22-4-625.
15. Kern S, Eichler H, Stoeve J, Klüter H, Bieback K. Comparative analysis of mesenchymal stem cells from bone marrow, umbilical cord blood, or adipose tissue. Stem Cells. 2006 May;24(5):1294-301. doi: 10.1634/stemcells.2005-0342.
16. Woods EJ, Perry BC, Hockema JJ, Larson L, Zhou D, Goebel WS. Optimized cryopreservation method for human dental pulp-derived stem cells and their tissues of origin for banking and clinical use. Cryobiology. 2009 Oct;59(2):150-7. doi: 10.1016/j.cryobiol.2009.06.005.
17. Marquez-Curtis LA, Janowska-Wieczorek A, McGann LE, Elliott JA. Mesenchymal stromal cells derived from various tissues: Biological, clinical and cryopreservation aspects. Cryobiology. 2015 Oct;71(2):181-97. doi: 10.1016/j.cryobiol.2015.07.003.
18. Hartong DT, Berson EL, Dryja TP. Retinitis pigmentosa. Lancet. 2006 Nov 18;368(9549):1795-809. doi: 10.1016/S0140-6736(06)69740-7.
19. Siqueira RC, Messias A, Voltarelli JC, Messias K, Arcieri RS, Jorge R. Resolution of macular oedema associated with retinitis pigmentosa after intravitreal use of autologous BM-derived hematopoietic stem cell transplantation. Bone Marrow Transplant. 2013 Apr;48(4):612-3. doi: 10.1038/bmt.2012.185.
20. Siqueira RC, Messias A, Messias K, Arcieri RS, Ruiz MA, Souza NF, Martins LC, Jorge R. Quality of life in patients with retinitis pigmentosa submitted to intravitreal use of bone marrow-derived stem cells

(Reticell -clinical trial). Stem Cell Res Ther. 2015 Mar 14;6(1):29. doi: 10.1186/s13287-015-0020-6.
21. NCD Risk Factor Collaboration (NCD-RisC). Worldwide trends in diabetes since 1980: a pooled analysis of 751 population-based studies with 4.4 million participants. Lancet. 2016 Apr 9;387(10027):1513-1530. doi: 10.1016/S0140-6736(16)00618-8.
22. Saaddine JB, Honeycutt AA, Narayan KM, Zhang X, Klein R, Boyle JP. Projection of diabetic retinopathy and other major eye diseases among people with diabetes mellitus: United States, 2005-2050. Arch Ophthalmol. 2008 Dec;126(12):1740-7. doi: 10.1001/archopht.126.12.1740.
23. Wong WL, Su X, Li X, Cheung CM, Klein R, Cheng CY, Wong TY. Global prevalence of age-related macular degeneration and disease burden projection for 2020 and 2040: a systematic review and meta-analysis. Lancet Glob Health. 2014 Feb;2(2):e106-16. doi: 10.1016/S2214-109X(13)70145-1.
24. Wong TY, Liew G, Mitchell P. Clinical update: new treatments for age-related macular degeneration. Lancet. 2007 Jul 21;370(9583):204-206. doi: 10.1016/S0140-6736(07)61104-0.
25. Jonas JB, Witzens-Harig M, Arseniev L, Ho AD. Intravitreal autologous bone marrow-derived mononuclear cell transplantation: a feasibility report. Acta Ophthalmol. 2008 Mar;86(2):225-6. doi: 10.1111/j.1600-0420.2007.00987.x.
26. Siqueira RC, Messias A, Gurgel VP, Simões BP, Scott IU, Jorge R. Improvement of ischaemic macular oedema after intravitreal injection of autologous bone marrow-derived haematopoietic stem cells. Acta Ophthalmol. 2015 Mar;93(2):e174-6. doi: 10.1111/aos.12473.
27. Park SS, Bauer G, Abedi M, Pontow S, Panorgias A, Jonnal R, Zawadzki RJ, Werner JS, Nolta J. Intravitreal autologous bone marrow CD34+ cell therapy for ischemic and degenerative retinal disorders: preliminary phase 1 clinical trial findings. Invest Ophthalmol Vis Sci. 2014 Dec 9;56(1):81-9. doi: 10.1167/iovs.14-15415.
28. Miller NR, Arnold AC. Current concepts in the diagnosis, pathogenesis and management of nonarteritic anterior ischaemic optic neuropathy. Eye (Lond). 2015 Jan;29(1):65-79. doi: 10.1038/eye.2014.144.
29. Katz DM, Trobe JD. Is there treatment for nonarteritic anterior ischemic optic neuropathy? Curr Opin Ophthalmol. 2015 Nov;26(6):458-63. doi: 10.1097/ICU.0000000000000199.
30. Chaon BC, Lee MS. Is there treatment for traumatic optic neuropathy? Curr Opin Ophthalmol. 2015 Nov;26(6):445-9. doi: 10.1097/ICU.0000000000000198.
31. Wingerchuk DM. Neuromyelitis optica spectrum disorders. Continuum (Minneap Minn). 2010 Oct;16(5 Multiple Sclerosis):105-21. doi: 10.1212/01.CON.0000389937.69413.15.
32. Jasiak-Zatonska M, Kalinowska-Lyszczarz A, Michalak S, Kozubski W. The immunology of neuromyelitis optica – current knowledge, clinical implications, controversies and future perspectives. Int J Mol Sci. 2016 Mar 2;17(3):273. doi: 10.3390/ijms17030273.
33. Weiss JN, Levy S, Benes SC. Stem Cell Ophthalmology Treatment Study (SCOTS) for retinal and optic nerve diseases: a case report of improvement in relapsing auto-immune optic neuropathy. Neural Regen Res. 2015 Sep;10(9):1507-15. doi: 10.4103/1673-5374.165525.
34. Lu Z, Ye D, Qian L, Zhu L, Wang C, Guan D, Zhang X, Xu Y. Human umbilical cord mesenchymal stem cell therapy on neuromyelitis optica. Curr Neurovasc Res. 2012 Nov;9(4):250-5. doi: 10.2174/156720212803530708.
35. Connick P, Kolappan M, Crawley C, Webber DJ, Patani R, Michell AW, Du MQ, Luan SL, Altmann DR, Thompson AJ, Compston A, Scott MA, Miller DH, Chandran S. Autologous mesenchymal stem cells for the treatment of secondary progressive multiple sclerosis: an open-label phase 2a proof-of-concept study. Lancet Neurol. 2012 Feb;11(2):150-6. doi: 10.1016/S1474-4422(11)70305-2.
36. Ceglie G, Papetti L, Valeriani M, Merli P. Hematopoietic stem cell transplantation in neuromyelitis optica-spectrum disorders (NMO-SD): State-of-the-Art and Future Perspectives. Int J Mol Sci. 2020 Jul 26;21(15):5304. doi: 10.3390/ijms21155304.

Authors' ORCID iDs and academic degrees
Tatiana Taralunga, MD, Scientific Researcher – https://orcid.org/0000-0002-8069-4975
Ala Paduca, MD, PhD, Associate professor – https://orcid.org/0000-0002-9879-8211
Viorel Nacu, MD, PhD, Professor – https://orcid.org/0000-0003-2274-9912

Authors' contributions
TT conducted literature review, obtained raw data and wrote the manuscript; AP and VN revised the manuscript critically. All the authors revised and approved the final version of the manuscript.

Funding
The study was supported by the State Program Project 2020-2023: "GaN-based nanoarchitectures and three-dimensional matrices from biological materials for applications in microfluidics and tissue engineering", No 20.80009.5007.20. The trial was the authors' initiative; they are independent and take responsibility for the integrity of the data and accuracy of the data analysis.

Ethics approval and consent to participate
The project was approved by the Research Ethics Committee of *Nicolae Testemitanu* State University of Medicine and Pharmacy (Protocol No14, 15.03.2019).

Conflict of interests
No competing interests were disclosed.

Moldovan Medical Journal. December 2021;65(2):69

Mihail Popovici – 80-year anniversary

Born on October 29, 1942, in the village of Podoima, Camenca district, Academician Mihail Popovici is one of the Lords of science in the Republic of Moldova. Mr. Mihail Popovici went through an exemplary career evolution and at a fast pace firmly moved up the steps of the scientific-practical career. He graduated from the State University of Medicine and Pharmacy, Chisinau (faculty of general medicine) in 1965. His activity in the period of 1965-1977 included: doctorate, assistant and associated professor at the biochemistry department. In 1986 Mr. M. Popovici obtained the scientific degree of Doctor Habilitatus in Medicine, and in 1990 – scientific title of University Professor.

Mr. Mihail Popovici achieved outstanding results in his scientific-practical career. We will not review the hundreds of works of the scholar Mihail Popovici which, throughout his life, placed him in a vanguard position in the modernization and reform of the medical services system. Throughout his successful career, he was actively participating in the reconstruction of both the medical society and the academic life. We will only remember that this important personality of our science is essentially related to the research in the field of cardiology. This was also one of the reasons why in 1977 he was entrusted with the founding within the State Institute of Medicine in Chisinau of the Research Laboratory in the Field of Cardiology, which through the insistence, perseverance, and tenacity characteristic for Mr. M. Popovici in just a few years became the clinical-experimental Sector and firmly established itself as an important research subdivision. In 1983 Mr. M. Popovici was appointed the director of the Scientific-Research Institute of Cardiology and in 1987 – the director of the Institute of Research in Preventive and Clinical Medicine of Moldova which embraces 4 important Research Institutes of the country – Cardiology, Preventive Medicine, Pneumo-Phthisiology and Oncology. Since 1997 he has continued to be the director of the Institute of Cardiology. This emblematic institution for both health, research and higher education in the Republic of Moldova, whose General Director until 2014 was Academician Mihail Popovici, in addition to saving hundreds of thousands of lives, also gave birth to many scholars, specialists in clinical and fundamental cardiology research as well as doctors of higher category. A remarkable group of almost 40 scientists who delivered their scientific degrees of PhD and Doctor Habilitate under the supervision of Mr. M. Popovici have honored a remarcable scientific school in cardiology recognized by wide world. Nowadays, a lot of them activate in the prestigious cardiological centers in USA, Germany, Italy, Spain, Romania, etc.

The active participation of academician Popovici in the socio-political life of our country is also highly appreciated. Being a deputy in the Parliament of the Republic of Moldova from the twelfth legislature (1990-1994), he is a signatory of the Declaration of Independence of the Republic of Moldova. The 1990s were perhaps the most difficult years in the modern history of medicine in the Republic of Moldova and as a Member of the Parliamentary Commission, Member of the Board of the Ministry of Health (1998–2004), Mr. M. Popovici is among the illustrious figures of shapers of the new system of medicine governance, management and operation dictated by the transition to the market economy.

Today academician Mihail Popovici continues to work assiduously, being vice-director for science of the Cardiology Institute, an emblematic institution in the Republic of Moldova, whose founder he was. The field of research that he leads represents, beyond the outstanding practical and research activities carried out, beyond the results and the recognition obtained over time is a catalyst of valuable ideas and continues to contribute to the appearance of many scientific works, which are published in magazines with national and international impact, are presented at the Congresses of the European Society of Cardiology, of the Romanian Society of Cardiology, and also of the Society of Cardiologists of the Republic of Moldova, whose Presidency he holds.

Through all his prodigious activity academician Popovici proves to us that it does not matter how many years of life you have accumulated, but how much life you have accumulated in the years you have gone through.

On your anniversary, we address you, both on behalf of all Institute of Cardiology collaborators, and on behalf of the scientific community, the Society of Cardiologists of the Republic of Moldova, the expression of our most sincere feelings and the full support of all your activities to cultivate standards of excellence in research and health. We wholeheartedly wish you health and full success in your noble mission of harnessing the scientific-practical potential. May you always succeed in combining research and innovation, so that you find and keep the key to a knowledge society!

Happy Birthday, our dear Academician! Happy birthday, fruitful, bright, and good!

Vitalie Moscalu, MD, PhD, Associate Professor
Director of the Institute of Cardiology
Chisinau, the Republic of Moldova

Oleg Calenici – 60-year anniversary

We are honored and happy to congratulate you on the occasion of a beautiful jubilee and your worthy achievements, because this year your birthday marks a real event for the Public Health Institution – Institute of Cardiology collaborators, who have known you for years.

Every time we pay tribute or appreciate a personality, we mention what he has achieved or experienced, but often the words are not enough to frame the multiple qualities, virtues that were bestowed upon Mr. Oleg Calenici, who is in his activity a skilled doctor, peerless clinician and prodigious scientist having national and international outstanding performance.

Thus, speaking about Doctor Oleg Calenici represents a challenge, but also a possible risk. The challenge means to explore all the aspects through which we can pencil his personality, and the risk threatens the one who would not succeed in catching all the essential aspects of a person passionately dedicated to saving lives. As it is difficult to encompass all his merits, we have selected only a few significant benchmarks, which define his great activity.

The stages of professional training that you have gone through are remarkable, from honors student, as a graduate of the faculty of general medicine of the State Institute of Medicine in Chisinau (1985), followed by secondary clinical studies (1985-1987) and postgraduate studies (1988-1991) cardiology specialty (at the Academy of Medical Sciences of the USSR, Moscow). The titanic effort resulted in writing the thesis of a doctor in medical sciences, then you had the ambition to take the post-doctorate in 2000, became a doctor habilitate in medicine.

Even so, the career is in a continuous ascent that extends on distinct levels, but which are interrelated and support each other. Thus, at the same time with your work as a doctor and manager of the Institute of Cardiology, you also carried out a prodigious research activity, starting from scientific researcher (1991-1992) to senior scientific researcher (1992-2000) and coordinator (2000-2010) in the scientific laboratory of Cardiomyopathies and Myocarditis of the Institute of Cardiology. We are proud to say that you have continued research in the field of science within the Institute of Cardiology, and several of its indispensable branches which have been founded through your concept idea. It refers to the creation of the Invasive Cardiology Service of the Institute of Cardiology (2000-2010).

You are a true professional, a perfectionist, who had and always has the will and perseverance to go beyond one's limit, to be the first to apply the newest conquests of science in the medical system. The results of the conducted scientific studies were reflected in more than 300 scientific publications, one of which, "Ischemic Cardiopathy in Figures and Tables", was selected for preservation in the United States Library of Congress. Under your supervision, 2 theses were also defended by doctors of medicine.

As a manager, exercising the position of deputy director of the Institute of Cardiology during the work itinerary 1997-2010, you were a competent manager, with a perfect spirit of a leader, with an outstanding professional and human demeanor, always willing to look for new ways to approach the complex problems defined by cardiovascular diseases. Being constantly concerned with ensuring a high level of cardiologic support, maintaining the necessary conditions for the care of the sick, you managed to obtain high performance indicators in the activity of the institution you had managed.

The managerial and scientific activity was combined with a rich and responsible medical practice. You are a doctor for whom saving human lives was and is above everything else. Your intelligence, tact and sensitivity warmed the hearts of many suffering patients, but also inspired many spirits of students and doctors who see in you a perfect example and a human image to follow.

Although your soul remained firmly with patients and students from the Republic of Moldova, in 2010 you went abroad with your family to continue your professional activity at the same levels of competence and responsibility. So, in a short time, your professional and human value was also recognized in France, where you work until now as a clinical cardiologist at the Center Hospitalier Intercommunal Caux Vallée de Seine, Lillebonne, France.

You have reached one of the most important heights of life and you have every reason to consider yourself realized, that is why we wish you to be glad and delighted with new achievements, to be healthy and enjoy the respect and affection from people.

On behalf of the collaborators, on the occasion of your jubilee, Mr. Oleg Calenici, we wish you health, wealth, joys, work power, perseverance, achievements, continued and increased national and international recognition.

Best regards,

Alexandru Caraus, MD, PhD, Professor
Head of the Arterial Hypertension Clinic
Medical Director of the Institute of Cardiology
Chisinau, the Republic of Moldova

GUIDE FOR AUTHORS

The manuscript has to be sent electronically to editor@moldmedjournal.md by the author, responsible for the correspondence, using the **Authorship Statement Form** and **License Agreement**.

The authors are kindly requested to visit our web site www.moldmedjournal.md and strictly follow the directions of the **Publication Ethics and Malpractice Statement.**

Details about submission and article processing charge can be found on the journal's website: www.moldmedjournal.md.

All papers are to be executed in the following manner:

1. The manuscript should be typed in format A4, 1.5-spaced, with 2.0 cm margins, printing type 12 Times New Roman, in Microsoft Word.

2. The original article (presents new and original scientific findings, explains research methodology and provides data) has to be less than 16 pages long and should consist of an Introduction, Material and methods, Results, Discussion, Conclusions and be followed by not more than 40 references.

3. The review article (provides an overview of a field or subject, synthesizes previous research) must not exceed 25 pages and contain not more than 100 references.

4. The title page should include the first and family name of all the authors, their academic degrees, the name of the department and institution from which the paper has arrived, the phone number and e-mail address of the corresponding author.

5. The abstract should be written on the title page and limited from 220 to 240 words.
The abstract of original article should have 4 parts: Background, Material and methods, Results, Conclusions.
The abstract of review article should have 2 parts: Background and Conclusions.
The abstract should end with 3 to 6 key words.

6. The tables and figures must be typed, consecutively numbered and followed by an explanatory text. The figures that have to emphasize a comparison or details are published in color. If colored figures are to be placed, the author must pay an additional fee of €100 per page (1-8 figures on a page).

7. The references are to be listed in order of their appearance in the text, and the appropriate numbers are to be inserted in the text in square brackets in proper places.

The list of references should contain more than 50% in Scopus or WoS, more than 80% with DOI and not more than 30% of monographs or conference abstracts.

The references must comply with the general format outlined in the Uniform Requirements for the Manuscripts Submitted to Biomedical Journals developed by the International Committee of Medical Journal Editors (www.icmje.org), chapter IV.A.9.

The references in the Cyrillic script should be transliterated into Latin script using the American Library Association and Library of Congress Romanization Tables as follows: А=A, Б=B, В=V, Г=G, Д=D, Е=E, Ё=E, Ж=ZH, З=Z, И=I, Й=I, К=K, Л=L, М=M, Н=N, О=O, П=P, Р=R, С=S, Т=T, У=U, Ф=F, Х=KH, Ц=TS, Ч=CH, Ш=SH, Щ=SHCH, Ъ=", Ы=Y, Ь=', Э=E, Ю=IU, Я=IA.

Immediately after the transliteration the translation of the title in English in the square brackets should follow. For example: Ivanov IV, Shchukin NF, Men'shikov VM, Ad"yunktov AM. Transplantatsiia organov i tkanei [Transplantation of organs and tissues]. Vestnik Khirurgii. 2010; 26(6):45-49. Russian.

Address of the Editorial Office

192, Stefan cel Mare Avenue, Chisinau, MD-2004, the Republic of Moldova
Telephone: +373 22 205 209, +373 79 429 274 mobile
www.moldmedjournal.md editor@moldmedjournal.md